

IDENTIFICATION OF ULTRASTRUCTURAL AND BIOCHEMICAL MARKERS OF
FROST AVOIDANCE IN THE CUTICULAR LAYER OF CORN

A Thesis

Submitted to the College of

Graduate and Postdoctoral Studies

In Partial Fulfillment of the Requirements

For the Degree of Master of Science

In the Department of Plant Sciences

University of Saskatchewan

Saskatoon

By

Kaila Hamilton Sadowski

© Copyright Kaila Hamilton Sadowski, December 2017. All rights reserved.

Permission to Use

In presenting this thesis in partial fulfilment of the requirements for a Postgraduate degree from the University of Saskatchewan, I agree that the Libraries of this University may make it freely available for inspection. I further agree that permission for copying of this thesis in any manner, in whole or in part, for scholarly purposes may be granted by the professor or professors who supervised my thesis work or, in their absence, by the Head of the Department or the Dean of the College in which my thesis work was done. It is understood that any copying or publication or use of this thesis or parts thereof for financial gain shall not be allowed without my written permission. It is also understood that due recognition shall be given to me and to the University of Saskatchewan in any scholarly use which may be made of any material in my thesis.

Requests for permission to copy or to make other use of material in this thesis in whole or part should be addressed to:

Head of the Department of Plant Sciences

College of Agriculture and Bioresources

University of Saskatchewan

Saskatoon, Saskatchewan S7N 5A8

ABSTRACT

Abiotic stresses are a critical factor in the reduction of yield. Corn has been identified as a highly economically important yet, frost sensitive crop. Climate change trends are showing increased frost damage. The global need for food production is increasing and current production will not meet demand. Corn is killed at the moment of freezing and therefore, developing frost avoidance is essential. The primary obstacle limiting production of new more cold sensitive crops in the Canadian prairies is the cooler climate and early frost events in both spring and fall which are preventing widespread expansion. While many studies have examined corn chilling and frost sensitivity, the impact of simulated autumn temperatures (termed chilling pre-treatment) preceding a frost has not been reported. The effect of chilling pre-treatment, on subsequent freezing avoidance was studied in mature hybrid grain corn of four contrasting genotypes (256 and 675 [chilling sensitive]; 884 and 959 [chilling resistant]). Chilling pre-treatment (18°C/6°C, 10 days) induced physical and biochemical changes in the cuticular wax layer in all four genotypes. These changes were measured using a suite of complementary techniques including: thermal imaging, hydrophobicity, Confocal Laser Scanning Microscopy (CLSM), Attenuated Total internal Reflectance (ATR-FTIR), and Gas Chromatography Mass Spectrometry (GC-MS). In all corn genotypes studied, chilling pre-treatment induced a warmer freezing temperature than non-chilled. No significant genotypic differences were observed, however, genotypes 675 and 959 were least responsive to the stressor which resulted in the smallest change in freezing temperature induced by chilling pre-treatment. Hydrophobicity was reduced following chilling pre-treatment in all genotypes with the most significant effect observed in genotype 675. Cuticular thickness ($\mu=3.25\text{ }\mu\text{m}$) remained unchanged over the ten-day chilling pre-treatment under controlled environment conditions. By contrast, over the five-week field conditions, cuticle thickness increased in all genotypes. Genotype 256 had a significantly thinner cuticle ($-0.25\text{ }\mu\text{m}$) than the other genotypes indicating genotypic variation is accentuated under field conditions and sensitive lines may have a thinner cuticle. In the growth chamber, chilling treatment induced increasing cutan, cutin, & cuticular wax only in Region 1 (CH₃ functional group) according to ATR-FTIR within 2 μm of the adaxial surface layer. By contrast, field treatment induced a reduction in cutan, cutin, and cuticular wax in all regions (1, 2, & 3) (CH₃, Asymmetrical CH₂, Symmetrical CH₂) to the same 2 μm depth of ATR sampling. A primary challenge of proofing cuticle based studies in the field is the extremely strong

environmental influence (high light intensity, wind abrasion, insects, temperature fluctuations) which induce modifications on the cuticle. Using GC-MS analysis, 142 known compounds were identified in both controlled environment (chilling treatment) and field samples from the adaxial cuticular wax extraction of mature grain hybrid grain corn. Of those identified compounds, 28 were found to represent significant ($P < 0.05$) variation between chilling treated and non-chilled treatments under both growth chamber and field conditions. This variation represented 5 Classes of key compounds (Alkane, Alcohol, Fatty Acid, Triterpenes and other). It is clear that chilling treatment modifies both physical and biochemical properties of the cuticular layer. The degree and rate of detectable chemical changes induced by chilling treatment indicate physical cuticular modifications likely are contingent on biochemical changes. This may be due to the great number of chemical modifications and signals needed to induce a physical modification. ATR applications are more reflective of the cuticular composition in cases where the entire cuticular thickness is within the depth of sampling ($2\text{ }\mu\text{m}$). The investigation of the dynamic process of cuticular wax modification following chilling treatment using complementary techniques in *Zea mays* appears to be a useful system with practical applications for evaluating the correlation between the cuticle as a barrier to abiotic stress and chilling treatment in a whole plant system.

ACKNOWLEDGMENTS

Dr. Karen Tanino has once again taken me under her wing and inspired a passion for academics through her immense commitment for students, science and collaboration. I cannot thank her enough for the breadth of opportunities she has provided. I would also like to thank my committee members, Drs. Y. Bai, C. Karunakaran and R. Chibbar (chair), for providing their diverse backgrounds to support me during this project. The many members of the Tanino Lab have been a constant encouraging resource with protocols, plant care, and lab techniques with specific note of Ian Willick, Gowri Valsala, Masoomah Etehadnia, Elena Benic, Pankaj Banik and Rensong Liu. Quality plant care was made possible by Jackie Bantle, Eldon Siemens, Dr. Waterer and phytotron team.

Without the numerous and generous funding sources this project would have not been possible; Special thanks to DuPont Pioneer, Western Grains Research Foundation, Robert P. Knowles Scholarship, Canadian Light Source, National Science Foundation, and Mitacs through the Japanese Society for the Promotion of Science. Ann Perera at the W.M. Keck Metabolomics Research Laboratory was an immense help running and analyzing the GC-MS as was Eiko Kawamura at our local WCVI imaging center using the CLSM. Microscopy techniques were learned from the imaging team at NMBU with special recognition of Yeonkyeon Lee and Jorunn Olsen. Special thanks to Drs Rosendahl and Reed of the CLS Mid-IR beamteam for their ongoing patience and support.

I would like to recognize my parents (Rod and Cheryl Hamilton), family (Carlee and Rylee Hamilton) and friends (especially Ellen Misfeldt) for their interest and unwavering support over the course of the project. And Lastly, but most importantly, to my husband Jason Sadowski for his incredible patience, problem solving and statistical analysis.

TABLE OF CONTENTS

	<u>page</u>
ABSTRACT	ii
ACKNOWLEDGMENTS	iv
TABLE OF CONTENTS	v
LIST OF TABLES	viii
LIST OF FIGURES	ix
LIST OF ABBREVIATIONS	xiv
1 INTRODUCTION	1
Research Problem	2
Purpose of the Study	3
2 LITERATURE REVIEW	5
2.1 Corn as a model system	5
2.2 Climate Change	6
2.3 Low Temperature	7
2.3.1 Biotic and Abiotic Factors	7
2.3.2 Low Temperature Stress Classification	8
2.3.3 Field Frost Conditions	8
2.3.4 Freezing Resistance	9
2.3.5 Freezing Avoidance	9
2.3.6 Freezing Tolerance	10
2.3.7 Cold Acclimation and Chilling Pre-Treatment	12
2.3.8 Leaf Factors of Freezing Avoidance	13
2.3.9 Corn Lipid Profile	16
2.3.10 Hydrophobicity	16
2.3.11 Ice Nucleation	17
2.4 Imaging and Chemical Techniques in Plant Science	18
2.4.1 Use of Thermal Imaging in Plant Exotherm Measurements	18
2.4.2 Confocal Laser Scanning Microscopy (CLSM)	19
2.4.3 Mid-Infrared Synchrotron Spectroscopy (FTIR)	19
2.4.4 Gas Chromatography Mass Spectrometry (GC-MS)	21
3 IMPACT OF CHILLING PRE-TREATMENT AND GENOTYPE ON SUBSEQUENT CORN LEAF FREEZING CHARACTERISTICS	22
3.1 Introduction	22
3.1.1 Ice Nucleation Sub-hypothesis	24
3.2 Material and Methods	24
3.2.1 Plant Material	24

3.2.2 Establishment of Corn Plants	24
3.2.3 Chilling Regime	25
3.2.4 Thermal Imaging.....	26
3.2.5 Hydrophobicity	31
3.3 Results	34
3.3.1 Leaf and Stem Ice Nucleation Temperature	34
3.3.2 Genotype Effect on Ice Nucleation Temperature	34
3.3.3 ‘Extreme’ Chilling Condition Freezing Point Depression.....	35
3.3.4 ‘Mild’ Chilling Condition Freezing Point Depression.....	39
3.3.5 Chilling Treatment and Genotypic Influence on Hydrophobicity	41
3.4 Discussion	49
4 LIPID COMPOSITIONAL CHANGES IN THE ADAXIAL CUTICLE IN LEAVES OF	
MATURE CORN	52
4.1 Introduction	52
4.1.1 Physical and Biochemical Changes Sub-hypothesis.....	54
4.2 Materials and Methods.....	54
4.2.1 Plant Material	54
4.2.2 Establishment of Corn Plants.....	54
4.2.3 Chilling Regime	56
4.2.4 Sample Preparation for CLSM.....	57
4.2.5 Leaf Cuticle Thickness using CLSM.....	57
4.2.6 CLSM Experimental Design.....	58
4.2.7 CLSM Image Analysis.....	58
4.2.8 ATR-FTIR Sample Preparation	58
4.2.9 Spectroscopy with ATR-FTIR.....	59
4.2.13 ATR and FPA-FTIR Analysis	59
4.2.14 Spectra CH ₂ Regions Defined.....	60
4.2.15 Cuticular Wax extraction	63
4.2.16 Derivatization.....	63
4.2.17 GC/MS Analysis	63
4.2.18 Data Analysis	64
4.2.19 GC-MS/MS Experimental Design	64
4.3 Results.....	66
4.3.1 Field Condition- CLSM Cuticle Thickness	66
4.3.2 ‘Mild’ Chilling Condition – CLSM Cuticle Thickness	69
4.3.3 ‘Mild’ Controlled Environment Chilling Conditions – Integrations by Genotype	71
.....	
4.3.4 ‘Mild’ Controlled Environment Chilling Condition – Integrations by Treatment	75
.....	
4.3.7 ‘Field’ Chilling Conditions – CH ₂ Regions Defined	76
4.3.8 ‘Field’ Chilling Conditions – Integrations by Genotype	81
4.3.9 ‘Field’ Chilling Conditions – Integrations by Treatment	85
4.3.10 Identification of Adaxial Cuticular Composition in ‘Mild’ Chilling Treatment	
and Field Produced Corn	90
4.3.11 ‘Mild’ Chilling Condition – Identification of Lipid Compounds under	
Controlled Environment conditions in Genotype 884 and 959	93

4.3.12 Field Condition – Identification of Lipid Compounds in Genotype 675, 884 and 959	99
4.4 Discussion	108
<u>5 GENERAL DISCUSSION</u>	<u>114</u>
5.1 Future Research Directions	117
5.2 Novel Findings	117
5.2 Conclusions	118
<u>LIST OF REFERENCES</u>	<u>120</u>
<u>APPENDIX A 2016 GROWING SEASON Daily temperatures</u>	<u>139</u>
<u>APPENDIX B ‘EXTREME’ CHILLING CONDITION ATR-FTIR RESULTS</u>	<u>144</u>
<u>APPENDIX C FOCAL PLANE ARRAY MAPPING</u>	<u>151</u>
<u>APPENDIX D. 10 DAY ‘CHILLING TREATED’ MATURE CORN PLANTS</u>	<u>154</u>
<u>APPENDIX E PRELIMINARY ULTRASTRUCTURAL STUDIES</u>	<u>155</u>

LIST OF TABLES

<u>Table</u>	<u>page</u>
Table 3.1 Chilling regimes for a ten-day period under controlled growth environments..	26
Table 3.2 Hybrid corn plant material used for hydrophobicity measurements.....	33
Table 3.3 Comparison of Means (HSD Tukey Method) of Freezing Point Measurement of ‘Mild’ Chilling Treatment mature corn by genotype with 95% confidence interval around the lower and upper range.....	41
Table 4.1 Field produced measurement periods, relative chilling comparison reference and Environment Canada weekly average temperatures by week (Government of Canada 2016)	57
Table 4.2 Two-way ANOVA comparing means of cuticle thickness of leaf (V6; adaxial side), field produced mature corn	66
Table 4.3 Comparison of Means (HSD Tukey Method) of cuticle thickness of leaf	68
Table 4.4 Two-way ANOVA comparing means of cuticle thickness of leaf (V6; adaxial side) ‘mild’ chilling condition, mature corn across genotypes (884, 959) and treatment (chilling treated, non-chilled); n=120.....	69
Table 4.5 Comparison of Means (HSD Tukey Method) of combined (Regions 1, 2 and 3) peak area integration of field produced	89
Table 4.6 Cuticular wax composition, localized by multiple linear regression to 28 key compounds, identified through GC-MS of chilling treatment differential between treatments under ‘Mild’ chilling	92

LIST OF FIGURES

<u>Figure</u>	<u>page</u>
Figure 2.1 Physical layers of the plant cuticle (Kourouniotti et al. 2013) above the epidermal cells. The typical thickness of cuticle is 2-3 μ m (Schreiber and Schonherr 2009).	15
Figure 3.1 Freezing Point Measurements Ramp Compared to Step	30
Figure 3.2 Sampling of mature corn at stage VT and collared leaf (V6) identified (circled)	32
Figure 3.3 Classification and characteristics of hydrophobic surfaces	34
Figure 3.4 Box plot of stem and leaf freezing temperatures	35
Figure 3.5 Box plot comparing temperature of ice nucleation across genotypes (959, 884, 675 and 256)	36
Figure 3.6 Thermal images of ice nucleation after a 10-day exposure of non-chilled conditions (28/22°C).	37
Figure 3.7 Thermal images of ice nucleation after a 10-day exposure to ‘mild’-chilling pre-treatment (18/6°C)	38
Figure 3.8 Freezing point measurement as a measurement of lethal freezing temperature of mature corn plants (R1-R3) by genotype (256, 675, 884, 959) and treatment (chilling treated, non-chilled)	40
Figure 3.9 Contact angle as a measurement of hydrophobicity of mature corn leaf (V6; adaxial side) by genotype (256, 675, 884, 959) and treatment (chilling treated, non-chilled)	43
Figure 3.10 Contact angle as a measure of hydrophobicity of mature corn leaf (V6; adaxial side) by genotype (256, 675, 884, 959) and treatment (chilling treated, non-chilled). ..	44
Figure 3.11 Main effect of contact angle as a measurement of hydrophobicity of mature corn leaf.....	45
Figure 3.12 Main effect of contact angle as a measurement of hydrophobicity of mature corn leaf.....	46
Figure 3.13 Box plot comparing combined genotype (256, 675, 884, 959) information to directly evaluate treatment effect	47
Figure 3.14 Box plot comparing combined genotype (256, 675, 884, 959) information to directly evaluate treatment effect	48

Figure 4.1 Field Planting Design at the U of SK Horticulture Field Site; Sutherland Clay series plot using Complete Randomized Design (CRD) with 1 meter on center paired row planting; 12 replicates for each genotype (256, 675, 884 and 959).....	56
Figure 4.2 Chilling treated and non-chilled average spectra by genotype with band regions 60	
Figure 4.3 Z-stack of autofluorescence of mature corn cuticle using 488nm laser taken with Confocal laser scanning microscope. (A) Example of orthogonal slice in x-direction; (B) Pre-processing of smooth and sharpen in imageJ; (C) Binary representation to remove noise within image for data collection.	61
Figure 4.4 Mid-IR Endstation Facility (A) Attenuated Total internal Reflectance (ATR-FTIR) with DTGS Detector at the Canadian Light Source (CLS), Saskatoon SK; (B) Fresh mature corn leaf (V6) sample clamped into 3mm ATR probe accessory (C) Endstations at the CLS Mid Infrared 01B1-1 Beamline	61
Figure 4.5 Averaged, normalized, lipid fingerprint region ($2840\text{-}3040\text{cm}^{-1}$) chilling treated (CT) and non-chilled (NC) spectra by genotype	62
Figure 4.6 Cuticle thickness of leaf (V6; adaxial side), field produced mature corn by genotype (256, 675, 884, 959) and treatment (early 2016-08-03, late 2016-09-12) using CLSM	67
Figure 4.7 Boxplot of cuticle thickness of leaf (V6; adaxial side), field produced mature corn by genotype (256, 675, 884, 959) with combined treatment (early-2016-08-03, late-2016-09-12) using CLSM.....	68
Figure 4.8 Cuticle thickness of leaf (V6; adaxial side) of mature corn plants under ‘mild’ chilling conditions by treatment by combined genotypes (884, 959) averaged results using CLSM,	70
Figure 4.9 Peak area integration (a.u.) of CH_3 (region 1) $2960\text{-}3040\text{cm}^{-1}$ of leaf (V6; adaxial side) ‘mild’ chilling condition mature corn by genotype (256, 675, 884, 959) and treatment (chilling treated, non-chilled) using ATR-FTIR.....	72
Figure 4.10 Peak area integration (a.u.) of asymmetrical CH_2 bend (region 2; $2910\text{-}2960\text{cm}^{-1}$) of leaf (V6; adaxial side) ‘mild’ chilling condition mature corn by genotype (256, 675, 884, 959) and treatment (chilling treated, non-chilled) using ATR-FTIR;.....	73
Figure 4.11 Peak area integration (a.u.) of symmetrical CH_2 bend (region 3; $2840\text{-}2880\text{cm}^{-1}$) of leaf (V6; adaxial side) ‘mild’ chilling condition mature corn by genotype (256, 675, 884, 959) and treatment (chilling treated, non-chilled) using ATR-FTIR;.....	74
Figure 4.12 Boxplot of peak area integration (a.u.) of asymmetrical CH_2 bending groups of leaf (V6; adaxial side) ‘mild’ chilling condition mature corn by treatment (chilling treated, non-chilled) using ATR-FTIR	75
Figure 4.13 Boxplot of peak area integration (a.u.) of symmetrical CH_2 bending group (region 3; $2840\text{-}2880\text{cm}^{-1}$) of leaf (V6; adaxial side) ‘mild’ chilling condition mature corn by treatment (chilling treated, non-chilled) using ATR-FTIR;.....	76

Figure 4.14 Lipid fingerprint (2840-3040cm ⁻¹) average spectra of genotype 256 with band regions (region 1, 2960-3040cm ⁻¹ ; region 2, 2910-2960cm ⁻¹ ; region 3, 2840-2880cm ⁻¹) assigned to the CH ₂ groups	77
Figure 4.15 Lipid fingerprint (2840-3040cm ⁻¹) average spectra of genotype 675 with band regions (region 1, 2960-3040cm ⁻¹ ; region 2, 2910-2960cm ⁻¹ ; region 3, 2840-2880cm ⁻¹) assigned to the CH ₂ groups	78
Figure 4.16 Lipid fingerprint (2840-3040cm ⁻¹) average spectra of genotype 884 with band regions (region 1, 2960-3040cm ⁻¹ ; region 2, 2910-2960cm ⁻¹ ; region 3, 2840-2880cm ⁻¹) assigned to the CH ₂ groups	79
Figure 4.17 Lipid fingerprint (2840-3040cm ⁻¹) average spectra of genotype 959 with band regions (region 1, 2960-3040cm ⁻¹ ; region 2, 2910-2960cm ⁻¹ ; region 3, 2840-2880cm ⁻¹) assigned to the CH ₂ groups	80
Figure 4.18 Peak area integration (a.u.) of CH ₃ (region 1; 2960-3040cm ⁻¹) of leaf (adaxial side). V6 field produced mature corn by genotype (256, 675, 884 and 959) and treatment 82	
Figure 4.19 Peak area integration (a.u.) of the asymmetrical CH ₂ bend (region 2; 2910-2960cm ⁻¹) of leaf (adaxial side). V6 field produced mature corn by genotype (256, 675, 884 and 959) and treatment	83
Figure 4.20 Peak area integration (a.u.) of the symmetrical CH ₂ bend, (region 3; 2840-2880cm ⁻¹) of leaf (adaxial side). V6 field produced mature corn by genotype (256, 675, 884 and 959) and treatment	84
Figure 4.21 Boxplot of peak area integration (a.u.) of the CH ₃ group average across all genotypes, region 1, 2960-3040cm ⁻¹	86
Figure 4.22 Boxplot of peak area integration (a.u.) of asymmetrical CH ₂ bending group average across all genotypes, region 2, 2910-2960cm ⁻¹	87
Figure 4.23 Boxplot of peak area integration (a.u.) of symmetrical CH ₂ bending group average across all genotypes, region 3, 2840-2880cm ⁻¹	88
Figure 4.24 Heat Map and Dendrogram of ‘Mild’ chilling treated (884, 959) and field produced (675, 884, 959) showing z-scores of adjusted metabolites	91
Figure 4.25 Heat Map and Dendrogram of ‘Mild’ chilling treated (884, 959) showing z-scores of adjusted metabolites.....	94
Figure 4.26 Cuticular wax composition of chilling treatment on the concentration of 28 compounds of the cuticular wax extracted and analyzed from leaf (V6; adaxial side) surface of mature corn leaves in genotype 884 under ‘Mild’ chilling condition...	95
Figure 4.27: Cuticular wax composition of chilling treatment on the concentration of 28 compounds of the cuticular wax extracted and analyzed from leaf (V6; adaxial side) surface of mature corn leaves in genotype 959 under ‘Mild’ chilling condition...	96

Figure 4.28 Cuticular wax composition of chilling treatment on the concentration of 28 compounds of the cuticular wax extracted and analyzed from leaf (V6; adaxial side) surface of mature corn leaves in genotypes (884, 959) under ‘Mild’ chilling condition	97
Figure 4.29. Percentage abundance of chemical classes (alcohol, alkane, ester, fatty acid, other and triterpene) of two ‘mild’ chilling condition genotypes (884, 959) across two treatments	98
Figure 4.30 Heat Map and Dendrogram of three field produced genotypes (675, 884, 959) by two treatments (early; 2016-08-22, late; 2016-09-30), showing z-scores of adjusted metabolites,	101
Figure 4.31 Field produced cuticular wax composition of two treatments (early; 2016-08-22, late; 2016-09-30) on the concentration of 28 compounds of the cuticular wax extracted and analyzed from adaxial surface of mature corn leaf (V6) in genotype 675 Three replicates. Error bars denote standard error.	102
Figure 4.32 Field produced cuticular wax composition of two treatments (early; 2016-08-22, late; 2016-09-30) on the concentration of 28 compounds of the cuticular wax extracted and analyzed from adaxial surface of mature corn leaf (V6) in genotype 884.....	103
Figure 4.33 Field produced cuticular wax composition of two treatments (early; 2016-08-22, late; 2016-09-30) on the concentration of 26 compounds (Methacrylic acid tetradecyl ester, n-Dodecyl methacrylate removed) of the cuticular wax extracted and analyzed from adaxial surface of mature corn leaf (V6) in genotype 884.	104
Figure 4.34 Field produced cuticular wax composition of two treatments (early; 2016-08-22, late; 2016-09-30) on the concentration of 28 compounds of the cuticular wax extracted and analyzed from adaxial surface of mature corn leaf (V6) in genotype 959.....	105
Figure 4.35 Field produced cuticular wax composition of two treatments (early; 2016-08-22, late; 2016-09-30) on the concentration of 26 compounds (Methacrylic acid tetradecyl ester, n-Dodecyl methacrylate removed) of the cuticular wax extracted and analyzed from adaxial surface of mature corn leaf (genotype 959)	106
Figure 4.36 Percentage abundance of chemical classes (alcohol, alkane, ester, fatty acid, other and triterpene) of three Field produced genotypes (675, 884, 959) across two treatments	107
Figure 5.1: Ultrastructural and Biochemical Cuticle Model Flowchart	116
Figure B.1 Chilling treated and non-chilled average spectra by genotype with band regions (region 1, 2960-3040cm ⁻¹ ; region 2, 2910-2960cm ⁻¹ ; region 3, 2840-2880cm ⁻¹)	144
Figure B.2 Peak area integration (a.u.) of CH ₃ group (region 1; 2960-3040cm ⁻¹) of leaf (V6; adaxial side) ‘extreme’ chilling condition mature corn by genotype (256, 675, 884, 959) and treatment (chilling treated, non-chilled).....	146

Figure B.3 Peak area integration (a.u.) of asymmetrical CH ₂ bend (region 2; 2910-2960cm ⁻¹) of leaf (V6; adaxial side) ‘extreme’ chilling condition mature corn by genotype (256, 675, 884 and 959) and treatment (chilling treated, non-chilled).....	147
Figure B.4 Peak area integration (a.u.) of symmetrical CH ₂ bend (region 3; 2840-2880cm ⁻¹) of leaf (V6; adaxial side) ‘extreme’ chilling condition mature corn by genotype (256, 675, 884 and 959) and treatment (chilling treated, non-chilled).....	148
Figure B.5 Boxplot of peak area integration (a.u.) of asymmetrical CH ₂ bending groups of leaf (V6; adaxial side) ‘extreme’ chilling condition mature corn by treatment (chilling treated, non-chilled)	149
Figure B.6 Boxplot of peak area integration (a.u.) of symmetrical CH ₂ bending group (region 3; 2840-2880cm ⁻¹) of leaf (V6; adaxial side) ‘extreme’ chilling condition mature corn by treatment (chilling treated, non-chilled)	150
Figure C.1 Heat map of ‘mild’ chilling treated and non-chilled 884 and 959 over three regions of integration. The color scale represents intensity of the spectra (warm colors; high intensity, low values; cool hues).	153
Figure D.1 (L to R): Early Golden Bantam, 3 (256), 3 (675), 3 (884), 3 (959).....	154

LIST OF ABBREVIATIONS

a.u.	Absorbance units
ACS	(American chemical society) grade
ANOVA	Analysis of Variance
ASTM	American society for testing and materials - International standard
ATR	Attenuated total reflectance
BSTFA+TCMS	N,O-Bis(trimethylsilyl)trifluoroacetamide + trimethylchlorosilane
CI	Confidence interval
CLS	Canadian Light Source, Saskatoon, SK, CAN
CLSM	Confocal laser scanning microscope
CRD	Complete random design
CT	Chilling treated
DTGS	(deuterated-triglycine sulfate) detector
FLIR	Forward Looking Infrared FLIR Systems Inc.
FTIR	Fourier transform infrared spectroscopy
GC-MS	Gas chromatography mass spectrometry
HSD	Tukey's (Honest significance difference) test
LCFA	Long chain fatty acid
Mid-IR	Mid-Infrared light
MSD	Mass selective detector
NC	Non-chilled
PTFE	Polytetrafluoroethylene
U of SK	University of Saskatchewan, Saskatoon, SK, CAN
VLCFA	Very long chain fatty acid

CHAPTER 1

INTRODUCTION

Biotic (pathogens, insects and weed competition) and abiotic (temperature, moisture, light intensity and nutrient availability) stresses play a key role in the reduction of realized yield potential in crops. Environmental stressors are one of the most critical factors in yield reduction (Boyer 1982). The effect of the environment on corn is known to significantly impact productivity (Food and Agriculture Organization of the United Nations 2013) and the impact of yield loss is significant to many economies.

Corn has been identified as a highly economically important yet, frost sensitive crop. It is Canada's third most important crop, based on tonnage (Statistics Canada 2015) and in the US, corn is the most valuable crop (Esteve Agelet et al. 2012). In addition to being a key North American crop, internationally, many developing countries rely on corn for a primary food source. It is a food staple crop for millions of people around the world (Vivek 2008).

Due to the widespread impact and need for corn there is strong interest and investment to move corn production into the Canadian prairies (Saskatchewan Ministry of Agriculture 2010, Monsanto Canada 2013, DuPont Pioneer 2017). This geography shift would provide new opportunities to meet production needs as well as diversity in cropping options and locally produced products for the producers and consumers, respectively. The primary obstacle limiting production in the Canadian prairies is the cooler climate and early frost events in both spring and fall which are preventing widespread expansion into the region.

The continuation of global warming likely will facilitate increased frost and freezing damage (Gu et al. 2008, Storey and Tanino 2012) due to pre-mature growth followed by subsequent cooling (Esteve Agelet et al. 2012). Global warming is predicted to affect the protection of plants due to reduced insulating quantities of snow. This reduction in snow load may cause premature de-acclimation of plants due to earlier warmer temperatures followed by erratic cooling and frost events (Hinch and Zuther 2014). Changes in snowmelt can also affect signaling in plants and subsequent ability to reproduce and survive (Inouye 2008). Studies of

freezing avoidance and tolerance will continue to provide value by creating methods for improving the ability of the crop to withstand environmental stresses associated with global warming and climate change, including the prairies.

Corn is generally considered to be sensitive to cold (Chichester 1979, Esteve Agelet et al. 2012, Food and Agriculture Organization of the United Nations 2013) and it has been specifically recognized as both chilling and frost sensitive. Chilling injury occurs in sensitive crops at low temperatures in the absence of ice nucleation. Frost injury occurs when ice is formed, and intracellular freezing occurs. Frost sensitive crops may be able to initially supercool (freezing avoidance) or withstand the presence of ice in the extracellular space (freezing tolerance) but if ice penetrates in to the intracellular space, the cell and tissues will die. Corn has long been identified as a useful model system due to its prevalence around the world, its genetic diversity and its long term comprehensive use as a model organism in agronomy (Smith and Betrán 2004, Strable and Scanlon 2009).

To evaluate the degree of sensitivity in corn and its potential for avoiding freezing, we will utilize cycles of chilling pre-treatment to simulate fall conditions. Fall conditions are known to trigger cold acclimation in species which adapt. Cold acclimation is an adaptive process where after exposure to non-freezing cold temperatures the plant is able to tolerate colder temperatures in subsequent exposures (Catalá et al. 2011, Hinch and Zuther 2014) as first described by Tumanov and Krasavtsev (1959). The ability of corn to cold acclimate is not well understood, however, corn, at the seedling stage, may have the ability to acclimate (Prasad et al. 1994). As the climate continues to change, it is significant to note that even now frost injury continues to be one of the key factors in limiting production as it was over 30 years ago (Lindow 1983). This is reinforced by more recent examples of frost damage due to early spring frost causing \$2 billion of damage over one weekend in the U.S. (Gu et al. 2008) and a 80% reduction in the 2012 spring apple blossoms in Ontario (Leung 2012, Scallan 2012).

Research Problem

Locally produced Canadian prairie grain corn is often not able to reach its full production potential due to its sensitivity to early fall frost. The first frost typically ends growth in the fall before the grain reaches physiological maturity. By improving frost avoidance in corn to avoid damage from the first frost, plants would gain additional time to reach physiological maturity. As

corn is not primarily grown in cooler climates, its interaction and ability to avoid and adapt to cool conditions is not well understood.

Purpose of the Study

In corn, the first radiation frost typically initiates ice on the adaxial (upper) cuticular leaf surface (Gusta et al. 2009). We want to pursue the investigation of the modifications that occur in the cuticle. The purpose of this study is to understand the cuticular and epidermal surface contributions to freezing avoidance and to identify the specific traits that will either physically or through compositional alteration, improve frost avoidance. These traits can then be used as selection criteria in breeding programs to expedite selection and release of more stress resistant types into cool temperature regions. Moreover, as drought stress becomes more prevalent, reducing transpirational water loss through the cuticle will be increasingly important. Therefore, the study of the cuticular layer has potential impact alleviating multiple stresses.

The overall hypothesis is: Chilling pre-treatment alters cuticular characteristics which are linked to ice nucleation avoidance. To more specifically address this overarching hypothesis, two sub-hypotheses and objectives have been developed.

1.1 Ice Nucleation Sub-hypothesis

Chilling pre-treatment will cause corn genotypes to initiate ice nucleation at cooler temperatures than non-chilled plants.

1.11 Objective (Freezing Temperature): To determine the ice nucleation temperature in mature hybrid grain corn plants of four contrasting chilling resistant lines in chilling pre-treated and non-chilled plants.

1.12 Objective (Hydrophobicity): To determine if differences in ice nucleation temperatures in mature corn plants are related to cuticular hydrophobicity.

1.2 Physical and Biochemical Changes Sub-hypothesis

Chilling treatment will cause hybrid grain corn of four contrasting chilling resistant genotypes to modify cuticular thickness or biochemical composition

1.2.1 Objective (Cuticle thickness): To determine if cuticular thickness is modified by chilling treatment in hybrid grain corn of four contrasting chilling resistant genotypes.

1.2.2 Objective (Cuticle Composition): To determine if a cuticle compositional trait is modified by chilling treatment in hybrid grain corn of four contrasting chilling resistant genotypes.

1.2.3 Objective (Frost Avoidance): To determine if cuticle thickness or composition is linked to frost avoidance in mature hybrid grain corn in four contrasting chilling resistant genotypes.

1.2.4 Objective (Chemical Structure): To determine if differences in lipid profile are present between chilling treated and non-chilled greenhouse and field grown mature hybrid grain corn of contrasting chilling resistant genotypes.

CHAPTER 2

LITERATURE REVIEW

2.1 Corn as a model system

Corn has the highest production based on total tonnage worldwide (Food and Agriculture Organization of the United Nations 2013) and it has diverse applications including: food, fuel and feed uses. The human consumption of corn ranks as the third most important food crop in the world following wheat and rice (Food and Agriculture Organization of the United Nations 2013, Statistics Canada 2015). The value of corn in the Canadian agriculture industry is vast. In Canada, corn production has generated over two billion dollars in farm cash receipts (Canada. Agriculture Agri-Food Canada issuing body 2015). In the United States, corn ranks first in cereal production by tonnage and is the most valuable national crop (United States Department of Agriculture 2015). The preferential production of corn over other grain crops, such as wheat and rice, is expected to continue to increase in future years (Alexandratos and Bruinsma 2012). Corn prices have been trending upward and the price per bushel of corn has doubled in the last ten years (United States Department of Agriculture 2015).

Corn (*Zea mays sp. mays*) is a monocot within the Poaceae family. Corn or Maize, is a diploid consisting of 20 chromosomes. The genetics of corn provides researchers with considerable diversity and recombination potential (Smith and Betrán 2004). Historically (sixteenth century), corn has been recognized for its ability to adapt across environments (Weatherwax 1955). Prior to formal breeding efforts, human influenced natural selection had been ongoing for thousands of years and is thought to have originated in Central America (Smith 1989). Selections in the 1920's and 1930's continued breeding efforts to improve open pollinated varieties. In the 1940's, there was a rapid shift into hybrid corn production as inorganic nitrogen became readily available (Smith and Betrán 2004, Gardner 2009). In the 70 years since hybrids were introduced, there has been a history of steady increases in yield and stress tolerance (Smith and Betrán 2004).

Corn is thought to have originated from a small population comprised of large diversity (Eyre-Walker et al. 1998). It has a history of sensitivities to an array of abiotic stresses including drought (Castiglioni et al. 2008), nitrogen, water stress (Rossini et al. 2016), and cold. The sequencing of the maize genome (Dolgin 2009) has aided in advances in abiotic stress resistance. DroughtGard (Waltz 2014) is an example of a genetic based physiology trait modification that improves susceptibility of corn to drought by induction of bacterial cold shock proteins (Castiglioni et al. 2008). The chilling sensitivity of corn remains a significant limitation in expanding the geographic growing areas of corn. Corn has an extensive breeding history, has been recently sequenced and there are known gaps in resistance to abiotic stresses, especially cold sensitivity which makes it an ideal model plant system for physiological studies.

2.2 Climate Change

Climate change will lead to an increase in temperature variability along with more extreme weather fluctuations. Significant losses are predicted for corn yields in the US (Brown and Rosenberg 1999, Kucharik and Serbin 2008). Over the last twenty years there has been increasing research interest in understanding the link between climate change and extreme weather events leading to yield loss (Gobin et al. 2013, Papagiannaki et al. 2014). Negative impact on production and yields are expected due to this increased environmental weather variability (Chhetri et al. 2010, Melillo et al. 2014). As the global climate continues to change, it is significant to note that frost injury has been for the last thirty years, and continues to be, one of the key factors limiting production (Lindow 1983). In order to meet the growing need for food to sustain the increasing global population, improved abiotic stress resistance will be required in all commercial crops (Palta 2014). The continuation of global warming is predicted to increase chilling and frost injury due to premature growth followed by subsequent frost (Gu et al. 2008).

In corn, chilling injury is an ongoing constraint for global production (Gao et al. 2009, Guan et al. 2015) and restricts production boundaries (Stamp 1984). Despite large investment from private industry, the primary obstacle preventing widespread production of corn into the Canadian prairies is the overall cooler climate and early fall frost events in the region (Monsanto Canada 2013, DuPont Pioneer 2017). Before the first fall frost, the mean temperatures in the first fourteen days of September (30 year average) are 18°C day and 6°C night (Environment and Climate Change Canada 1981-2010). The freezing avoidance response following chilling pre-

treatment is relatively unknown in our corn genotypes. The ability of annual crops of sub-tropical origin to modify freezing avoidance mechanisms under temperate production regions, is important for expanded production. It represents a unique opportunity to evaluate the direct response of the plant without extensive protective mechanisms (Allen and Ort 2001). The need for adaptation in response to climate change extends beyond basic plant freezing avoidance mechanisms and will also necessitate production systems and farming approaches to respond to new environmental conditions (Howden et al. 2007, Arbuckle et al. 2013, Roesch-McNally et al. 2017).

2.3 Low Temperature

2.3.1 Biotic and Abiotic Factors

Within basic plant mechanisms, there are many factors which impact the overall productivity of plants. Plant stress can be defined as any outside factor that negatively affects the plant (Levitt 1972). These stress or factors can be sub-divided into two classes: Biotic and Abiotic. Biotic stressors are defined as living organisms impacting plant performance and includes pathogens (fungi, bacteria, virus and insects) and other competitive plants. Abiotic stress is characterized by the non-living factor impact on plant performance. Major losses experienced by abiotic stresses can include water deficit (Araus et al. 2002), drought, salinity (Ashraf and Wu 1994), and cold stresses (Gu et al. 2008). It is common for a combination of biotic and abiotic stress to affect the overall performance of the plant (Hirt 2004). It is also common for plants to be continually exposed to stresses (Zhu 2002, Mahmoud and Narisawa 2013, Bakhsh and Hussain 2015). Great economic losses are experienced in crop production each year due to abiotic stresses, with cold stress being a key loss factor (Xiong and Zhu 2001).

Cold-tolerance in corn has long been considered an extremely complex trait (Sevilla 2006). Some researchers have found additive genes responsible for cold survival (Grogan 1970), while others indicate non-additive genes (Eagles and Hardacre 1979) responsible to cold-tolerance in maize. Additive genes are those which work together toward a phenotype while non-additive genes have no summation toward the effect on the phenotype. Corn is considered chilling sensitive (Stamp 1984) and generally not freezing tolerant. However, native cold-tolerant corn populations have been established (Sevilla 2006). Species, such as corn, with origin

of tropical and sub-tropical nature can be sensitive to chilling stress and may be unable to cold acclimate (Sanghera 2011). One possible explanation for the lack of cold tolerance in these species is the lack of ABA. Exogenous application of ABA has shown to improve cold hardening in winter wheat (Chen and Gusta 1983), potato (Chen and Li 1982) and tobacco (Bornman and JANSSEN 1980). Tropical and sub-tropical originating species are of scientific interest as their response to cold is rapid, typically irreversible (Wang 1990) and simplified due to its reduced level of protective responses (Allen and Ort 2001). Low temperature stress slows plant growth leading to yield reduction and losses (Xin 2000) and is a key abiotic stress that needs to be managed to mitigate increasing risks caused by climate change.

2.3.2 Low Temperature Stress Classification

Low temperature stress can be classified into chilling stress and freezing stress. Levitt (1980) defined chilling low-temperature stress to occur at temperatures above 0°C, with a range from 0°C to 15°C. Freezing low-temperature stress is defined to occur at sub-zero temperatures (Levitt 1980, Thomashow 1999). Irreversible plant damage can be induced under either of the low temperature stress conditions (Palva 1994). Freezing stress can be characterized by damaging ice formation at sub-zero temperatures (Thomashow 1999, Kolaksazov et al. 2013). The origin of the species (Sub-tropical, tropical or temperate) can be good indicator of the type of low temperature stress most likely to affect the plant (Palva 1994). It is likely that plants have developed a complementary suite of adaptive functions including biochemical, physical and genetics to improve response to low temperature stress (Shinozaki et al. 2003). The most common low temperatures stress that causes yield reduction and lethal losses is late season freezing injury caused by radiation frost.

2.3.3 Field Frost Conditions

Radiation frosts are characterized by localized cool, dry air on clear nights where heat radiates directly from the plants and soil to the sky (Biel 1961, Rosenberg et al. 1983). This type of frost occurs on calm nights when the plants are actively growing. Radiation frost causes the plants to rapidly lose heat to the night sky and atmosphere and can cause complete and drastic losses to the crop (Gusta et al. 2009). A combination of morphology and environment will affect

losses to the plant caused by the transfer of heat from the leaf and soil to the sky (Leuning 1988, Leuning and Cremer 1988). Heat will always transfer from warmer regions to cooler regions. There are three ways which heat can transfer: conduction, convection and radiation. Conduction is the most common form and is defined as heat transfer from direct contact between substances. Convection is the movement of heat in a circular pattern through a liquid or gas as it continuously exchanges heat from hotter to cooler areas. As the hot air rises, it is displaced by cooler denser air which is pushed down. Lastly, radiation transfer is characterized by heat transfer without contact (Whitaker 2013). In plants, latent heat, following the suppression beyond the dew point, also has implications for the severity of a radiation frost. Latent heat is characterized by a phase change rather than temperature change and can be measured through evaporative loss of water in plants (Buttner 1934, Huber 1935). During a radiation frost event, a combination of heat transfer methods will be employed between the plant, the soil, the air and the sky (Raschke 1960).

2.3.4 Freezing Resistance

Freezing resistance is a general term used to describe the mechanisms encompassing both individual and compounding effects of freezing avoidance and freezing tolerance (Levitt 1972). Freezing resistance is defined as survival in plant tissue by avoidance or tolerance of ice formation (Levitt 1958). Corn has been characterized as having variable chilling tolerance among sensitive genotypes (Stamp 1984) but is not considered to be freezing tolerant.

2.3.5 Freezing Avoidance

The type and location of freezing is critical in determining the outcome for a plant during a frost event. Intracellular freezing is a process by which ice formation first occurs inside the protoplasm resulting in cell death (Burke et al. 1976, Levitt 1980, Pearce 2001). Freezing avoidance refers to the plants ability to avoid intracellular ice formation as it causes instant and irreversible cell death (Levitt 1972, Burke et al. 1976, Levitt 1980). This can be achieved through various means including reducing the temperature where the biological water freeze occurs (KB Storey and JM Storey 2005), accumulation of antifreeze proteins (Griffith and

Antikainen 1996), and cell dehydration which can reduce the intracellular freezing temperature (Levitt 1972, Levitt 1980). At the cellular level, freezing avoidance involves the process whereby cells deep supercool their intracellular water (Burke et al. 1976, George 1982) and have a deficiency of ice nucleators to avoid ice formation within the cell (Ishikawa and Sakai 1982). It has been noted that supercooled cells are typically more rigid and thicker than non-supercooled (Fujikawa et al. 1999). Species which avoid freezing by supercooling do not have the mechanism to tolerate any ice formation (George et al. 1974, Burke et al. 1976). Supercooling can be a valuable survival approach. For example, a group of tree-like species from the tropical high Andes was found to employ supercooling as their primary freezing resistance mechanism (Goldstein et al. 1985, Rada et al. 1987). This study also found that, in general, taller alpine species were freeze avoiders while lower lying species were tolerators (Goldstein et al. 1985, Rada et al. 1987, Azócar et al. 1988) indicating that targeted agronomic traits maybe good indicators for determining freezing resistance type. Freezing avoidance is not a mechanism exclusive to C4 crops such as corn, rather is a common attribute across most plants in the form of supercooling (Burke et al. 1976, Lindow 1983, Ashworth and Kieft 1995, Jain and Minocha 2013). The degree of supercooling between plant species is variable. Certain tissues, such as shoot primordia (Sakai 1979), winter cereal crowns (Vose and Blixt 2012) and florets (Ishikawa and Sakai 1982) have shown much higher freezing avoidance than surrounding tissues

The first wave of ice nucleation occurs on the leaf surface (Burke et al. 1976, Pearce and Ashworth 1992, Wisniewski et al. 1997, Carter et al. 1999, Wisniewski and Fuller 1999, Workmaster et al. 1999) and following that event, the ice spreads radially from the surface into the extracellular spaces (Sakai 1979, Beck et al. 1984, Guy 1990). Freezing avoidance is the only mechanism of freezing resistance in sensitive plants thus possessing the inability to tolerate freezing.

2.3.6 Freezing Tolerance

Freezing tolerance refers to the ability of the plant, tissue or organ to live, grow or develop in the presence of ice (Levitt, 1980). It is a process by which water preferentially freezes in the extracellular space which inhibits intracellular freezing (Burke et al. 1976, Levitt 1980). There are two ways by which ice can enter the intracellular spaces (Mazur 1969). The first is spontaneous internal ice nucleation (Levitt and Scarth 1936) and the second, ice entering

from the extracellular space into the intracellular space (Steponkus et al. 1983). Freezing tolerance also refers to the plants ability to tolerate dehydration stress in a duration effect as water migrates out of the cell down its vapor pressure gradient to form ice in the extracellular space (Burke et al. 1976, Ishikawa and Sakai 1982). A low water vapor pressure deficit draws water out of the cells until water potential equilibrium is reached between the ice and intracellular space (Pearce 2001). The loss of water results in freeze dehydration stress. This extracellular freeze dehydration stress may or may not result in cell death. The mechanism of cellular dehydration damage appears to be caused by the eventual collapse of the cell wall. This results in cell shrinkage. Cellular dehydration causes increased concentration of solutes, further depressing the freezing temperature (Wisniewski and Fuller 1999). In this case, the cell is injured due to desiccation stress. The advantage to properly managed water supply is that plants can slowly dehydrate and the water can transition as ice into the extracellular space. Plants can only tolerate a reasonable amount of freeze dehydration prior to having deleterious effects (Pearce 1988). In order for non-lethal extracellular freezing to occur, the freeze event must move slowly, stay in the extracellular space, and not compromise the protoplasm (Olien 1961, Levitt 1972).

During extracellular freezing there is significant stress placed upon the plant caused by dehydration as the water becomes tied up as ice (Mazur 1969). The time it takes the water to relocate will determine survival (Levitt and Scarth 1936). For example, in bark of apple voids corresponding a reduction in water in the cortical cells have been found suggesting a re-allocation of water (Ashworth et al. 1988). In addition to avoiding freeze induced cellular dehydration, another survival technique associated with freezing tolerance is controlled extracellular freezing. It is important to identify the adaptations needed for freezing tolerance. Work by Olien (1961), Mazur (1969), KB Storey and JM Storey (2005) identified one of the critical factors of freezing tolerance being a slow extracellular freeze. This means having sufficient stored carbohydrates to support basic functions, sufficient gas exchange despite ice barriers, and recovery from dormancy. Cold hardy plants which can withstand temperatures beyond the homogenous ice nucleation point are typically considered freezing tolerant (Sakai 1960).

It is important to note that these mechanisms are not isolated and often work in a dependent fashion. It is not uncommon to find both freezing tolerance and avoidance mechanisms acting in tandem to best resist freezing. In addition to combined freezing resistance

mechanisms, organ specific freezing has been shown in some species to protect critical points. Very low temperature supercooling (freeze avoidance) has been observed in the floral meristem and xylem parenchyma of temperate plants and other organs such as buds and seeds have expressed long durations of deep supercooling (Sakai 1979, Ishikawa and Sakai 1982). Following supercooling of the bud and seed, the extraorgan spaces were able to tolerate freezing by relocating water to less sensitive and critical adjacent tissues for freezing in less damaging preferential locations (Sakai and Larcher 1987). Extraorgan freezing is defined by separation of a supercooled region from a specific space outside the target organ (Sakai 1979). Once acclimated, winter cereal crowns have been shown to possess a high degree of both freezing avoidance (supercooling) and tolerance (altering water stores) (Gusta et al. 1982, Li 2012), while other structures such as leaves and roots are not highly freezing tolerant and subsequently die back. There are additional variations between these structures, with many studies finding that roots are more sensitive to freezing injury than shoots however the mechanism is not well understood (Pellett 1971, Wildung et al. 1973, Gusta et al. 1978, Chen et al. 1983). In corn, ice formation seems to be site specific. Research evidence by Ashworth and Pearce (2002) suggests that in corn, ice will form both in the extracellular and intracellular space. Ice forms in the extracellular space, preferentially in the mesophyll, causing cellular dehydration. In the intracellular space, ice forms, at -3.1°C, in epidermal and bundle sheath cells. (Ashworth and Pearce 2002).

2.3.7 Cold Acclimation and Chilling Pre-Treatment

Cold acclimation is a process by which plants increase freezing tolerance when exposed to prior low non-lethal above zero temperatures (Levitt 1980, Sakai and Larcher 1987). According to Weiser (1970) there are three stages of cold acclimation. The first stage is characterized by exposure to shorter day length triggering slowed growth followed by resting. The second stage of acclimation is characterized by cool, non-freezing temperature exposure, signaling key physical and metabolic cold survival preparative processes. The final stage is frost induced physical and biochemical changes in the plant including dehydration resistance and protein and water bond organization (Weiser 1970).

Following the final stage of cold acclimation, plants can expand their ability to withstand freezing following exposure to non-freezing cool temperatures (Thomashow 1999). The response

of plants to resist freezing following the process of cold acclimation has two primary constituents: 1) the change in cell function and biological metabolism in response to cold exposure and 2) the ability to tolerate freezing (Guy 1990). These two mechanisms are termed freezing avoidance and freezing tolerance, respectively. In general, crops at the plant level, such as tomato, rice and corn which originate from sub-tropical and tropical regions are known to lack ability to cold acclimate (Zhu et al. 2007, S. Sanghera et al. 2011) however some isolated and unpublished works indicate it may be possible at the juvenile seedling stage. Similarly in work by Chen and Li (1982), they found that *S. tuberosum* was unable to cold harden and implicated the importance of high osmotic concentrations for triggering an acclimation response.

2.3.8 Leaf Factors of Freezing Avoidance

As discussed previously, many plant organs (shoot primordia, roots, buds, seeds, crowns, and florets) function mutualistically within the plant utilizing varied freezing resistance mechanisms to best tolerate and avoid freezing. Leaf factors have important implications on the leaf surface and its interaction with cold temperature exposure. One way of classifying corn leaves is to identify key components based on their proximity and characteristics in a specific plane. In work by Freeling and Walbot (2013) they describe the leaf components by examining them from three dimensions. The first being longitudinal dimension consisting of the sheath and the blade. The second being the transverse dimension; the adaxial, abaxial and vascular bundle surfaces are asymmetrical and highly polarized areas in this plane. Lastly, the lateral dimension; this plane depicts the bilateral symmetry around the midrib (Freeling and Walbot 2013).

The specific tissues within the leaf fall into one of three tissues systems: epidermis, ground and vasculature. The epidermis is composed of the cuticle, pavement cells, guard cells and trichomes. The ground tissue encompasses: parenchyma, collenchyma and sclerenchyma. The vascular system comprises: xylem and phloem (Evert 2006). Since the first point of contact of ice is on the epidermal surface, this tissue becomes the most critical to regulate ice formation.

2.3.9.1 Structure and Composition of the Leaf Epidermis

Cuticle Layer

The cuticle is essential to support plant life (Kersters 1996). However, the contribution of the cuticular wax layer to freezing avoidance remains relatively unknown. Environmental

conditions have a strong impact on cuticular waxes. The cuticle seems to act as a barrier in freezing resistance in leaves (Wisniewski and Fuller 1999). The evolution of a hydrophobic covering over the surface of plants in the form of a cuticular layer is considered one of the most important evolutionary developments. This development has aided in survival and the transition to terrestrial environments (Yeats and Rose 2013) based on findings in sporophytes (Edwards 1993) and gametophytes (Budke et al. 2012). Lipids compose a large group of compounds which constitute a wide array of biological functions (Rojas et al. 2014). They play key roles in metabolism, cell membrane and cell wall, including cuticular wax. They have been recognized as critical for survival to plant stress (Welti et al. 2007). The cuticle serves as a thin protective cover on the surface of the plant (Jenks and Hasegawa 2008). The cuticle layer is the outermost layer which interacts with the environment. Its primary purpose is to act as a barrier (Bird and Gray 2003) against water loss (Goodwin and Jenks 2005). Other biotic and abiotic pressures such as temperature, light and humidity were shown to cause changes in wax. Decreases in humidity and temperature caused the greatest wax deposition (Baker 1974). The layer is physically and chemically important for function in regulating temperature changes, water movement and environmental contaminants (Sturaro et al. 2005).

Structural Characteristics

The cuticle has a multilayer, complex and ubiquitous surface structure (Martin 1970). The cuticle is composed of three distinct layers (Figure 2.1).

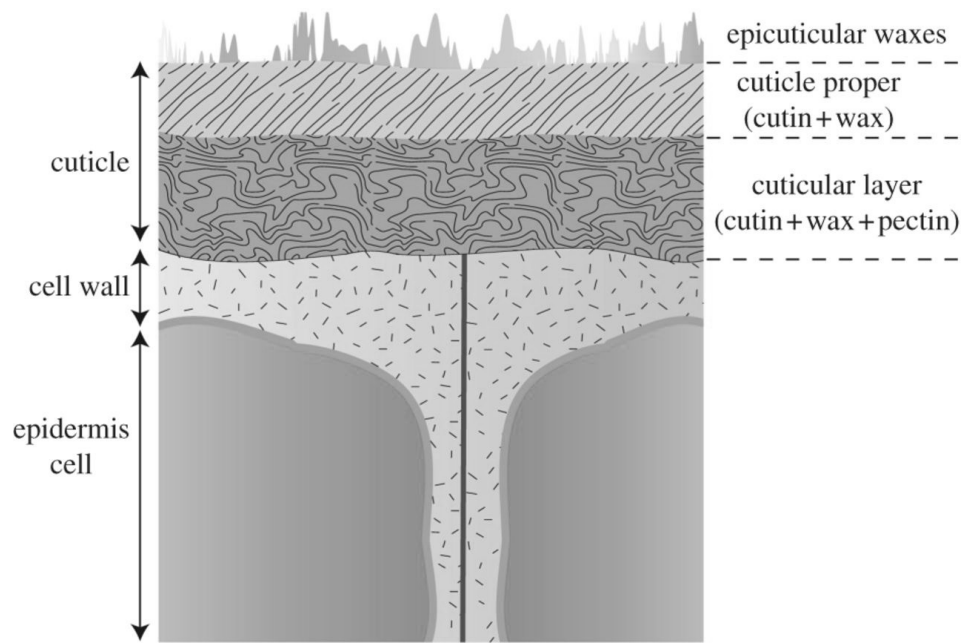


Figure 2.1 Physical layers of the plant cuticle (Kourounioti et al. 2013) above the epidermal cells. The typical thickness of cuticle is 2-3 μm (Schreiber and Schonherr 2009). Cuticular thickness measured with in these experiments had cuticular thickness means ranging from 3.3 μm to 4 μm .

The outermost layer of the cuticle consists of wax crystals. This delicate layer develops characteristic shapes as it organizes on the surface (Ensikat et al. 2010). Beneath the thin layer of cuticle are pavement cells. This cell type also has unique characteristic shapes and is determined by the underlying epidermal layer. Pavement cells are readily occurring simple surface cells that act as a barrier to more differentiated cells beneath and are generally in a puzzle like interlocking formation (Glover 2000). It is thought that the cuticle originates from these epidermal cells (Sturaro et al. 2005). The central layer in the cuticle is called the cuticle proper and the inner most layer of the cuticle is the intracuticular layer or cuticular layer and is contained within the matrix of the cell wall (Sturaro et al. 2005, Kourounioti et al. 2013). The cuticle proper arises from the procuticle and is formed of thin layers of polysaccharides and cutin (Bird and Gray 2003).

Biochemical Properties

The cuticle is heterogeneous with an insoluble wax layer over a soluble layer (Villena et al. 1999). The composition of the cuticle is primarily a combination of cutin and epicuticular waxes. The cuticle is primarily comprised of aliphatic compounds ranging from 16-34 length carbon chains. Each chain consisting specifically of: alkanes, esters, fatty acids, alcohol and aldehydes (Baker et al. 1982, Bianchi et al. 1989, Kolattukudy 1996, Sturaro et al. 2005).

Cutin is composed of a combination of hydroxy, epoxy fatty acids and esterified aliphatic acids (Kolattukudy 1980). The complementary cuticular waxes are long-chain fatty acids (LCFA) and very long chain fatty acids (VLCFA). The prevalence of the cuticle on all terrestrial land plants has made cuticular wax one of the most highly abundant sources of very long chain fatty acids (Perera 2005). VLCFA's are classified as 20 carbon chain length and greater.

2.3.9 Corn Lipid Profile

The history of interest in the cuticle dates back to the early 1800's when it was initially described in the literature (Brongniart 1834). The composition of wax is a complex, heterogeneous structure which appears to represent large variation across species (Riederer and Markstadter 1996, Bargel et al. 2004). In addition to species variation, the cuticle has also been found to be pliable with high variation between plants, structures, environment and age (Jeffree 1996, Jenks and Ashworth 1999). The composition of cuticular waxes in maize is a mixture of the long chain aliphatic compounds containing n-alkanes, alcohols, aldehydes, free fatty acids and esters (Bianchi et al. 1989). The research of Avato et al. (1987) described the composition of wax as varying greatly from immature to mature leaves and that the total amount of wax was depleted over time (Avato et al. 1987).

2.3.10 Hydrophobicity

The properties of a leaf can be defined by the wettability of a surface with a liquid at the surface interface. Hydrophobicity or hydrophilicity can be described, using a metric of contact angle, when the liquid phase in the system is water. Water droplets having greater than 90° contact angle at the liquid to surface interface are considered hydrophobic and to have a low affinity for water (ASTM Compass C813 2014). Hydrophilic surfaces have less than 90° contact angle and are highly wettable with high affinity for water (ASTM Compass C813 2014). Due to

the hydrophobic nature of plant lipids, notably waxes, water is repelled from the surface of the plant (Zia et al. 2016). The purpose of these waxes is to act as a hydrophobic defense barrier (Albersheim et al. 2010).

Hydrophobicity of the cuticle is of interest as it has been identified as an effective barrier against ice nucleation (Wisniewski and Fuller 1999), and imperfections in the cuticle have been shown to be sources for ice entry (Wisniewski et al. 2002). The ice-phobic nature of material had been linked to hydrophobicity (Heydari et al. 2013), however, the term ice-phobicity is a relatively new term and there is some controversy over whether ice-phobicity is directly correlated to hydrophobicity. The general consensus is that hydrophobicity, specifically superhydrophobicity, is not directly correlated to ice-phobicity (Kulinich et al. 2010, Jung et al. 2011, Nosonovsky and Hejazi 2012). The material used in this study did not fall into the superhydrophobic classification and therefore there is no established icephobicity link. However, in plant systems there appears to be a link between hydrophobicity and freezing avoidance (Wisniewski and Fuller 1999, Wisniewski et al. 2002, Fuller et al. 2003). Exogenously applied hydrophobic barriers have been shown to be very effective in preventing or delaying the propagation of lethal ice nucleation into the plant (Wisniewski et al. 2002, Fuller et al. 2003, Koch and Ensikat 2008, Wisniewski et al. 2015). In addition, Single and Marcellos (1974) found that physically removing the cuticle had a negative effect on the ability of the plant to withstand freezing, thus the hydrophobic nature of the cuticle was important for protection from external ice formation in field conditions.

2.3.11 Ice Nucleation

Regardless of the point of ice entry, ice nucleation must occur for freezing to take place (Lucas 1954, Steponkus 1984). When water freezes, it forms an ordered hexagonal crystal lattice which occupies a larger volume than its liquid state. The presence of an impurity, or ice nucleators catalyze the lattice formation (Franks 1985). The presence of many substances such as dust, fungi, bacteria or wind can all function as ice nucleating agents (Workmaster 2001). In order for ice nucleation to occur, water must be present (Pearce 2001). There are two classes of ice nucleators: intrinsic and extrinsic. Intrinsic nucleators occur naturally and are produced within the plant; whereas extrinsic nucleators are foreign substances not inherently produced in the plant (Wisniewski et al. 2009). Plants with greater hydrophobicity have been shown to better

resist extrinsic ice nucleation compared with plants with high leaf wettability (lower contact angle) (Fuller et al. 2003, Neuner and Hacker 2012).

2.4 Imaging and Chemical Techniques in Plant Science

Imaging and chemical techniques including: Thermal imaging, Confocal laser scanning microscopy (CLSM), Mid-IR light Spectroscopy (ATR-FTIR and FPA-FTIR) and Gas chromatography mass spectrometry (GC-MS) are a useful suite of tools to evaluate cuticular wax. These techniques were used in the investigation of the mechanism of cuticular wax modification following chilling and pre-treatment. These tools are powerful for both data collection and physiological understanding of the underlying processes.

2.4.1 Use of Thermal Imaging in Plant Exotherm Measurements

The use of thermal imaging has been long established as a method in evaluating stress tolerance (Clawson and Blad 1982, Ellenson and Amundson 1982, Hashimoto et al. 1984). Thermal imaging is a useful tool for measuring freezing events. Each pixel of the thermal images essentially acts as a thermocouple providing a temperature measurement and is useful to observe both initial ice nucleation and subsequent propagation of ice through plants (Ceccardi et al. 1995, Wisniewski et al. 1997, Workmaster et al. 1999, Carter et al. 2001). Ice nucleation and propagation is detectable as a change in thermal radiation when water freezes due to the exothermic nature of the reaction producing heat. During a freeze event, water transitions from liquid to solid state and as it transitions latent heat of fusion is released and this what is detected by the thermal imager.

In recent years, infrared thermography has gained acceptance as a high-throughput method for phenotyping crops for a multitude of traits (Fahlgren et al. 2015, Mutka and Bart

2015). High-throughput evaluations of traits include salinity stress, pathogen damage (Chéné et al. 2012), plant growth (Matos et al. 2014), heat, chilling and drought stress (Jansen et al. 2009). Another important application of this in-situ technology includes evaluation of abiotic stressors (Masuka et al. 2012, Zia et al. 2013) with direct implications for maize. Thermal imaging represents a unique opportunity to evaluate freezing point measurements in a mature whole plant system.

2.4.2 Confocal Laser Scanning Microscopy (CLSM)

Confocal laser scanning microscopy can provide a relatively high-throughput option for evaluation of the micromorphology of the plant cuticle (Urban et al. 2016). In contrast, previous methods such as bright field polarized light and fluorescence (Buda et al. 2009), proved prohibitively time consuming (Dilcher 1974). Autofluorescence of the cuticle presents a unique opportunity to visualize the three-dimensional features of the cuticle, including cuticle thickness (Fernández et al. 1999) without the use of fluorescing stains. Investigation of the thickness of the cuticle using CLSM is of interest due to its correlation to impacts on many abiotic stresses. Many important physiological responses have been linked to cuticle thickness and include: drought resistance (Gibson 1996), high temperatures stress (Casado and Heredia 2001) and UV response (Holmes and Keiller 2002). In addition, the mechanics and strength of the leaf tissues have been linked to cuticle thickness (Taylor 1971, Bargel et al. 2006) and this is of interest to ice penetration resistance.

2.4.3 Mid-Infrared Synchrotron Spectroscopy (FTIR)

Although traditional methods in plant science research of biochemical components exist, the preparation can be destructive, with extraction and processing of samples leading to long duration and costly experiments (Türker-Kaya and Huck 2017). In comparison to other methods,

harsh extractions and disruptive sample preparation are not required for FTIR spectroscopy (Largo-Gosens et al. 2014). FTIR spectroscopy using Mid-IR light has been recognized as a high-throughput method (Leugers et al. 2003, Kazarian and Chan 2010). The ability to use in-situ plant samples enables complex heterogeneous compounds in plant structures to interact with light resulting in spectra. This results in a non-destructive approach that is fast, efficient, easy to use with reproducible results (Barron 2011, Li et al. 2014, Türker-Kaya and Huck 2017). Despite the recognition of FTIR spectroscopy as a convenient and high-throughput method, the Mid-IR beamline (01B1-1) endstation at the Canadian Light Source (CLS) continues to be an underutilized tool in plant science research (Vijayan et al. 2015, Kumar et al. 2016).

Mid-IR light is ideal for cuticular wax studies as it allows for identification of absorbance spectra peaks associated with lipids (Safar et al. 1994, Lahlali et al. 2014). The peaks are associated with the vibration mode of the molecule or group of molecules with the height of the peak representing intensity or prevalence of the compound. Numerous previous studies have measured individual cuticle fraction modifications caused by chemical preparation using IR light (Benitez et al. 2004, Chefetz 2007, Girard et al. 2012), and were able to create band assignment recommendations from isolated cuticle (Girard et al. 2012, Heredia-Guerrero et al. 2014). The lipid fingerprint region is typically defined in the region from $2800\text{-}3000\text{cm}^{-1}$ (Fernández et al. 2011, Heredia-Guerrero et al. 2014, Lahlali et al. 2014). However, extensive intact IR tissue measurement of the cuticular layer have not been conducted.

FTIR spectroscopy is a useful and powerful tool to evaluate biochemical modifications, however, complementary use of this technique with others, such as GC-MS, improves the chemical characterization (Heredia-Guerrero et al. 2014) and should be performed.

2.4.4 Gas Chromatography Mass Spectrometry (GC-MS)

Metabolomics research has been used in recent studies to examine whole environment interaction on plants (Steinfath et al. 2010, Heuberger et al. 2014) as well as specific abiotic stress responses (Shi et al. 2014, Ganie et al. 2015, Sanchez-Martin et al. 2015). The study of metabolic signatures as markers for model predictors of traits that would otherwise be cost or duration prohibitive in field studies, is another important emerging research area (Steinfath et al. 2010, Xu et al. 2016). Mass spectrometry is ideal for measuring physiological response of primary and secondary plant metabolites. This is because they are detectable at low limits and are suitable for classing out compounds. In addition, non-targeted metabolomics, using GC-MS, can allow for a shotgun approach to detect the complete set of compounds without previous knowledge of the compounds involved in the abiotic stress response (Heuberger et al. 2014). The use of GC-MS has long been established for qualitative and quantitative understanding of the cuticle (Audisio et al. 1987).

CHAPTER 3

IMPACT OF CHILLING PRE-TREATMENT AND GENOTYPE ON SUBSEQUENT CORN LEAF FREEZING CHARACTERISTICS

3.1 Introduction

A plants' ability to withstand chilling and frost damage will dictate the landscapes in which production can occur. The continuation of global warming is predicted to increase chilling and frost injury due to premature growth followed by subsequent frost (Cannell and Smith 1986, Inouye 2000, Gu et al. 2008). As the climate continues to change, it is significant to note that frost injury has been for the last 30 years, and continues to be, one of the key factors limiting production (Lindow 1983). A study conducted by the Food and Agriculture Organization, (Snyder and De Melo-Abreu 2005) found that frost damage in the USA has caused more monetary losses than any other abiotic stressors. In corn, chilling injury is an ongoing constraint for global production (Gao et al. 2009, Guan et al. 2015). Cooler climates and early fall frosts are the primary obstacles preventing widespread production of corn in the Canadian prairies, despite the availability of arable land.

Corn is considered to be sensitive to cold (Chichester 1979, Jian et al. 2004, Food and Agriculture Organization of the United Nations 2013) and is generally known to be both chilling and frost sensitive. Chilling injury in corn can occur at warm non-freezing conditions at temperatures below 12°C (Stamp 1984). The main difference between chilling injury and frost injury is the presence or absence of ice. Chilling injury occurs in sensitive crops at low temperatures in the absence of ice nucleation and frost injury occurs when ice is formed. In frost sensitive plants, the avoidance of freezing is the main mechanism of survival under sub-zero conditions (Sakai and Larcher 1987).

While there is increased interest to move the corn belt northward, the limiting factor of early fall frost is a major constraint. Frost is normally preceded by chilling temperatures in fall. However, to our knowledge, no one has yet investigated the genotypic or environmental influence of the preceding temperatures on subsequent frost

avoidance. The 30 year average temperature in Saskatoon, SK for the 10 days preceding the first fall frost is 18/6°C day/night (Environment and Climate Change Canada 1981-2010). To evaluate the degree of sensitivity in corn and its potential for avoiding freezing, cycles of a chilling pre-treatment on freezing avoidance were assessed (Figure 3.2) using in-situ whole specimen imaging.

Thermal imaging is a relatively high-throughput technique to accurately and quickly resolve freezing events on a mature plant system as a measure of lethal ice nucleation temperature. Freezing point measurement can act as a powerful imaging technique to measure the latent heat of fusion released during freezing to determine the temperature at which freezing occurs (Wisniewski and Fuller 1999).

The relationship between freezing temperature and contact angle, as a measure of hydrophobicity, is well established. Increased hydrophobicity of a surface will delay ice nucleation (Huang et al. 2012). In addition, particle films such as hydrophobic barriers will also delay ice nucleation (Glenn et al. 2001, Wisniewski et al. 2002, Fuller et al. 2003, Sharma et al. 2015).

The cuticle can serve as a hydrophobic barrier to ice propagation in leaves (Wisniewski and Fuller 1999). Hydrophobic surfaces are defined as having a contact angle greater than 90° (Goddard and Hotchkiss 2007). The cuticle is the first line of defense and acts as an interaction site of the plant to the environment (Bird and Gray 2003). It has long been known to be a barrier to both biotic and abiotic stresses including ice crystal formation (Thomas and Barber 1974). Both the physical and biochemical compositional properties of the cuticle are of interest. The cuticle has been identified as an effective physical barrier to ice propagation as well as enabling avoidance of freezing through increased hydrophobicity (Wisniewski and Fuller 1999).

The composition of the cuticle is primarily a combination of cutin and epicuticular waxes. Cutin is composed of a combination of hydroxy, epoxy fatty acids and esterified aliphatic acids (Kolattukudy 1980). The complementary cuticular waxes are long chain and very long chain fatty acids. The purpose of these waxes is to act as a hydrophobic defense barrier. The specific composition of cuticular waxes varies between species (Perera 2005, Albersheim et al. 2010) and environmental conditions

(Baker 1974). Hydrophobicity has been linked to the ability to avoid ice nucleation which is dependent on interface of water to the leaf and the environment.

The purpose of this initial study was to determine if a chilling pre-treatment (at average temperatures typical of the first two weeks of September in Saskatoon, Saskatchewan, Canada) will influence the subsequent temperature of freezing in corn leaves. Our hypothesis is chilling pre-treatment will cause corn genotypes to initiate ice nucleation at cooler temperatures than non-chilled plants due to increased epicuticular hydrophobicity which is genotype-dependent. Our intent is to determine ice nucleation temperatures in mature hybrid grain corn plants using four contrasting chilling resistant lines with cold treatments (chilling pre-treated; non-chilled).

3.1.1 Ice Nucleation Sub-hypothesis

Chilling pre-treatment will cause corn genotypes to initiate ice nucleation at cooler temperatures than non-chilled plants.

Objective (Freezing Temperature): To determine the ice nucleation temperature in mature hybrid grain corn plants of four contrasting chilling resistant lines in chilling pre-treated and non-chilled plants.

Objective (Hydrophobicity): To determine if differences in ice nucleation temperatures in mature corn plants are related to epicuticular hydrophobicity.

3.2 Material and Methods

3.2.1 Plant Material

Four genotypes of hybrid (256, 675, 884, 959) (DuPont Pioneer Johnston, Iowa, USA) *Zea mays* sub sp. *mays* (grain corn) were used in these experiments. The genotypes were from older breeding material of interest to the company for chilling and frost related characteristic evaluation.

3.2.2 Establishment of Corn Plants

The plants were grown in the A3 Agriculture Greenhouse (45 Innovation Boulevard, University of Saskatchewan, Saskatoon, SK., Canada) at 28°C/22°C

(day/night) under 16-h photoperiod (average PhaR 154 $\mu\text{moles/m}^2$). Four presoaked corn seeds per 10 cm^2 pot were planted at a depth of 3 cm. SM#4 Mix (Sunshine Mix No. 4, Sungro Horticulture Canada Limited) was the potting media used. During the V2 growth stage, at approximately 14 days, the seedlings were transplanted into standard 4 liter pots with SM#4. Nutricote 18-6-8, (Floracan, Sarasota, FL, USA), a 100-day slow release fertilizer, was incorporated into the bottom half of the soil at a rate of 3.5kg/m³ at time of transplanting. The 3.5kg/m³ is half rate for a heavy feeding crop and is used to supplement between weekly watered soluble fertilizer application and sustain the crop through chilling periods. Pots were fertilized twice a week during vegetative stages and during reproductive stages fertilizer was applied daily (N: P: K 20:20:20 + micronutrients, @1g/L for 100 ppm of nitrogen).

3.2.3 Chilling Regime

CONDITION 1 ('extreme' chilling treatment): In the initial experiments, corn plants were subjected to more extreme chilling conditions. This was done in a controlled environmental chamber, to simulate harsh fall field conditions under parameters of 10°C/5°C, with a 12-h photoperiod for a period of 10 days.

CONDITION 2 ('mild' chilling treatment): Subsequent experiments exposed mature corn plants to conditions of 18°C/6°C under 12-h photoperiod for 10 days. This parameter was selected to represent the 30-year average of Saskatoon, Saskatchewan environmental conditions during the first two weeks of September. This occurs just prior to the first fall frost (Environment and Climate Change Canada 1981-2010). In all subsequent experiments in this chapter, this treatment is designated as "chilling pre-treatment".

Table 3.1 Chilling regimes for a ten-day period under controlled growth environments

		CONDITION 1	CONDITION 2
		10°C/5°C	18°C/6°C
		‘extreme’	‘mild’
CHILLING TREATMENT			
EXTREME	DAY	10°C	
	NIGHT	5°C	
MILD	DAY		18°C*
	NIGHT		6°C*

* day/night 30 year average for first two weeks of September in Saskatoon, SK.

Lat: 52°10’00.00” N Long: 106°43’00.00” W (Environment and Climate Change Canada 1981-2010)

3.2.4 Thermal Imaging

3.2.4.1 Sample Preparation

To avoid sub-zero ice nucleation temperatures in the soil within the pot, whole plants at anthesis vegetative transition stage (age 7-10 weeks) were protected at the base with a thermal blanket. Appropriate plant staging was used for selection over plant age to account for greenhouse growing conditions over various seasons. This simulated the natural effect of soil to act as a large heat sink and prohibit ice nucleation in the roots. The absence of ice nucleation originating from the soil in the pot was verified through thermal imaging. Plants were allowed to nucleate naturally without the addition of ice nucleating substances.

3.2.4.2 Experimental Design

Three complete experimental repeats were conducted with three replications per experiment (three whole plant specimens per rep) with an additional non-chilled control from each of the four genotypes. Plants were subjected to chilling pre-treatment followed by freezing exposure. The temperature at of ice nucleation was used to determine the effects of chilling pre-treatment and genotype.

3.2.4.3 Thermal Imaging Set Up

The freezing response of the plants was measured using infrared image capture using a FLIR T640BX (Manufactured 2013, FLIR Systems Inc, Wilsonville, Oregon). The camera and samples were set up following the protocols of Wisniewski et al. (2014) on a stationary tripod. The camera was set using a continuous auto adjustment of the temperature span, which corrected as the temperature reduced in the programmable freezing chamber. Visual temperature output was in the form of a false colour heat map (warm colour for warm temperatures; cool colors – cooler temperatures). This camera has 640x480 pixel resolution, and 0.035°C sensitivity.

3.2.4.4 Leaf and Stem Temperature

Temperature measurements during cold exposure were captured at 30-second intervals across the 4 plants in the frame. Each pixel within the image acts as a thermal sensor and measures the specific temperature at that location of the leaf or stem. Resultant temperature readings, as an indicator of latent heat released during freezing was used to determine freezing temperature.

3.2.4.5 Cold Temperature Exposure

Whole plants were exposed to temperature conditions in a programmable controlled environment chamber at a steady ramp from 2°C to -10°C at a rate of -2°C/hr. to the final temperature of -10°C.

3.2.4.6 Thermal Imaging Analysis

Images from the camera were pre-processed using FLIR ThermaCam Researcher PRO 2.8 (FLIR Systems Inc, Wilsonville, Oregon) to extract the temperature spot measurements over time for each spot on the leaf and stem. Freezing point measurement was determined by plotting the plant spot temperature against the chamber reference temperature over time, using the second derivative of the curve to identify the exotherm. The measured exotherm corresponded to the temperature at which the leaf and stem freezing occurred. The two-way analysis of variance (2-way-ANOVA) of the freezing temperatures was conducted for each treatment, with a post hoc Tukey test, using R-Studio.

3.2.4.7 Ice nucleation temperature

The temperature at which ice nucleation was first initiated is indicated by an exotherm, or increase in plant temperature at the time of freezing. Exotherm identification was first observed using a step method. Step method is defined as the temperature instantaneously arriving at the next set point. The temperature change and the freezing event was measured through latent heat released during the initiation, to the next set point of the next cooler temperature (Figure 3.1A). Ice nucleation was allowed to occur naturally without any exogenous nucleators. The exotherm event was extracted through thermal information of random pixels on the stem and leaf between the region of leaf five to leaf seven. The extracted data was analyzed using the second derivative of time with respect to temperature (Figure 3.1 B) on a large body of images (1200 images per freeze cycle). The time which freezing occurred was evaluated using the second derivative of the spot temperature. The freezing event was verified through visual examination of the images and plant recovery. The step method had extensive noise, as it was observed that the chamber temperature would frequently overshoot the chamber set point during this step. The freezing event occurring during the temperature overshoot (instantaneous step) in both chilled and non-chilled genotypes led to no measurable differences of either genotype or treatment.

In subsequent experiments, the ramp method was favored. Ramp method is defined by an increase/decrease in temperature over a period of time at a defined rate. The ramp method was advantageous in these experiments as the temperature change was more gradual and the trend of the chamber temperature and set point were well aligned (Figure 3.1 C). In addition, the noise was greatly reduced leading to clear exotherm identification using the second derivative (Figure 3.1 D).

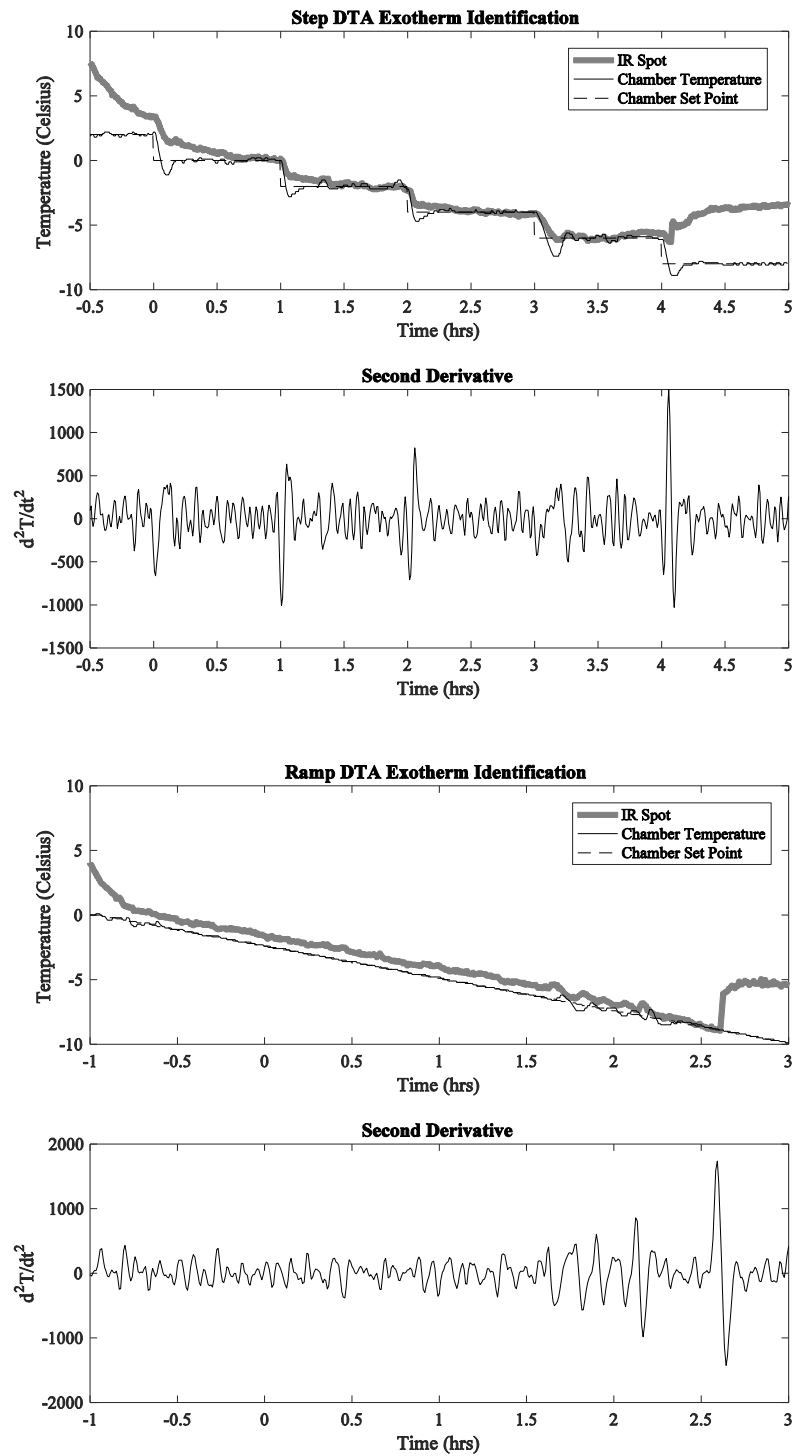


Figure 3.1 Freezing Point Measurements Ramp Compared to Step. (A) Freezing point measurement under -2°C per hour step cold temperature exposure over 5.5 hours. (B) Second derivative of plant temperature with respect to time. (C) Freezing point analysis under continuous ramp of -2°C per hour over 4 hours. (D) Second derivative of plant temperature with respect to time.

3.2.5 Hydrophobicity

3.2.5.1 Sample Preparation for Hydrophobicity

Fresh leaf tissue was excised from collared leaf 5-7 within 30 cm of the tip of the leaf. A leaf collar is the white band at the base of the leaf that protrudes away from the stem. Leaf sampling position was 30cm from the leaf tip (Figure 3.2). This location was selected based on thermal imaging demonstrating initial environmental impact of freezing affecting the leaf tip (Pearce and Fuller 2001), as well as large scale commercial reports of chilling and frost damage having occurred in this region (Nielsen and Christmas 2001). Leaf samples approximately 5 cm x 5 cm were mounted flat onto a standard glass slide securing all outer edges with satin transparent tape. The control material used was a sheet (4.76mm x 30.5cm x 30.5cm) of polytetrafluoroethylene (PTFE) (WD Plastics Ltd. Saskatoon, SK.) which has known hydrophobic properties (ASTM Compass C813 2014). Plants were sampled immediately following chilling treatment.

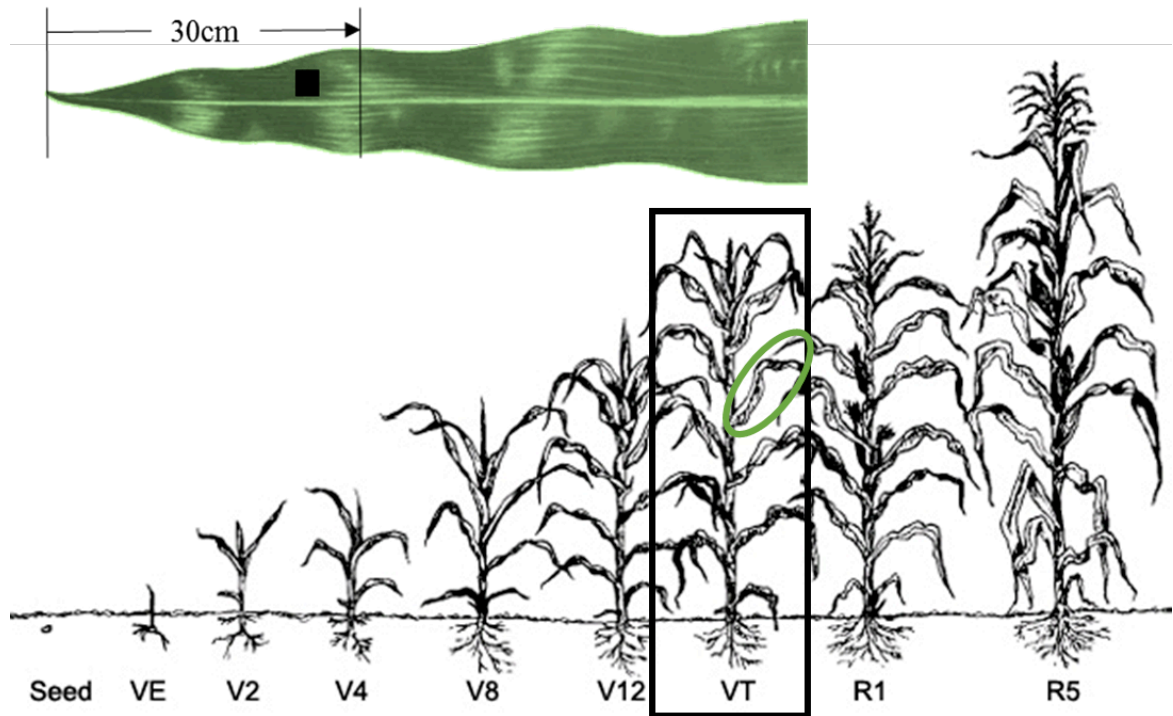


Figure 3.2 Sampling of mature corn at stage VT and collared leaf (V6) identified (circled)
 Modified from: <https://extension.entm.purdue.edu/fieldcropsipm/corn-stages.php>.
 Localized Sampling location within 30cm of collared leaf V6. Modified from:
<https://www.pioneer.com/home/site/us/agronomy/library>.

Table 3.2 Hybrid corn plant material used for hydrophobicity measurements

GENOTYPE	SENSITIVITY	TREATMENT	PLANTS PER TREATMENT	EXPT REPEATS
256	S	Non-chilled	3	3
675				
884	R			
959				
256	S	Chilled		
675				
884	R			
959				

3.2.5.2 Leaf Surface Hydrophobicity Measurements

The contact angle of chilled and non-chilled leaves was evaluated for hydrophobicity (Figure 3.2) using a standard contact angle measurement technique (ASTM Compass C813 2014) to determine the leaf surface interaction with water. The contact angle was measured of instilled metered droplets (3-5uL) of distilled water from a syringe mounted directly perpendicularly above the surface of the leaf. Topographical images of each droplet were collected using a tripod mounted iPhone 5S with a focal length of 4.10mm. Images were analyzed using ImageJ protractor function to determine the contact angle (Figure 3.3) the image describes the hydrophobic assumptions where a surface with a contact angle greater than 90° is considered hydrophobic and surfaces with a smaller contact angle are more hydrophilic.

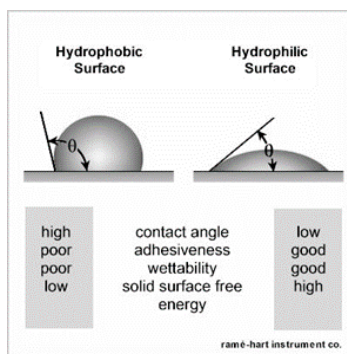


Figure 3.3 Classification and characteristics of hydrophobic surfaces

Source: <http://www.ramehart.com/contactangle.htm>

3.3 Results

3.3.1 Leaf and Stem Ice Nucleation Temperature

The comparison of leaf and stem spot temperatures indicated no difference between the stem and leaf freezing temperatures in either chilled or non-chilled samples. Following this observation measurements of leaf and stem spot temperature were amalgamated under ‘mild’ (18°C/6°C Condition 2) chilling conditions (Figure 3.4). The freezing event occurred rapidly throughout the whole plant in both chilling treated and non-chilled samples. This was also visually observed in the images (Figures 3.6 and Figure 3.7). Reported results were additive means for the sum total of the plant including both leaf and stem spots.

3.3.2 Genotype Effect on Ice Nucleation Temperature

Genotype 959 had the lowest freezing temperature and was significantly different from the three other genotypes (Figure 3.5) under ‘mild’ chilling conditions and was best able to avoid freezing. Genotypes 256, 675 and 884 were not significantly different. Genotypes 675 and 959 were the least influenced by chilling pre-treatment with a range of $\pm 1^{\circ}\text{C}$. In contrast, genotypes 256 and 884 varied about the median by $\pm 2^{\circ}\text{C}$ with a response twice as strong to the chilling pre-treatment.

3.3.3 ‘Extreme’ Chilling Condition Freezing Point Depression

There were limited measurable differences among genotypes or treatments under ‘extreme’ chilling treatment (10°C/5°C Condition 1). ‘Extreme’ chilling with step treatment (Figure 3.1 A) resulted in an artefact due to the overshoot of the chamber temperature. The chamber temperature would overshoot the temperature rapidly cooling the actual chamber temperature below to the set point which artificially caused nucleation in the plant during the 2°C step.

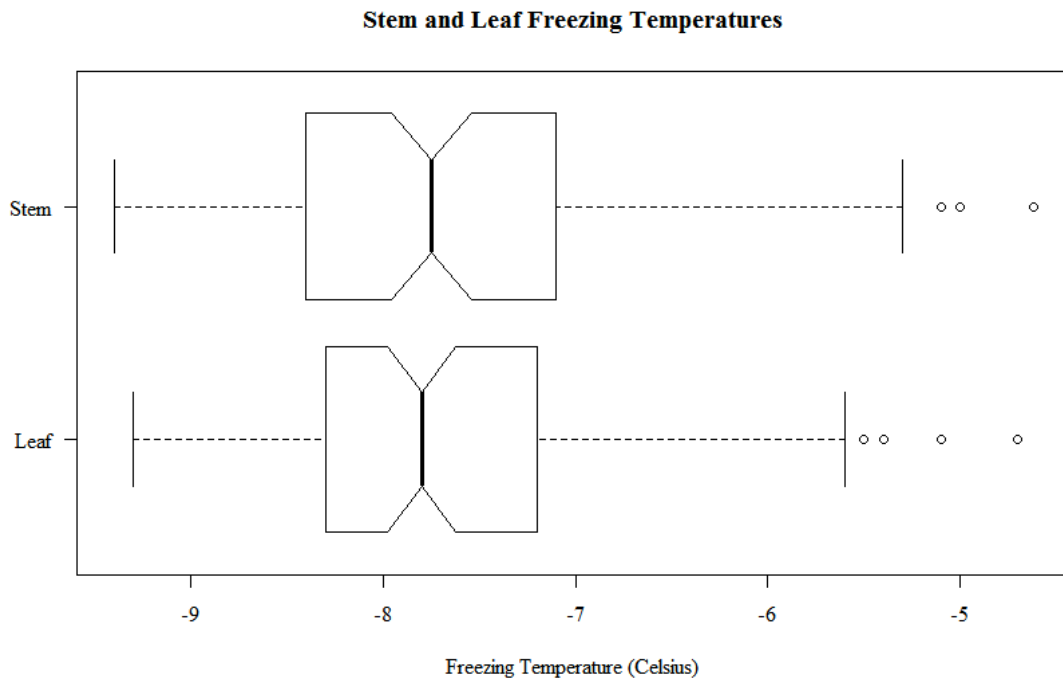


Figure 3.4 Box plot of stem and leaf freezing temperatures . Box Plot comparing leaf and stem freezing temperatures measured through representative selected spots of thermal images displaying exotherm of four corn genotypes Condition 2 ‘Mild’ treatment (256, 675, 884, 959). Six replicates, $F_{0.05}(1,189)=0.25$, $p=0.6177$, o outliers).

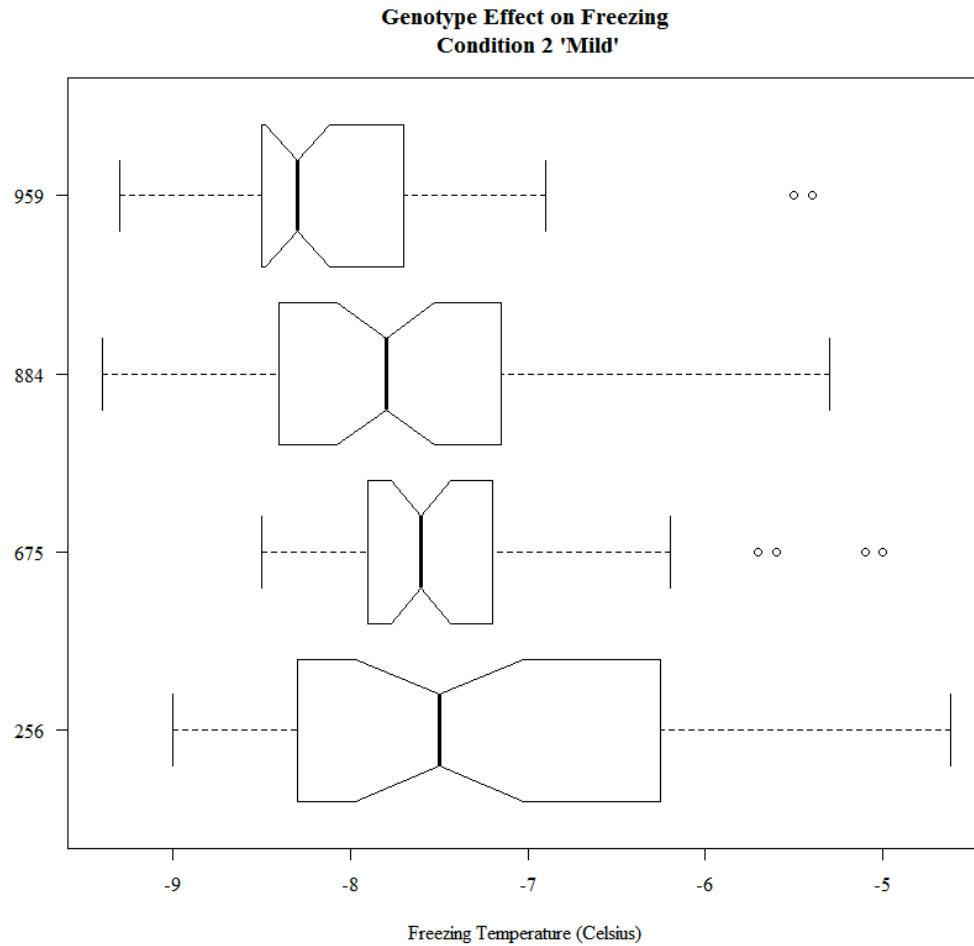


Figure 3.5 Box plot comparing temperature of ice nucleation across genotypes (959, 884, 675 and 256) after exposure to 10 days of 'mild' 18/6°C chilling treatment (Table 3.1 Condition 2) measured through exotherm identification based on thermal images over time. Three complete experimental repeats were conducted with three replications per experiment (three whole plant specimens per rep), $F_{0.05}(3,187) = 6.54$, $p = 0.0003$, o (outliers).

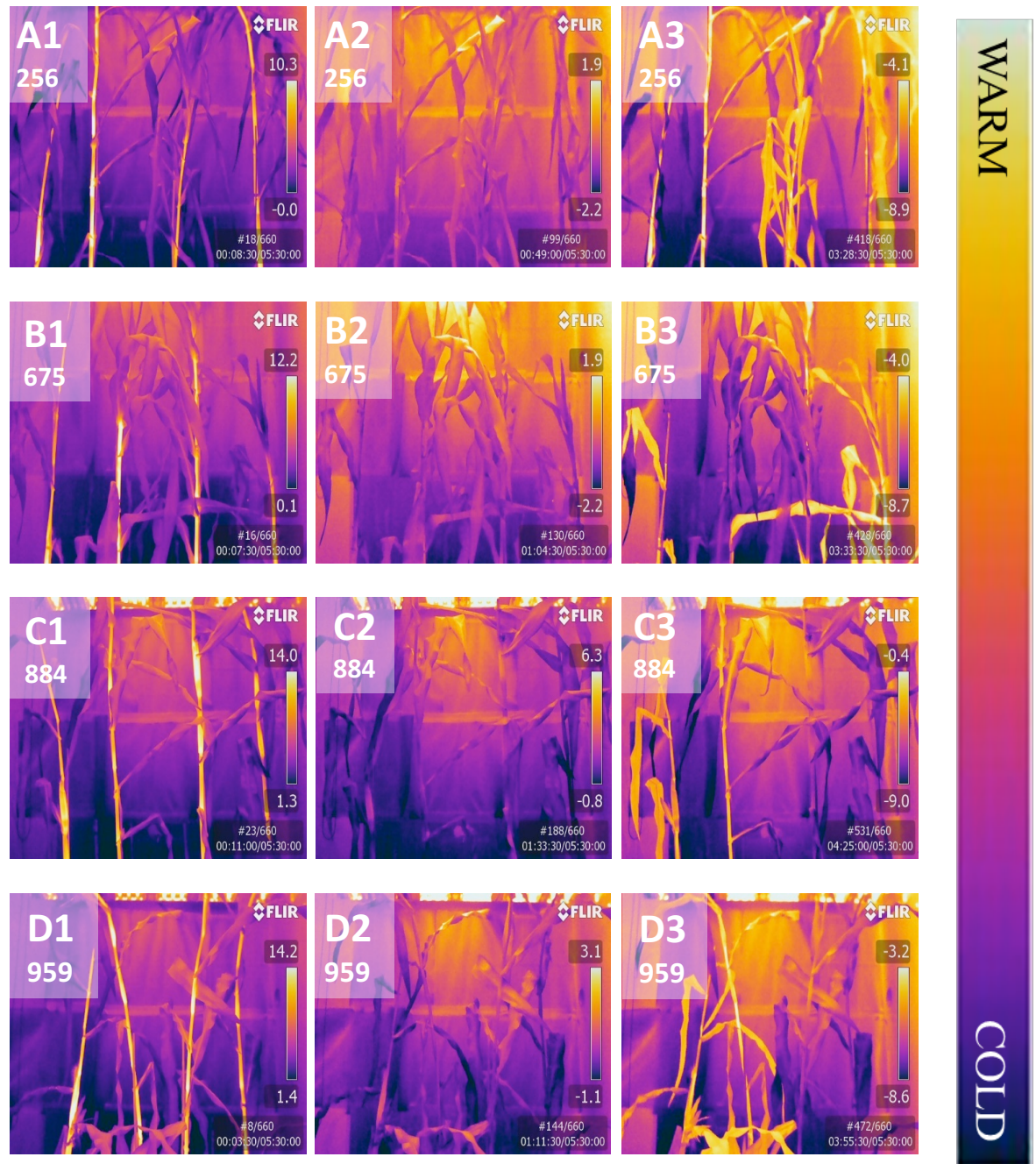


Figure 3.6 Thermal images of ice nucleation after a 10-day exposure of non-chilled conditions (28/22°C). (A1) 256 start (A2) 256 at air-plant temperature equilibrium (A3) 256 freezing. (B1) 675 start (B2) 675 at air-plant temperature equilibrium (B3) 675 freezing. (C1) 884 start (C2) 884 at air-plant temperature equilibrium (C3) 884 freezing. (D1) 959 start (D2) 959 at air-plant temperature equilibrium (D3) 959 freezing.

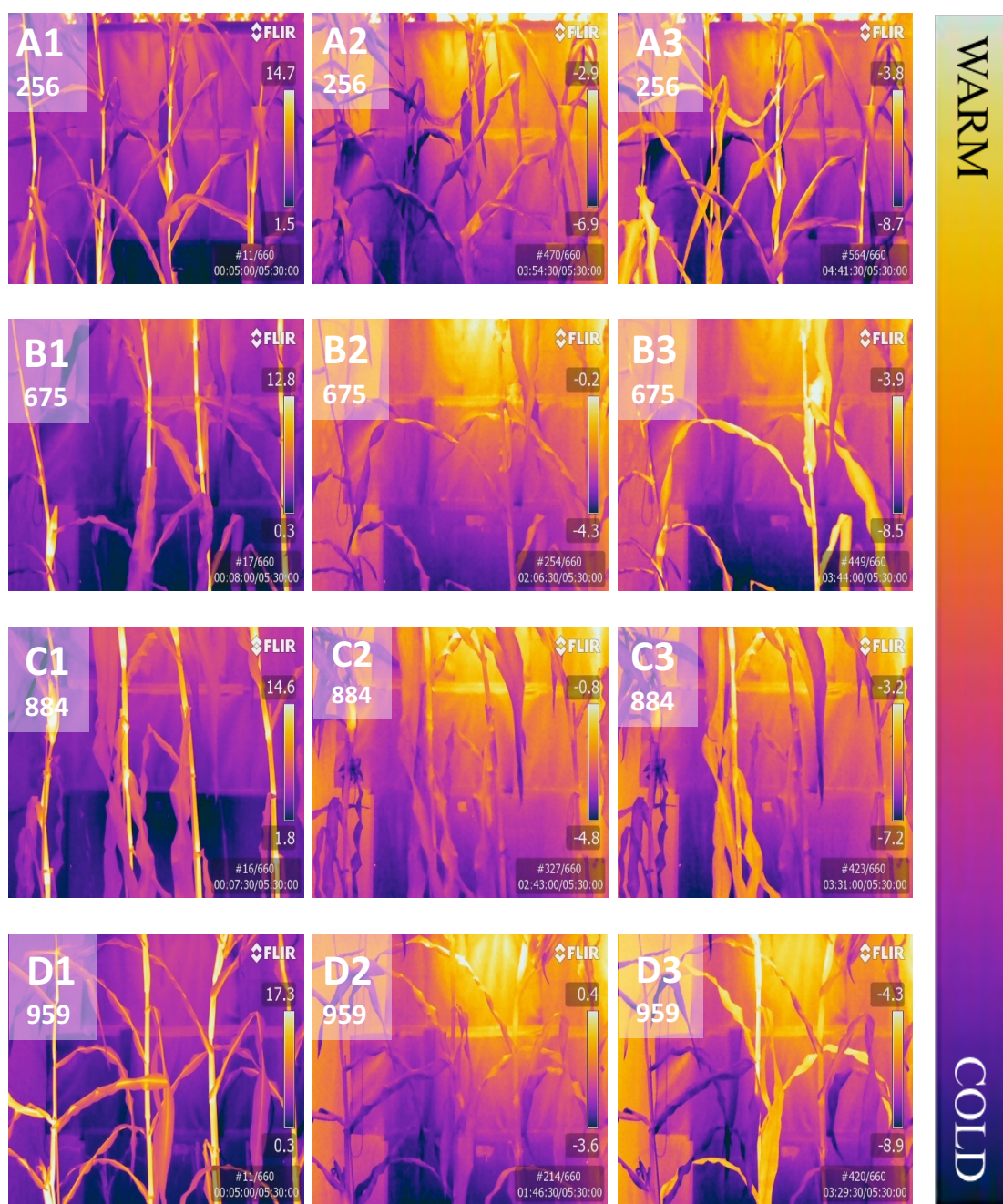


Figure 3.7 Thermal images of ice nucleation after a 10-day exposure to ‘mild’-chilling pre-treatment (18/6°C) (Table 3.1 for conditions). (A1) 256 start (A2) 256 at air-plant temperature equilibrium (A3) 256 freezing. (B1) 675 start (B2) 675 at air-plant temperature equilibrium (B3) 675 freezing. (C1) 884 start (C2) 884 at air-plant temperature equilibrium (C3) 884 freezing. (D1) 959 start (D2) 959 at air-plant temperature equilibrium (D3) 959 freezing.

3.3.4 ‘Mild’ Chilling Condition Freezing Point Depression

Using the FLIR T640BX thermal imager to capture visual and thermal images at 30 second intervals, the temperature at which the latent heat of fusion was measured was captured. Latent heat was used as an ice nucleation indicator and was measured over the course of freezing temperature exposure from +2 to -10°C. The freezing point in chilling pre-treated samples occurred at warmer temperatures than their non-chilled controls (Figure 3.8). This suggests pre-exposure to even very ‘mild’ chilling conditions (18°C/6°C) can increase the temperature of ice nucleation. There were no visible signs (Appendix D) of leaf chilling injury following ten days chilling pre-treatment under ‘mild’ chilling conditions. On average, non-chilled plants induced whole plant freezing at a significantly cooler temperature of -7.84°C compared with chilling treated plants at -7.24°C. The temperature differential indicated there were both treatment and genotypic differences. The treatment effect was present in all samples where warmer freezing temperatures followed exposure to chilling pre-treatment (Figure 3.8). The genotype effect was present in non-chilled samples where genotypes 256 and 675 (generally more sensitive) froze at warmer temperatures than genotypes 884 and 959 (generally more resistant). Post hoc analysis in Table 3.3 indicated that genotype 959 froze at significantly colder temperatures than all other genotypes (Figure 3.8). This was consistent with the results from 3.3.2 Genotype Effect on Ice Nucleation Temperature demonstrating strongest freezing avoidance. This is aligned with results from previous chilling tests under ‘extreme’ chilling conditions (data not shown).

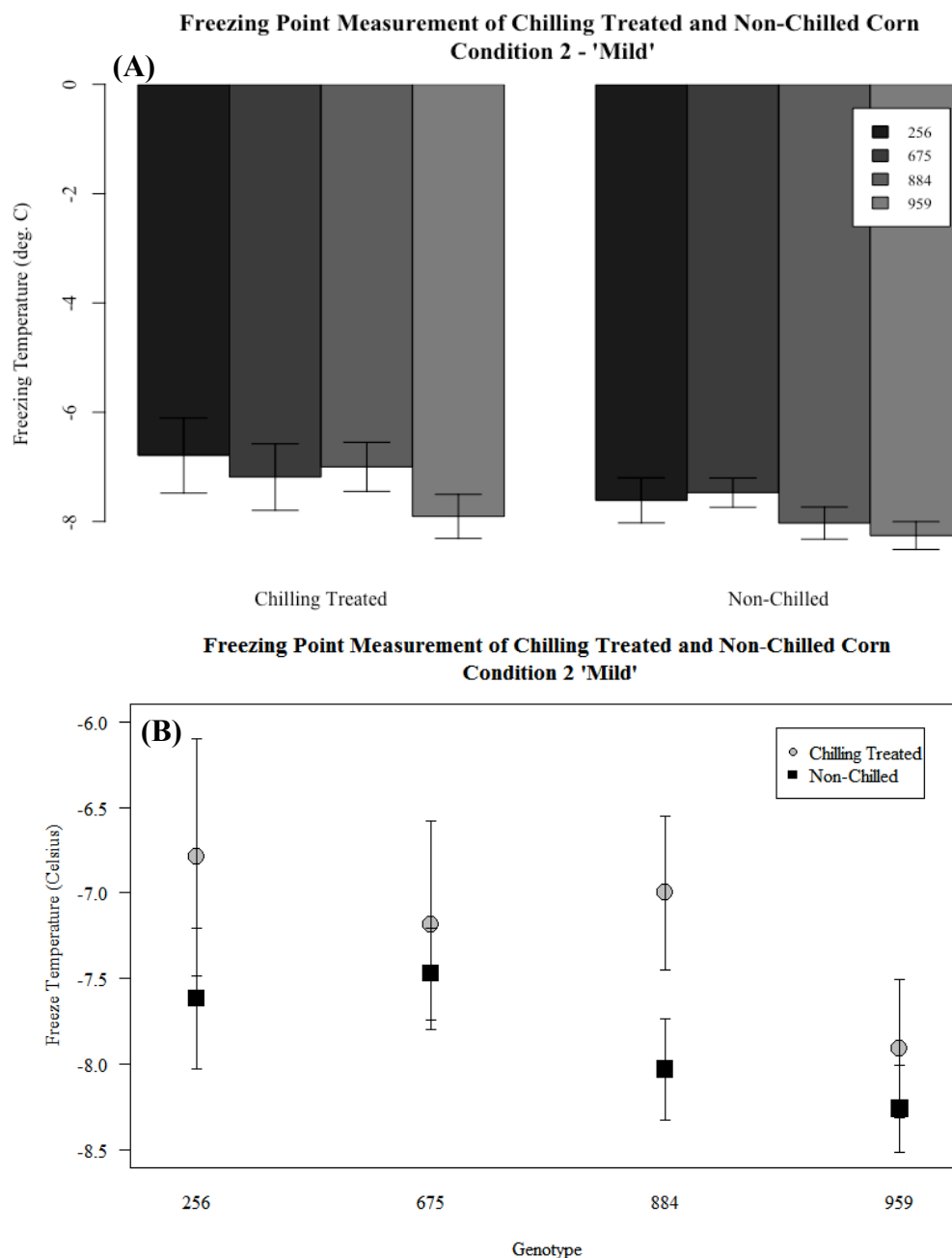


Figure 3.8 Freezing point measurement as a measurement of lethal freezing temperature of mature corn plants (R1-R3) by genotype (256, 675, 884, 959) and treatment (chilling treated, non-chilled) after exposure to 10 days of 'mild' chilling condition (18/6°C); Total $F(1,189) = 16.22$, $p < 0.0005$; NC $F(3,111) = 5.43$, $p = 0.0016$, $\mu = (-7.8478^\circ\text{C})$, $\sigma = 0.86495^\circ\text{C}$; CT $F(3,72) = 3.89$, $p = 0.0124$, $\mu = (-7.2472^\circ\text{C})$, $\sigma = 1.1944^\circ\text{C}$; (A) Barplot demonstrates difference in freezing temperature between genotypes. Error bars denote 95% confidence interval ($P0.05$); (B) Interaction plot illustrates the freezing temperature response for different combinations of factors (genotype and treatment)

Table 3.3 Comparison of Means (HSD Tukey Method) of Freezing Point Measurement of ‘Mild’ Chilling Treatment mature corn by genotype with 95% confidence interval around the lower and upper range.

TUKEY HSD MULTIPLE COMPARISON OF MEANS				
	diff	lwr	upr	p-value
675-256	-0.0668	-0.5880	0.4545	0.9873
884-256	-0.3611	-0.8613	0.1390	0.2437
959-256	-0.8527	-1.3627	-0.3428	0.0001
884-675	-0.2944	-0.8034	0.2146	0.4400
959-675	-0.7860	-1.3046	-0.2673	0.0007
959-884	-0.4916	-0.9890	0.0058	0.0541
NC-CT	-0.6006	-0.8802	-0.3210	<0.0005

3.3.5 Chilling Treatment and Genotypic Influence on Hydrophobicity

Extreme chilling conditions caused a greater shift in hydrophobicity with a median around 80°(extreme) (Figure 3.9) compared with 75° (mild)(Figure 3.10). Exposure to chilling caused a decrease in hydrophobicity in all genotypes (Figures 3.90, 3.10). The main effect of ‘extreme’ chilling treatment was to decrease the contact angle by 30°. However, genotype 675 demonstrated a different main effect with a contact angle reduction of 7.5° following chilling treatment. The more ‘mild’ chilling temperature regime resulted in the same trend as the ‘extreme’ chilling pre-treatment where all genotypes significantly decreased in hydrophobicity following chilling exposure. Plants were measured immediately following chilling treatment.

Under extreme chilling conditions, the main effect of chilling treatment was to reduce the hydrophobicity of corn leaves. Chilling treated plants exhibited a mean contact angle of 74.56° (hydrophilic), while non-chilled plants had a mean contact angle of 96.87° (hydrophobic). (Figures 3.9-3.11). The same trend was also observed under mild chilling conditions. Further investigation showed the genotype modified the effect of chilling response. Under extreme chilling conditions the hydrophobicity of genotype 675 was not modified to the same degree as the remaining genotypes (Figure 3.8). In the main effects plots for hydrophobicity, under both conditions, there was significant interaction of genotypes post chilling treatment (Figures 3.11, 3.12). Under ‘mild’ Condition 2, there was a clear grouping for the resistant and sensitive genotypes which

clustered together. There was no interaction between 256 and 675 indicating the treatment effect was the only significant factor. ‘Mild’ chilling treatment had less effect on reducing hydrophobicity than ‘extreme’ chilling. The main effect of ‘mild’ chilling treatment in sensitive genotypes 256 and 675 was a contact angle reduction of 15°. By contrast in resistant genotypes 884 and 959, the average reduction in contact angle was 7°.

By combining genotypes to evaluate treatment effect under both conditions (Figures 3.13, 3.14), the chilling pre-treatment significantly reduced hydrophobicity, despite a large variation about the mean, representing the contact angles. The differences between chilling treatments of non-chilled (control) samples between 96.87°(extreme) and 86.69°(mild) could be attributed to different growing cycles, especially natural light quality, in the greenhouse however experimental analysis was significant within each experiment and relative differences are valid.

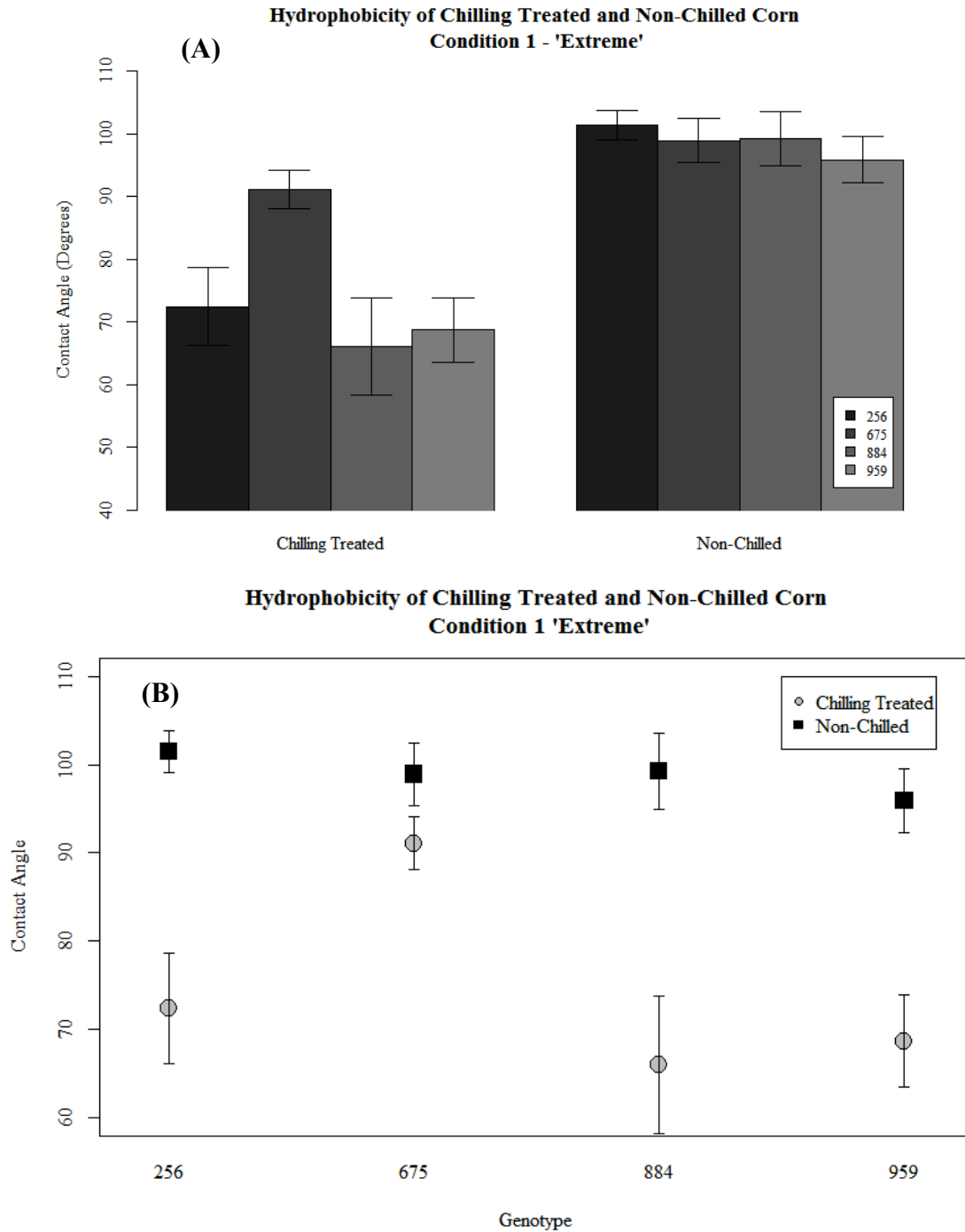


Figure 3.9 Contact angle as a measurement of hydrophobicity of mature corn leaf (V6; adaxial side) by genotype (256, 675, 884, 959) and treatment (chilling treated, non-chilled) after exposure to 10 days of 'extreme' (10/5°C) (Condition 1 Total F0.05 (1,286) =170.97, $p < 0.0005$; NC F0.05 (3,140) =1.72, $p = 0.1649$, $\mu = 96.868^\circ$, $\sigma = 10.514^\circ$; CT F0.05 (3,140) =15.57, $p < 0.0005$, $\mu = 74.556^\circ$, $\sigma = 19.68^\circ$; (A) Barplot demonstrates difference in contact between genotypes. Error bars denote 95% confidence interval (P0.05); (B) Interaction plot illustrates the contact angle response for different combinations of factors (genotype and treatment)

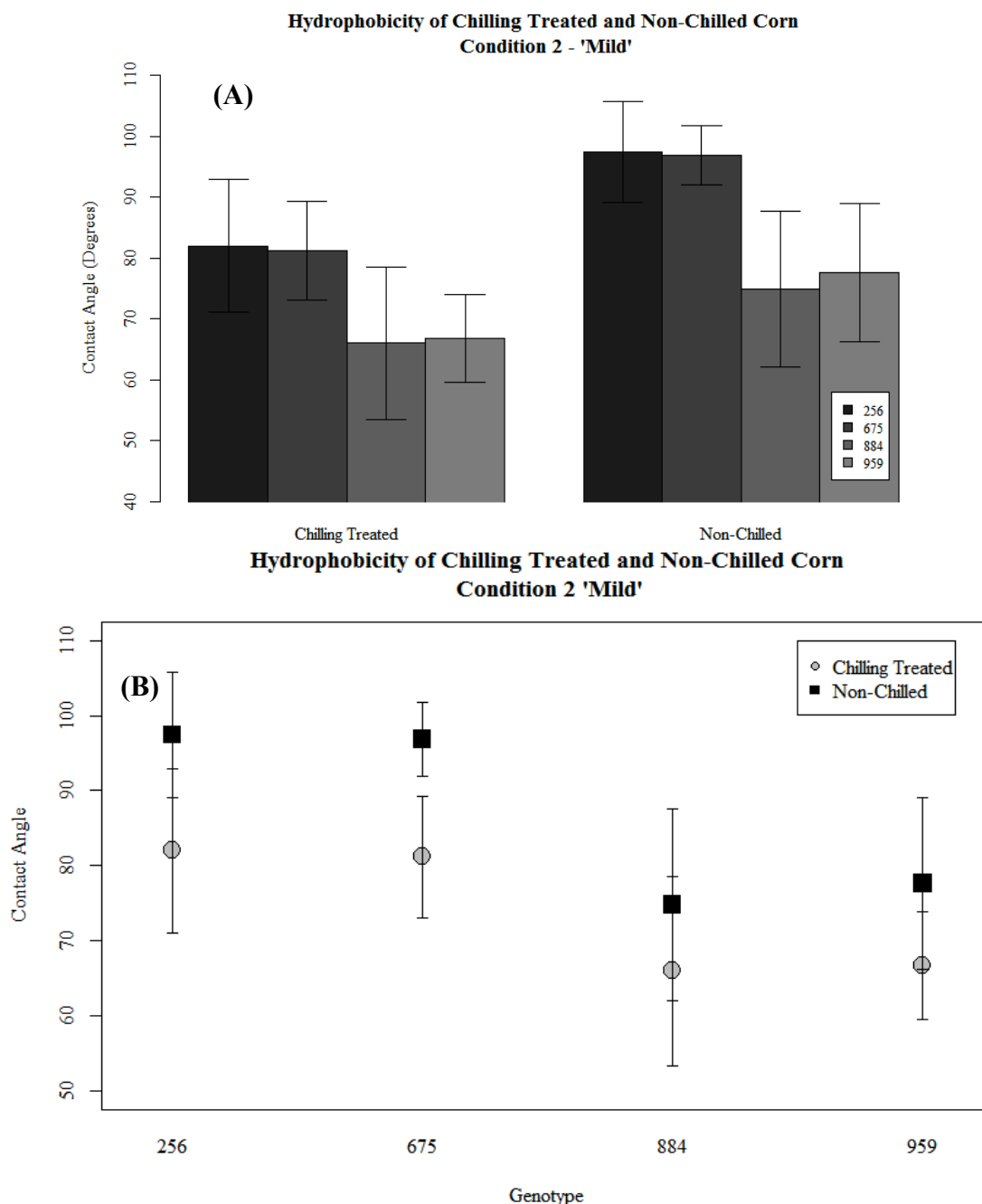


Figure 3.10 Contact angle as a measure of hydrophobicity of mature corn leaf (V6; adaxial side) by genotype (256, 675, 884, 959) and treatment (chilling treated, non-chilled).post exposure to 10 days of 'mild' (18/6°C) (Condition 2). Total $F_{0.05}(1,94) = 12.41$, $p = 0.0007$; NC $F_{0.05}(3,44) = 7.36$, $p = 0.0004$, $\mu = 86.69^\circ$, $\sigma = 18.33^\circ$; CT $F_{0.05}(3,44) = 3.79$, $p = 0.0168$, $\mu = 73.98^\circ$, $\sigma = 16.99^\circ$; **(A)** Barplot demonstrates difference in angle between genotypes. Error bars denote 95% confidence interval ($P_{0.05}$); **(B)** Interaction plot illustrates the angle for different combinations of factors (genotype and treatment)

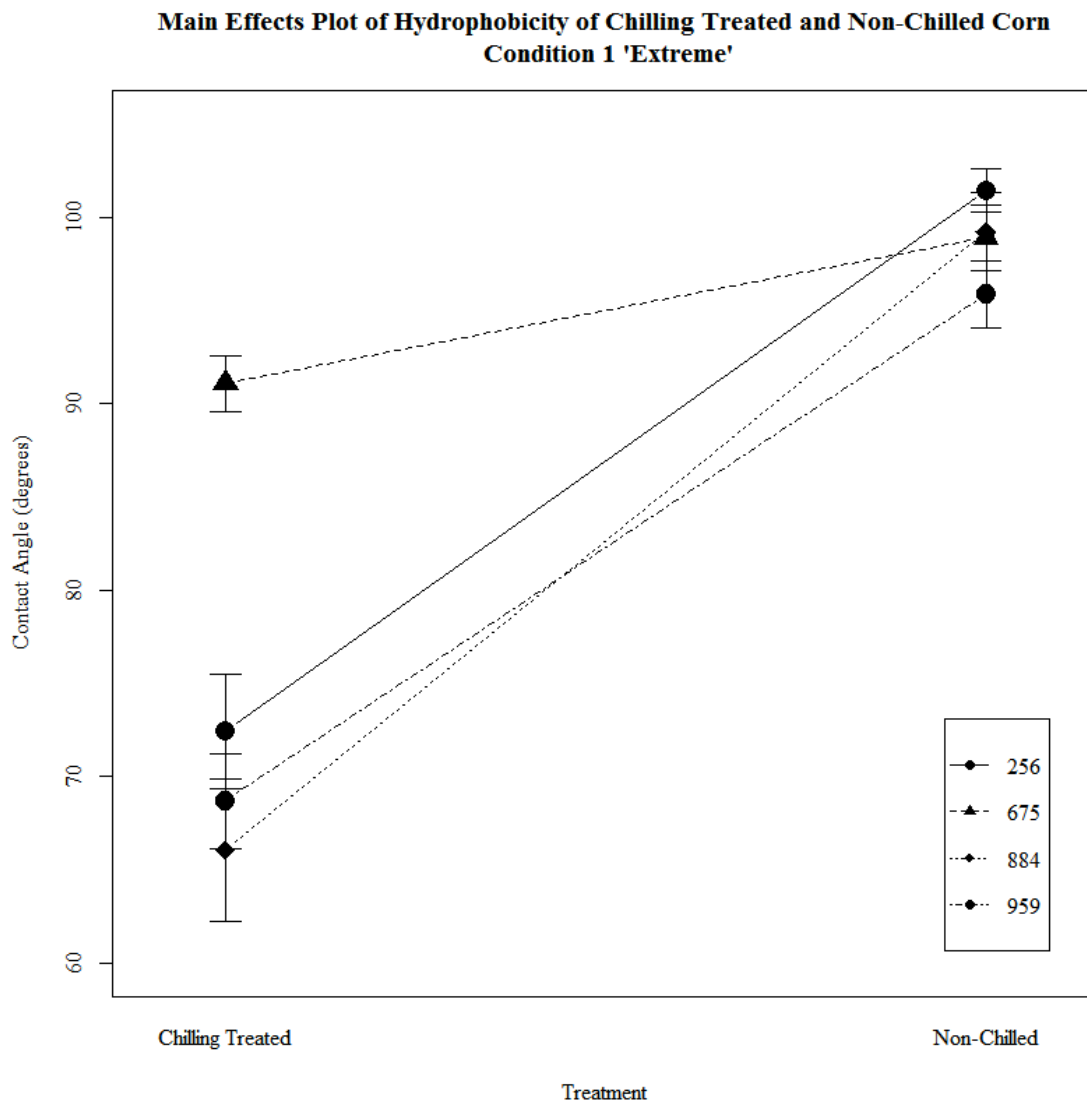


Figure 3.11 Main effect of contact angle as a measurement of hydrophobicity of mature corn leaf (V6; adaxial side) by genotype (256, 675, 884, 959) and treatment (chilling treated, non-chilled) after exposure to 10 days of ‘extreme’ chilling condition (10/5°C) (Condition 1).

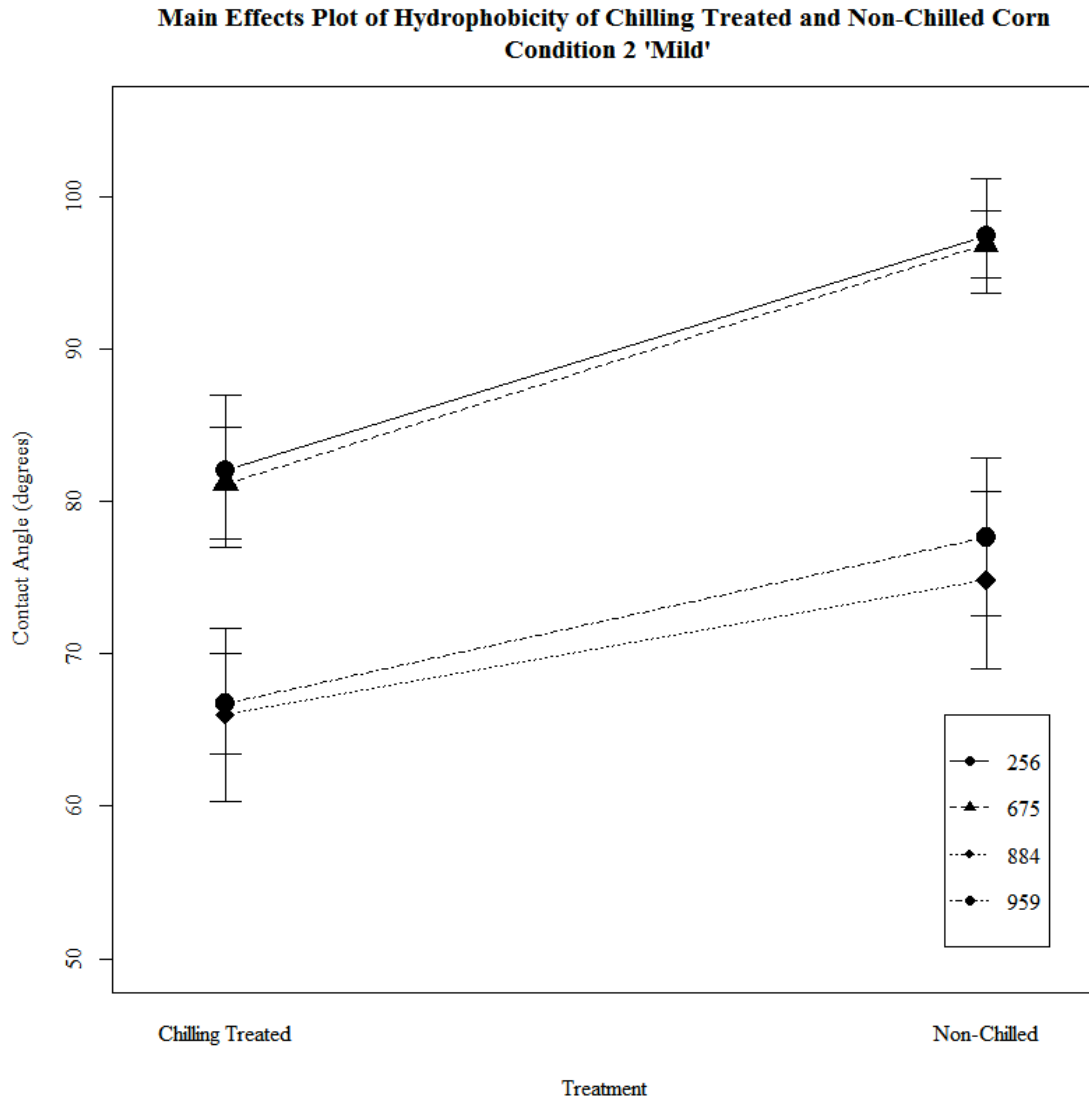


Figure 3.12 Main effect of contact angle as a measurement of hydrophobicity of mature corn leaf.(V6; adaxial side) by genotype (256, 675, 884, 959) and treatment (chilling treated, non-chilled) after exposure to 10 days of ‘mild’ chilling condition (18/6°C) (Condition 2)

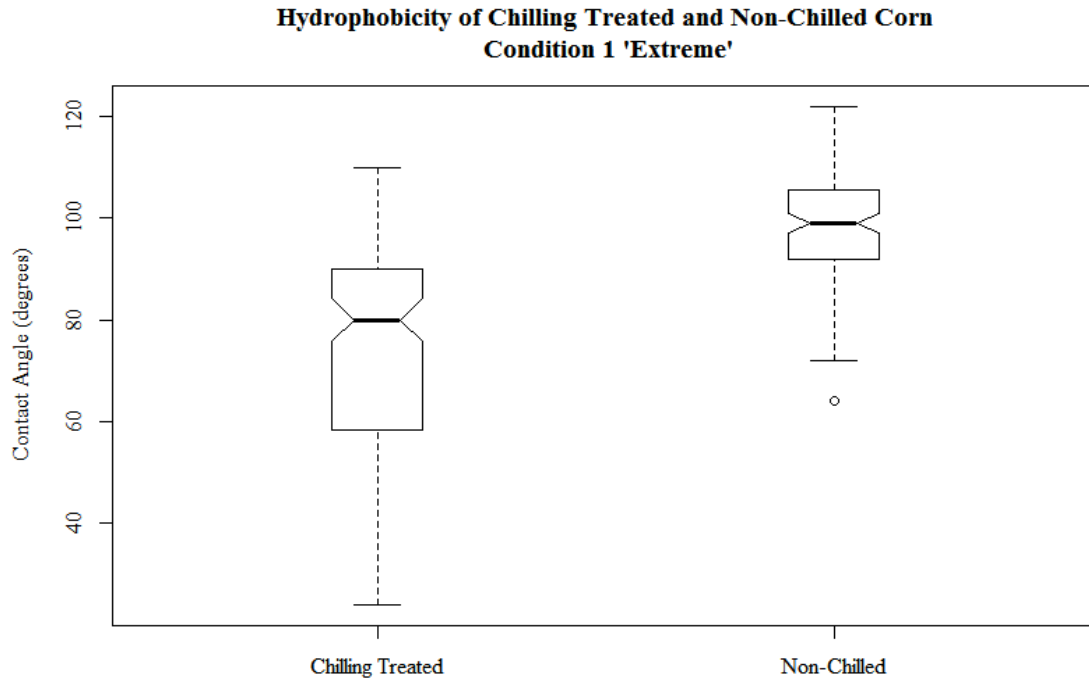


Figure 3.13 Box plot comparing combined genotype (256, 675, 884, 959) information to directly evaluate treatment effect (chilling treated, non-chilled) under 'extreme' chilling treatment Condition 1; Total $F_{0.05}(1,286) = 170.97$, $p < 0.0005$; NC $F_{0.05}(3,140) = 1.72$, $p = 0.1649$, $\mu = 96.868^\circ$, $\sigma = 10.514^\circ$; CT $F_{0.05}(3,140) = 15.57$, $p < 0.0005$, $\mu = 74.556^\circ$, $\sigma = 19.68^\circ$, o (outlier)

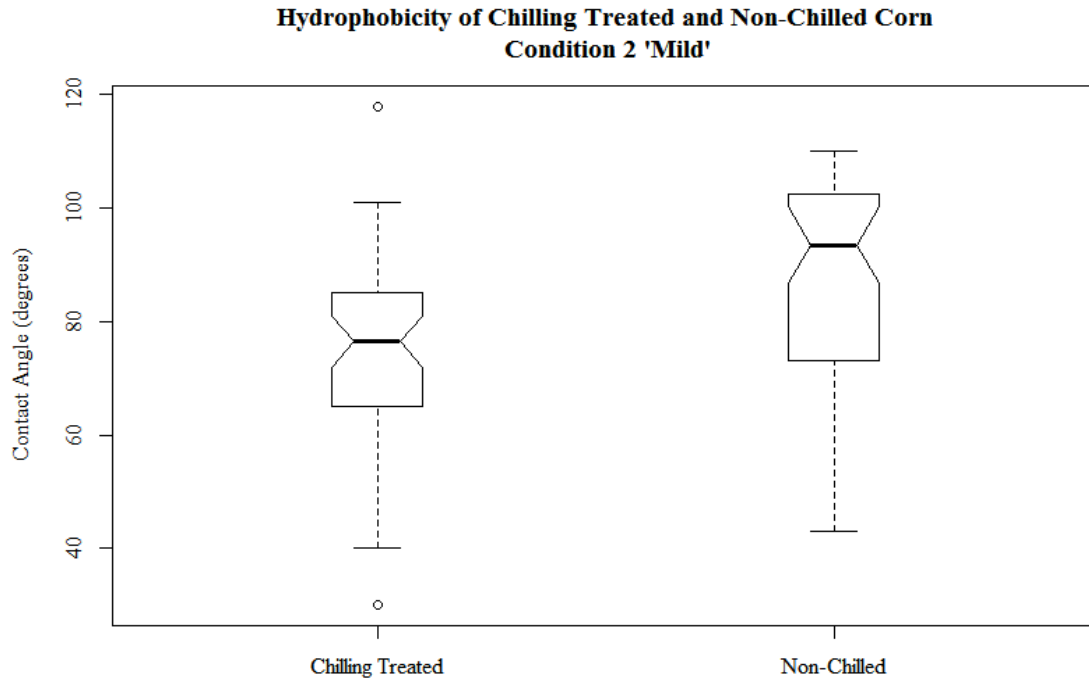


Figure 3.14 Box plot comparing combined genotype (256, 675, 884, 959) information to directly evaluate treatment effect (chilling treated, non-chilled) under 'mild' chilling treatment Condition 2; Total $F_{0.05}(1,94) = 12.41$, $p = 0.0007$; NC $F_{0.05}(3,44) = 7.36$, $p = 0.0004$, $\mu = 86.688^\circ$, $\sigma = 18.333^\circ$; CT $F(3,44) = 3.79$, $p = 0.0168$, $\mu = 73.979^\circ$, $\sigma = 16.985^\circ$, o (outlier)

3.4 Discussion

Long term food security is an area of great importance. Corn represents the single most important global grain crop by tonnage however is currently restricted in its northern production by its cold sensitivity. The first fall frost is typically expected within the first two weeks of September in Saskatoon, Saskatchewan. Once this event occurs it is followed by two to three weeks of subsequent frost free days. Plant survival into these frost-free days allow for additional and critical maturation time for longer season crops such as corn. Plant modifications induced by chilling pre-treatment (simulated pre-freezing temperature fall conditions) are of interest as it represents an opportunity for recognition of critical physiological crop traits involved in freezing avoidance preparation. The impact of chilling pre-treatment prior to first fall frost is not well understood. Our intent to investigate ice nucleation avoidance, and cuticular alterations following chilling pre-treatment, could aid in identification of traits for freezing avoidance enabling expansion of corn into new areas of production.

Although chilling injury has been observed at temperatures below 12°C (Stamp 1984) there is evidence to support that corn seedlings can be successfully chilling-acclimated (Anderson et al. 1994). The findings of this study do not support this conclusion, instead mature corn plants in this study were unable to cold acclimate. This may be attributed to the overall biomass of the plant as one of the primary factors involved in determining the freezing temperature (Ashworth and Kieft 1995) Other examples can be found in works by Kaku (1975), where the group found that in *Pinus* increasing leaf size caused greater variability in freezing temperatures. The group also found that as leaves matured in *Buxus* there was a decreasing range in freezing temperatures (Kaku 1975). Studies that used thermal imaging and evaluating freezing processes to develop new understanding have also identified plant size, specifically the total surface area and plant weight, as being a modifier of ice nucleation temperature (Workmaster et al. 1999, Carter et al. 2001, Pearce and Fuller 2001, Wisniewski et al. 2002). Larger masses of water can buffer temperature changes over longer periods of time. Temperature directly affects biological processes and metabolic rates and these

process are shown to be a function of size (Gillooly et al. 2001). In *Buxus*, it was found that ice nucleator quality was important to leaf maturity and following maturity quantity of ice nucleators drove freezing temperature (Kaku 1971). Another reasonable explanation that the hybrid grain corn was unable to acclimate may be related to age. Larcher (2003) found that as plants age they become more susceptible to abiotic stress caused by the reduction in speed of metabolic processes. Wax degradation indicators have been linked to a reduction in the intensity to the methylene groups of the asymmetrical and symmetrical groups (Chefetz 2007) which we observed in all field produced genotypes over time. Specific to maize, the transition between juvenile and adult waxes has been shown to occur very rapidly compared with other cereals having a much more gradual transition to distinct adult waxes (Bianchi et al. 1985, Moose and Sisco 1994). This rapid change to adult waxes represents a composition with less alcohol and aldehydes and an increase in esters and alkanes (Avato et al. 1990). These results align with our GC-MS findings preferentially synthesizing these increasingly hydrophobic longer chain fatty acids (VLCFA).

The reduction in hydrophobicity following chilling pre-treatment corresponds with the freezing results indicating a reduced ability to withstand cold. It has been widely demonstrated that higher hydrophobicity should better avoid ice nucleation (Wisniewski and Fuller 1999, Workmaster et al. 1999, Wisniewski et al. 2002, Sharma et al. 2015). These previous works support our findings where a link between ability to withstand freezing and reduced hydrophobicity was established. The effects of chilling pre-treatment, however, remain relatively unknown. The link between hydrophobicity and freezing is important because it allows us to define and localize the changes to specific hydrophobic compounds found on the adaxial surface of the leaf. The hydrophobic biochemical compounds of cuticular wax have been well established (Chibnall et al. 1934, Kolattukudy and Walton 1973) and are comprised primarily of aliphatic compounds including: alcohols, fatty acids and alkanes (Koch and Ensikat 2008).

In response to our sub-hypothesis that chilling pre-treatment will cause corn genotypes to initiate ice nucleation at cooler temperatures than non-chilled plants, we reject the hypothesis and conclude that chilling pre-treatment negatively modifies plant ability to avoid ice nucleation.

The future directions of this study will be to continue to investigate the mechanisms and biocomponents behind hydrophobicity in the cuticular layer and how these characteristics link to ice nucleation avoidance. One area of interest would be to conduct the hydrophobicity results under field produced conditions as well as to expand the model into other grain crops of high economic importance which represent diverse responses to frost avoidance. Other directions for hydrophobicity studies could include development of a correlation between freezing temperature and contact angle. This would be best done with genotypically similar material with varying hydrophobicity properties such a waxy and waxless mutants. Primary targets for additional studies will focus on the lipids in the cuticular layer of mature leaves through non-destructive Mid-infrared light attenuated total internal reflectance Fourier transform infrared spectroscopy (ATR-FTIR) and gas chromatography mass spectrometry (GC-MS).

In summary, the establishment of a link between freezing temperature following chilling pre-treatment with a corresponding reduction in hydrophobicity was unexpected and provided good evidence to continue to investigate the cuticular layer as an important barrier to ice nucleation. It appears that chilling pre-treatment has a negative impact to the overall freezing avoidance, and ultimately survival and ability to complete grain filling of mature corn plants. This study has provided insight into the impact of chilling pre-treatment in corn indicating hydrophobicity and the cuticular layer as a meaningful physical trait as a means of advancing frost avoidance for production into new regions.

CHAPTER 4

LIPID COMPOSITIONAL CHANGES IN THE ADAXIAL CUTICLE IN LEAVES OF MATURE CORN

4.1 Introduction

In the previous chapter, thermal imaging and hydrophobicity were used as a first step towards addressing the overall hypothesis that chilling treatment alters cuticular characteristics which are linked to ice nucleation avoidance. The freezing temperature following chilling treatment induced a warmer lethal freezing point and a strong link between freezing time and hydrophobicity was demonstrated. Having established that hydrophobicity is modified by chilling treatment to confer reduced hydrophobicity, this chapter will examine cuticular thickness and specific biochemical modifications to the hydrophobic cuticular layer using confocal laser scanning microscopy (CLSM), attenuated total internal reflectance Fourier transform infrared spectroscopy (ATR-FTIR) and Gas Chromatography Mass Spectrometry (GC-MS).

Globally, cold stress is one of the leading abiotic causes of yield reduction in agriculturally important crops (Kasuga et al. 1999, Lang et al. 2005). Corn is one of the most widely economically important grain crops across the world (Food and Agriculture Organization of the United Nations 2013). It is considered sensitive to chilling and cold stress (Larcher 2003). The contribution of cuticular wax layer to freezing avoidance remains relatively unknown. The cuticle acts as a barrier in protection against abiotic and biotic stresses. To continue to address the issues of climate change and shifts of production landscapes of commercially important crops into previously underutilized regions, it is important to consider the physiological barriers (physical and biochemical) of the plant and how they will interact with the environment. Current models suggest that there will be an increase in widespread frost damage as global warming progresses (Gu et al. 2008). Damage caused by cold stress will also be more prevalent as plants have less insulating snow cover, become de-acclimated, and are forced into new geographies.

To understand the mechanism of cuticular wax modifications following chilling treatment, this study investigated the physical (cuticular thickness) and biochemical (lipid fingerprint spectra and GC-MS lipid quantification) changes to this critical epi-cuticular barrier layer.

Confocal laser scanning microscopy (CLSM) allows for a relatively high throughput, non-destructive means of investigating cuticular thickness (Buda et al. 2009, Nadiminti et al. 2015). The mid-infrared beamline (Mid-IR) at the Canadian Light Source (CLS) generates specific wavelengths of brilliant synchrotron light optimized for analyzing large biomolecules (May et al. 2007) and can provide significant opportunities for plant based research (Vijayan et al. 2015). The Mid-IR has two endstations, Offline Attenuated Total internal Reflectance (ATR-FTIR), and Focal Plane Array (FPA-FTIR) mapping both of which were used for complementary non-destructive cuticular wax analysis. Utilizing CLSM, ATR-FTIR and GC-MS techniques, this project investigated physical cuticular thickness as well as biochemical, conformation and positional biochemical markers that could lead to improved understanding of freezing avoidance in corn.

The initial portion of this study examined the adaxial cuticular wax surface of *Zea mays* mature leaf specimen using a Global sourced ATR-FTIR broad probe accessory and FPA-FTIR Mapping under chilling treated and non-chilled conditions. The purpose of Mid-IR spectra-based biochemical vibration evaluations following chilling exposure is to identify whether chilling modifies the relative prevalence of the biomolecules in the lipid fingerprint region and determine a cuticular compositional trait linked to chilling treatment.

In addition to the above-mentioned techniques, further lipidomics analysis using GC-MS was conducted to further quantify chilling treatment induced modifications identified from the spectra. Metabolomics research has been used in recent studies to examine whole environment interaction on plants (Steinfath et al. 2010, Heuberger et al. 2014) as well as specific abiotic stress responses (Shi et al. 2014, Ganie et al. 2015, Sanchez-Martin et al. 2015). The study of metabolic signatures as markers for model predictors of traits that would otherwise be cost or duration prohibitive in field studies is another important emerging research area (Viant 2008, Steinfath et al. 2010, Xu et al. 2016).

In this subsequent study, we examine how chilling treatment induces a chemical modification to cuticular wax and identify both classes and specific cuticular wax compounds. We are interested in examining both genotype and treatment effect of chilling in both controlled environment and field produced conditions on cuticular wax composition and relative abundance.

4.1.1 Physical and Biochemical Changes Sub-hypothesis

Chilling treatment will cause hybrid grain corn of four contrasting chilling resistant genotypes to modify cuticular thickness or biochemical composition

Objective (Cuticle thickness): To determine if cuticular thickness is modified by chilling treatment in hybrid grain corn of four contrasting chilling resistant genotypes.

Objective (Cuticle Composition): To determine if a cuticular compositional trait is modified by chilling treatment in hybrid grain corn of four contrasting chilling resistant genotypes.

Objective (Frost Avoidance): To determine if cuticle thickness or composition is linked to frost avoidance in mature hybrid grain corn in four contrasting chilling resistant genotypes.

Objective (Chemical Structure): To determine if differences in lipid profile are present between chilling treated and non-chilled greenhouse and field grown mature hybrid grain corn in contrasting chilling resistant genotypes.

4.2 Materials and Methods

4.2.1 Plant Material

Greenhouse and Field

Four genotypes of hybrid (256, 675, 884, 959) (DuPont Pioneer Johnston, Iowa, USA) *Zea mays* sub sp. *mays* (grain corn) were used in the experiments. The genotypes were from older breeding material of interest to the company for chilling and frost related characteristic evaluation. They were grown in the Agriculture Greenhouses (45 Innovation Boulevard, University of Saskatchewan, Saskatoon, SK., Canada) at 28°C/22°C (day/night) under 16-h photoperiod (average PhaR 154 $\mu\text{moles/m}^2$) as per Chapter 3.

4.2.2 Establishment of Corn Plants

4.2.2.1 Greenhouse

Plants are grown and transplanted as described in 3.2.2 Establishment of Corn Plants

4.2.2.2 Field

Untreated corn seeds were planted into Sutherland Series clay soil prepared by rotovating to a depth of 15cm on June 1, 2017. They were planted using a hand seeder, at approximately 4cm depth with a seed spacing of 10cm. Planting design was in paired rows, 2m in length, with 1m on center spacing between all rows. A solid seeded guard row was planted around the entire plot to normalize the microenvironment and limit edge effects. The experimental design of the field was a completely randomized design with 12 replicates (Figure 4.1). The pH of the soil was 7.8, Electrical Conductivity 1.1 dS/cm and had greater than 700 lbs./a of available Potassium and greater than 500 lbs./a of available Phosphorous. The residual levels of Nitrogen were less than 20 lbs./a in the 0-12" soil profile. 100 lbs./a of Nitrogen was added as 46-0-0 as part of the soil preparation process. The previous crop represented a mix of plots of various field crops.



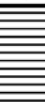





















































		RANGE												
		1	2	3	4					5	6	7	8	
ROW	1					IRRIGATION LINE					2M. Line Length			
	2													
	3													
	4													
	5													
	6													
	7													

Figure 4.1 Field Planting Design at the U of SK Horticulture Field Site; Sutherland Clay series plot using Complete Randomized Design (CRD) with 1 meter on center paired row planting; 12 replicates for each genotype (256, 675, 884 and 959).

4.2.3 Chilling Regime

The two chilling regimes for greenhouse experiments are as described in 3.2.3 Chilling Regime. Field material was exposed to natural outdoor chilling temperatures (Table 4.1).

Table 4.1 Field produced measurement periods, relative chilling comparison reference and Environment Canada weekly average temperatures by week (Government of Canada 2016)

Experiment	Measurement	DATE	Relative Chilling Period	Weekly Average Temperature °C		
				Max	Average	Min
FTIR	F1	2016-08-16	Early	24	18	11
FTIR	F2	2016-08-24	-	22	15	9
FTIR	F3	2016-08-31	Mid	23	16	8
FTIR	F4	2016-09-07	-	19	12	4
FTIR	F5	2016-09-12	Late	21	13	4
FTIR	F6	2016-09-14	Below 0°C event frost but no	17	9	2
GC-MS	-	2016-08-22	Early	22	15	9
GC-MS	-	2016-09-30	Late	18	11	4
CLSM	-	2016-08-03	Early	25	19	13
CLSM	-	2016-09-12	Late	21	13	4

4.2.4 Sample Preparation for CLSM

Fresh leaf samples of mature corn at the reproductive growth VT stage with sampling within 30cm of the tip (Figure 3.2) of collared leaf V6 (approximately 1cm x 3cm) were mounted adaxial side down onto FisherBrand 12-545J cover glass (Thermo Fisher Scientific, Waltham, MA, USA) modified to 55mm length and secured on all sides with clear satin tape. Leaf sampling position was 30cm from the tip and was selected based on thermal imaging demonstrating initial environmental impact of freezing affecting leaf tip (Pearce and Fuller 2001), as well as large scale commercial reports of chilling and frost damage having occurred in this region (Nielsen and Christmas 2001).

4.2.5 Leaf Cuticle Thickness using CLSM

Fresh leaf samples from mature corn were mounted on cover glasses and inserted into the TCS SP5 by Leica (Leica Microsystems GmbH, Wetzlar, Germany) CLSM with a 20X air objective (modified from Celler et al. (2016) Methods 3.1.2 [Steps 10, 11 13 and 14]) Confocal Laser Scanner Microscopy was performed. Microscope settings were adjusted to 1089 gain, -0.3

offset, line average of 4, format 1024 X 512, 300 Hz with emission capture 500-545nm of excitation with a 488nm Argon laser set at 25%.

4.2.6 CLSM Experimental Design

Two CLSM experiments were performed: ‘mild’ chilling treated and field produced. The field study was conducted at two time points of mature corn at the reproductive stage (early; 2016-08-03, late; 2016-09-12) with sampling of leaf V6 (adaxial side) to simulate chilling treated and non-chilled conditions, respectively. All four genotypes of contrasting chilling resistance (256, 675, 884, and 959) were evaluated with six biological replicates at each time point.

CLSM was performed on two genotypes (884 and 959) of greenhouse produced hybrid grain corn at the reproductive growth stage with sampling of leaf V6 (adaxial side) using chilling treated and non-chilled samples (‘mild’ 18°C/6°C for 10 days) with six replicates (two technical by three biological). Two resistant types were selected based on results from freezing point depression indicating a varying degree of response within the resistant types to chilling pre-treatment. They were selected with an interest to compare differences within the resistant response for cuticular thickness

4.2.7 CLSM Image Analysis

Three-dimensional views of the z-stack were generated using the orthogonal view function in ImageJ Fiji (Schindelin et al. 2012). Image contrast range was adjusted to greyscale level of 350 to 15000 (16-bit)(Figure 4.2). Two replicates were selected for analysis from a total of six replicates for each sample treatment and ten measurements were taken across each still image in the X and Y direction. Three images of each in the X direction and Y direction were captured for each sample. The total data captured for each treatment by genotype was 180 measurements (two reps by three X-direction by three Y-direction by ten measurements). Each image was preprocessed by using the smooth and sharpen function before making the image binary and zooming to a perspective of 600X to take the ten measurements of cuticle thickness.

4.2.8 ATR-FTIR Sample Preparation

Fresh leaf samples: Mature corn at the reproductive growth VT stage (Figure 3.2) with sampling of collared leaf V6 (adaxial side)(Figure 3.2) was measured with a 3mm ATR probe accessory

(Figure 4.4B). Fresh samples were collected from whole plants within 30cm of the leaf tip, rinsed with distilled water and surface air dried and placed directly into the probe vice holding chamber adaxial face down. Each replicate and treatment was a separate plant of the same age ('mild', field conditions). For field produced samples, each replicate was a separate plant randomly selected from the Complete Randomized Design (CRD) in the field. Fresh leaf samples secured in the ATR probe accessory have been evaluated in attenuated total reflectance spectra collection mode with an average of 512 scans per spot and were normalized using a background scan which was taken of the empty probe with a collection average of 512 scans.

4.2.9 Spectroscopy with ATR-FTIR

The adaxial leaf surfaces were evaluated with non-destructive leaf cuticle surface evaluation using Spectroscopy with Attenuated Total internal Reflection (ATR). The ATR endstation was a Pike MiracIATR with a 45° Ge ATR Crystal equipped with a deuterated-triglycine sulfate (DTGS) detector at room temperature Figure 4.4A. The Pike MiracIATR probe accessory was secured down onto the leaf sample with standard pressure. The infrared light is generated through a globar equipped with a silicon carbide source. Spectra were collected in the range of 800-4000 cm^{-1} with spectral resolution of 4 cm^{-1} .

4.2.13 ATR and FPA-FTIR Analysis

The spectra from both the ATR-FTIR (IFS 66V) and FPA-FTIR (Vertex 70V) were evaluated using OPUS Software (v. 7.0 Pro, Bruker Optics, Ettlingen, Germany) and R-Studio to generate compositional maps to distinguish the compositional contribution of cuticular wax through peak area integration across the lipid fingerprint region. All spectra resultant from ATR-FTIR measurements were ATR corrected and were averaged by genotype by treatment in OPUS. Resultant spectra were preprocessed in Orange (V3.3.10 Open Source) with a rubber band correction with positive peak direction and background action set at subtract. Integrations were performed at CH_3 (region 1), asymmetrical CH_2 (region 2) and symmetrical CH_2 (region 3). Limits of integration regions are defined in section 4.2.14 Spectra CH_2 Regions Defined.

4.2.14 Spectra CH₂ Regions Defined

To measure the integration areas under the curve for lipid quantification, the lipid peak regions were assigned according to the second derivative peak identification for congruity among the experiments (Figure 4.5). The limits of the integration regions were defined as follows (Figure 4.2)

Region 1 (CH₃) was assigned to 2960-3040cm⁻¹,

Region 2 (asymmetrical CH₂ bending) 2910-2960 cm⁻¹ and

Region 3 (symmetrical CH₂ bending) 2840-2880 cm⁻¹

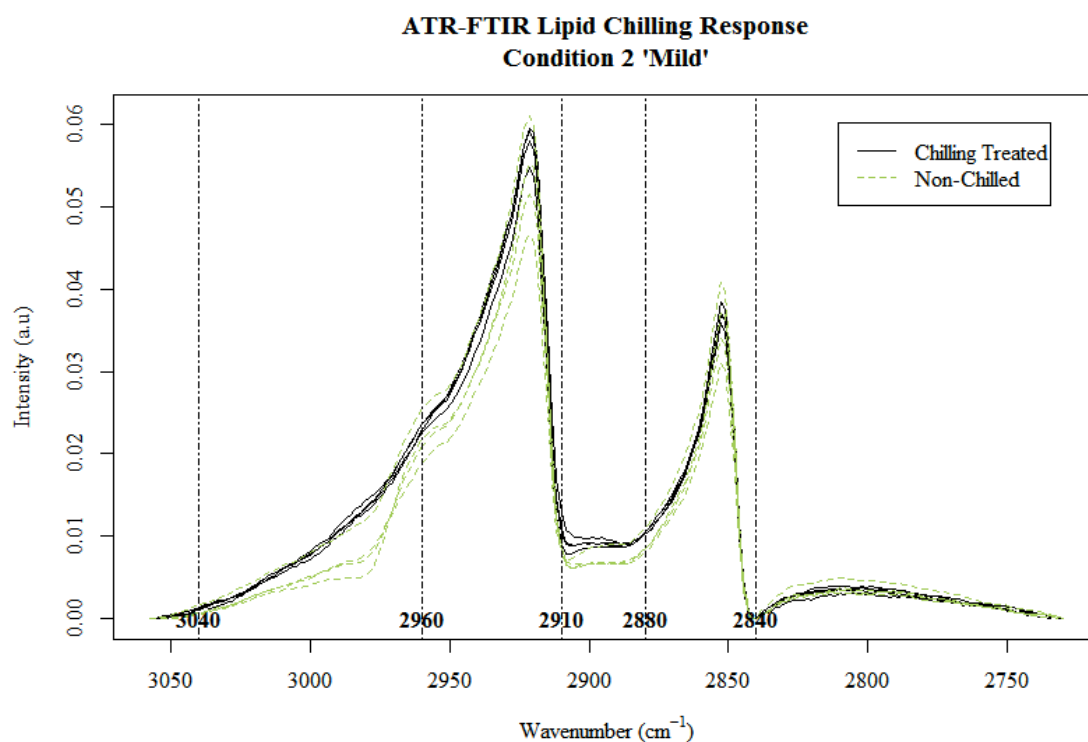


Figure 4.2 Chilling treated and non-chilled average spectra by genotype with band regions (region 1, 2960-3040cm⁻¹; region 2, 2910-2960cm⁻¹; region 3, 2840-2880cm⁻¹) assigned to the CH₂ groups under 'mild' chilling condition of mature corn leaf (V6; adaxial side).

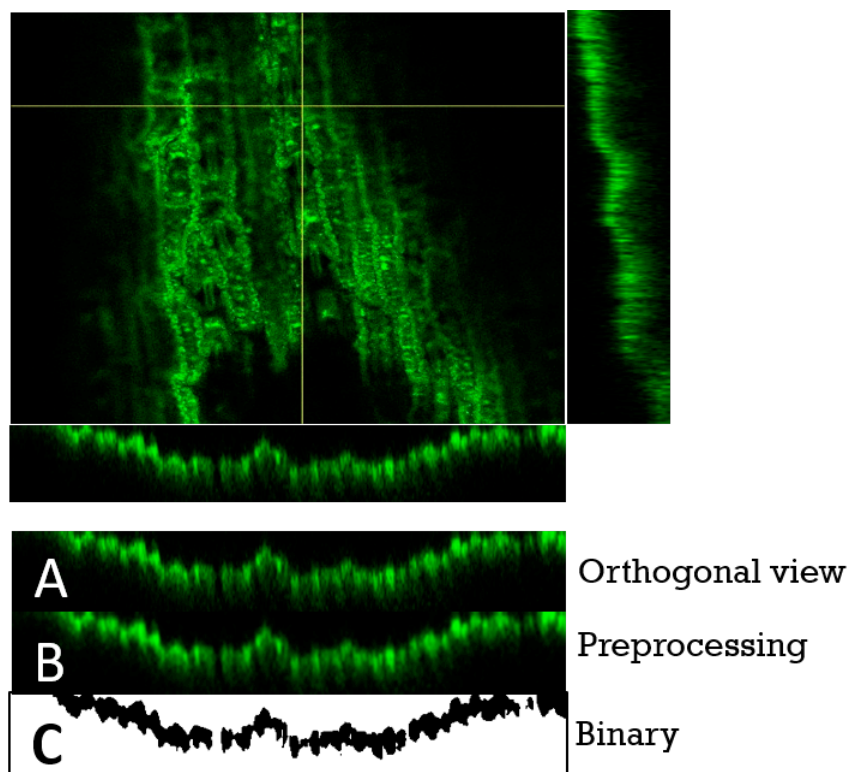


Figure 4.3 Z-stack of autofluorescence of mature corn cuticle using 488nm laser taken with Confocal laser scanning microscope. (A) Example of orthogonal slice in x-direction; (B) Pre-processing of smooth and sharpen in imageJ; (C) Binary representation to remove noise within image for data collection.

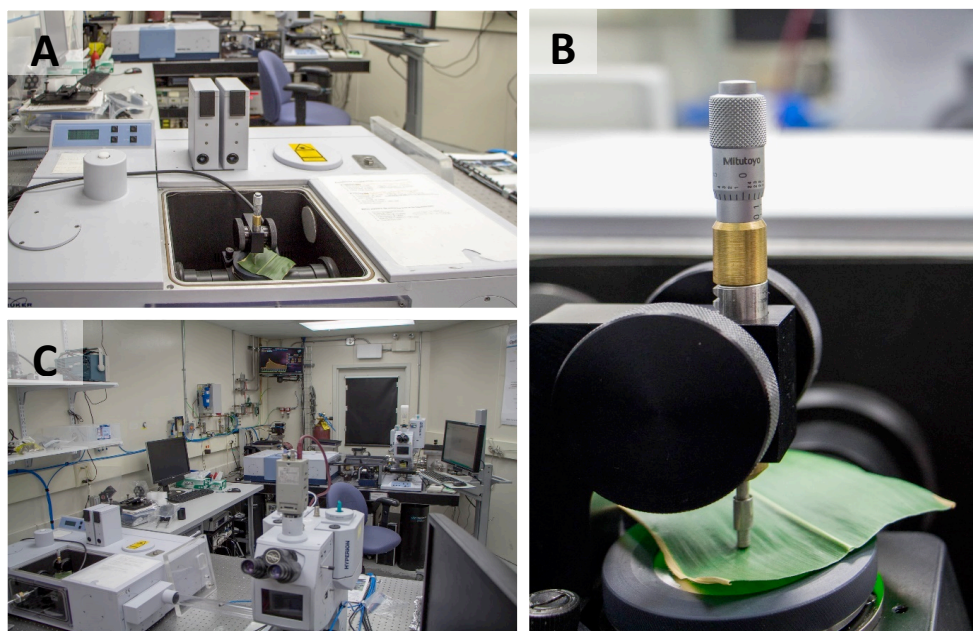


Figure 4.4 Mid-IR Endstation Facility (A) Attenuated Total internal Reflectance (ATR-FTIR) with DTGS Detector at the Canadian Light Source (CLS), Saskatoon SK; (B) Fresh mature corn leaf (V6) sample clamped into 3mm ATR probe accessory (C) Endstations at the CLS Mid Infrared 01B1-1 Beamline

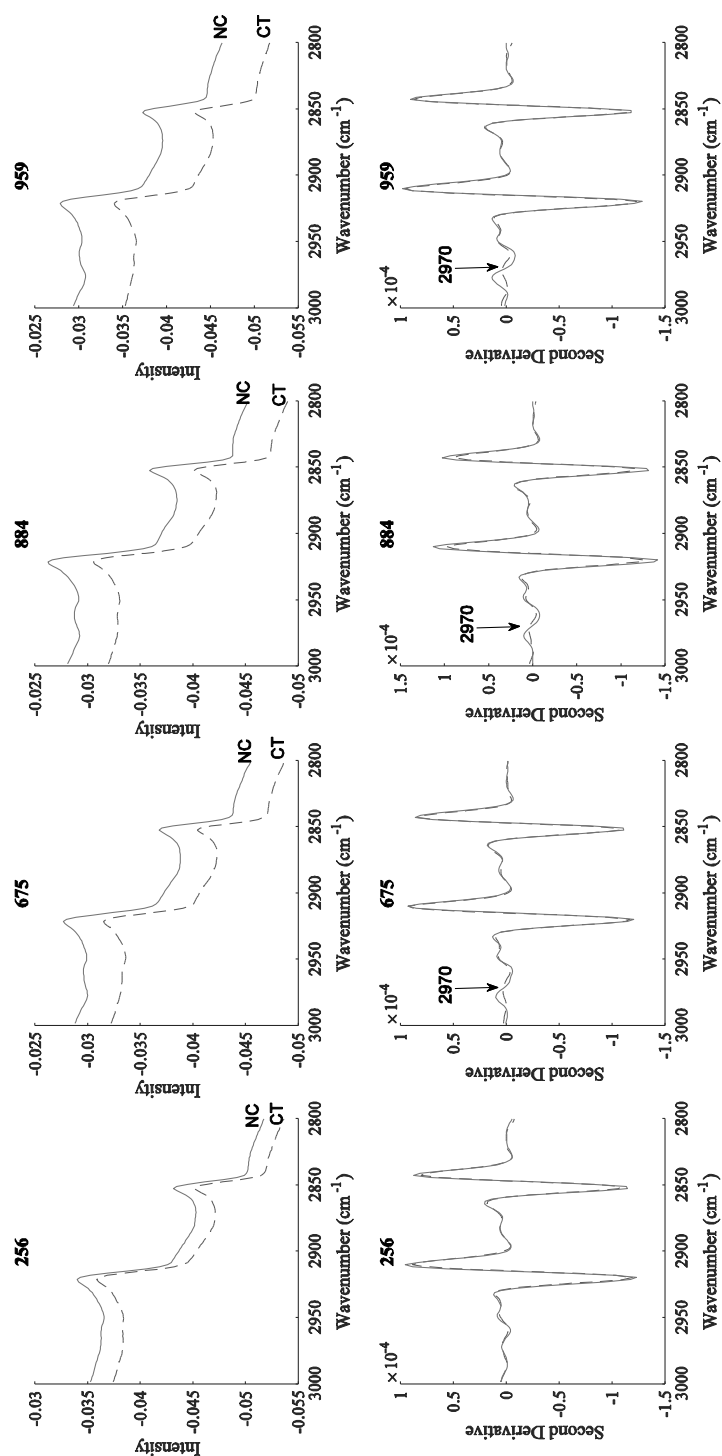


Figure 4.5 Averaged, normalized, lipid fingerprint region (2840-3040cm⁻¹) chilling treated (CT) and non-chilled (NC) spectra by genotype with corresponding second derivative across genotypes (256, 675, 884, 959) in ‘mild’ chilling conditions on mature corn leaf (V6; adaxial side) samples.

4.2.15 Cuticular Wax extraction

Analysis was conducted on fresh leaf tissue of mature corn at the reproductive growth stage with sampling within 30cm of the leaf tip of adaxial side of leaf V6 (Figure 3.2). The samples were triple rinsed with distilled water and surface air dried prior to cuticular wax extraction. Wax extraction protocol was modified from (Dietrich et al. 2005) for adaxial cuticular leaf wax extraction. The cuticular wax extraction was performed on the adaxial surface of the leaf using ACS grade Chloroform (BDH VWR Analytical, Radnor, PA, USA). Plant material weighing approximately 300mg was washed with 10ml chloroform over the adaxial surface of the tissue ten times using a 1ml pipette. 1 µg of *n*-tetracosane as an external standard was added to each extract and was vortexed for 30 seconds. Lastly, samples were dried under a gentle stream of nitrogen gas. Extracted leaf material was recovered, dried and weighed (Dietrich et al. 2005).

4.2.16 Derivatization

The derivatization for GC-MS analysis was performed with the addition of 200 µL HPLC-Grade acetonitrile (ACN) and 75µL BSTFA+TCMS to the dried wax extract and was incubated at 60°C for 20 minutes. In preparation for the GC-MS analysis, the sample was reduced with a gentle stream of nitrogen to approximately 50 µL. The sample was placed in an insert run on the GC-MS with the following protocol (Dietrich et al. 2005).

4.2.17 GC/MS Analysis

GC-MS was performed on prepared samples using an Agilent 7890A GC instrument coupled to an Agilent 5975 inert mass selective detector (MSD) with triple axis detector. Sample extract was loaded (injection volume 1 µL) with an Agilent G2614A auto-sampler. The column was a DB-1MS fused silica column (15 m x 250 µm; 0.25 µm film thickness). The GC oven, of the Agilent 7890A, was programmed with a thermal gradient starting at 80°C, first ramp to 220°C at 15°C/min, then ramp to 340°C at 7.5°C/min, hold at 340°C for 15min. Helium was used

as a carrier gas with a flow rate of 1.2 mL/min. The injector temperature was set at 280°C MSD temperature (Dietrich et al. 2005).

4.2.18 Data Analysis

GC-MS Chromatograms were converted to Peak areas using ChemStation (Agilent Technologies, Santa Clara, CA, USA) at WM Keck Metabolomics Laboratory Iowa State University. Peaks areas were converted to concentrations in moles per gram (Equation 4.1). Equation 4.1 Determination of concentration (mole/gram) for chromatogram produced peak area.

$$\text{mole/gram} = \left(\frac{\text{area of each peak}}{\text{internal standard area}} \right) * \left(\frac{\text{amount of internal standard added}}{\text{mg of tissue used}} \right)$$

Heatmaps were generated using the corrplot package in R. Z-scores were calculated using the mean and standard deviation of all observations for each cuticular wax component. The master dendrogram was generated in Orange (3.3.7 Open Source), with Z-scores calculated according to the same procedure.

4.2.19 GC-MS/MS Experimental Design

Greenhouse experiment

The experimental design of the GH samples for GC-MS consisted of two treatments (chilling treated and non-chilled), under ‘mild’ condition (See 3.2.3 Chilling Regime for condition parameters), two genotypes (884 and 959) and three biological replicates per sample. Two resistant types were selected based on results from freezing point depression and cuticle thickness with an interest to compare differences within the resistant response.

Field experiment

iCuticular wax was extracted across four genotypes of contrasting chilling resistance (256, 675, 884 and 959) for GC-MS analysis during four periods spanning five weeks beginning August 22, 2016 concluding September 30, 2016 (APPENDIX A). The design of the GC-MS

run was based on two treatments, early (2016-08-22) (non-chilled) and late (chilling treated) (2016-09-30), three genotypes were selected (675, 884, 959). Based on hydrophobicity and thermal imaging results, each contained three biological replicates.

4.3 Results

4.3.1 Field Condition- CLSM Cuticle Thickness

Both response variables (genotype [256, 675, 884, 959] and treatment [early 2016-08-03 and late 2016-09-12 field sampling]) were found to be statistically significant ($P < 0.05$) (Table 4.2) under field conditions for cuticle thickness response, however we must recognize this finding is approaching and potentially exceeding the estimated resolution detection limits for diffraction limited light for the z-direction in this system .

Table 4.2 Two-way ANOVA comparing means of cuticle thickness of leaf (V6; adaxial side), field produced mature corn across genotype (256, 675, 884, 959) and treatment (early 2016-08-03, late 2016-09-12); n=120.

	Sum of Squares	df	Mean Square	F	p-value
Sample Period	14.9	1	14.941	25.504	<0.001
Genotypes	15.4	3	5.150	8.791	<0.001
Residuals	559.5	955	0.586		

Under field produced conditions, there was an increase in cuticle thickness. The increase in thickness was observed across all genotypes (including 884 and 959) and between early 2016-08-03 and late 2016-09-12 measurements over a five-week period (Figure 4.6). The main effect for sample period yielded an F-ratio of $F_{0.05}(1,955) = 25.50$, $p < 0.001$, indicating a highly significant difference between early ($\mu = 3.80 \mu\text{m}$, $\sigma = 0.73 \mu\text{m}$) and late ($\mu = 4.05 \mu\text{m}$, $\sigma = 0.81 \mu\text{m}$) sampling periods. There was a differential in cuticle thickness of $0.25 \mu\text{m}$ between early and late, with a narrow upper and lower limit ranging from 0.15 and $0.35 \mu\text{m}$, respectively (Table 4.3). These narrow limits indicated low variability and stability amongst the traits. The main effect for genotypes yielded an F-ratio of $F_{0.05}(3,955) = 5.15$, $p < 0.001$, indicating a significant difference in cuticle width between genotypes. A post-hoc analysis (Table 4.3) showed genotype 256 is significantly ($P < 0.05$) different than each of the three other genotypes with a considerably thinner cuticle. Comparison of means of genotype 884 and 959 under field conditions also indicates significant differences ($P < 0.10$) (

Table 4.3) although to a lesser degree than genotype 256 ($P < 0.05$). Genotypes able to withstand colder freezing temperatures, or more freezing avoidant types, had a thicker cuticle.

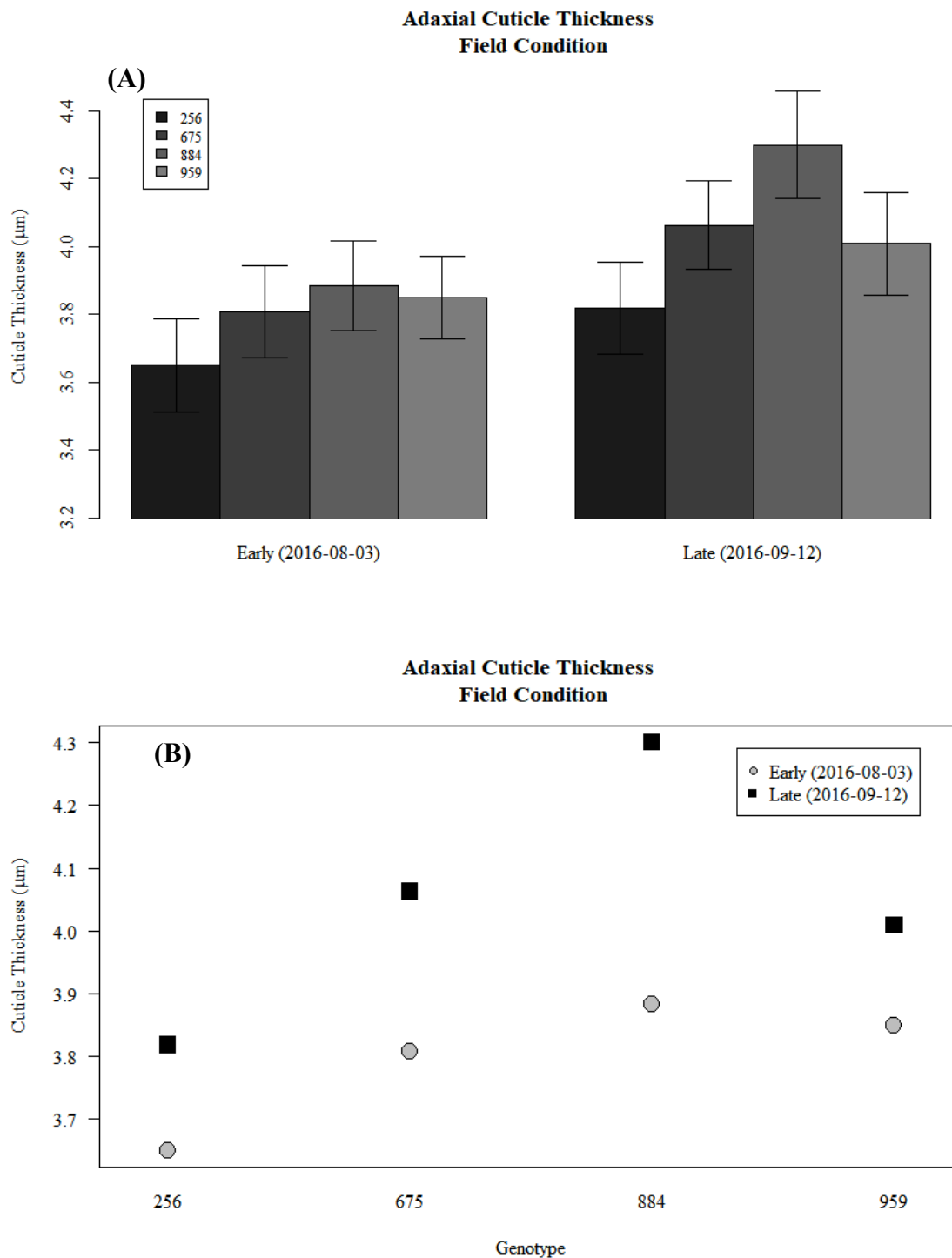


Figure 4.6 Cuticle thickness of leaf (V6; adaxial side), field produced mature corn by genotype (256, 675, 884, 959) and treatment (early 2016-08-03, late 2016-09-12) using CLSM; $n=120$; (A) Barplot demonstrates difference in cuticle thickness between genotypes. Error bars denote 95%

CI ($P_{0.05}$); (B) Interaction plot illustrates the cuticle thickness response for combinations of factors (genotype and treatment). Late treatment samples show increased cuticle thickness relative to early treatment.

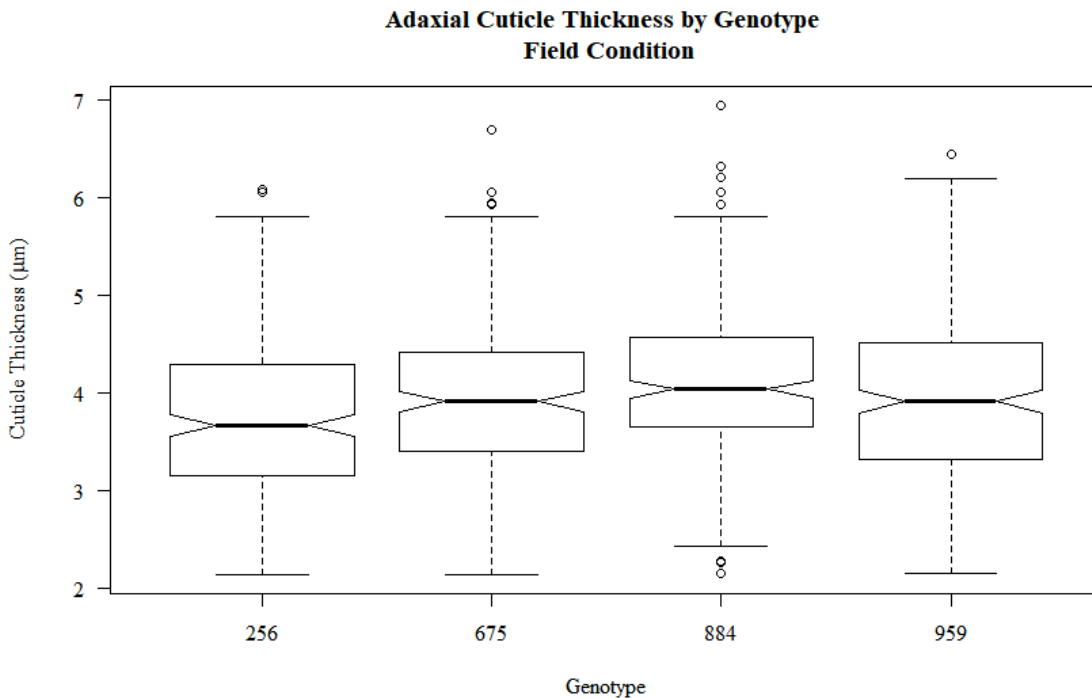


Figure 4.7 Boxplot of cuticle thickness of leaf (V6; adaxial side), field produced mature corn by genotype (256, 675, 884, 959) with combined treatment (early-2016-08-03, late-2016-09-12) using CLSM; n=240; o represent outliers.

Table 4.3 Comparison of Means (HSD Tukey Method) of cuticle thickness of leaf (V6; adaxial side) field produced mature corn by genotype (256, 675, 884, 959) and treatment (early 2016-08-03, late 2016-09-12) with 95% confidence interval around the lower and upper range.

TUKEY HSD MULTIPLE COMPARISON OF MEANS				
	diff	lwr	upr	p-value
675-256	0.2010	0.0212	0.3808	0.0213
884-256	0.3577	0.1779	0.5376	<0.0005
959-256	0.1949	0.0151	0.3748	0.0275
884-675	0.1567	-0.0231	0.3365	0.1125
959-675	-0.0061	-0.1859	0.1737	0.9998
959-884	-0.1628	-0.3426	0.0170	0.0920
Late-Early	0.2495	0.1525	0.3465	<0.0005

4.3.2 ‘Mild’ Chilling Condition – CLSM Cuticle Thickness

In response to the field study, where all genotypes were found to increase in cuticle thickness over time, two resistant genotypes were selected (885, 959) under ‘mild’ chilling condition to evaluate cuticle thickness response. Two resistant types were selected based on results from freezing point depression indicating a varying degree of response within the resistant types to chilling pre-treatment. They were selected with an interest to compare differences within the resistant response for cuticular thickness. There were no significant effects of either treatment or genotype (884, 959) on the adaxial cuticle thickness ($P < 0.05$) (

Table 4.4 and Figure 4.8) under the ‘mild’ 10 day chilling treatment. The non-chilled samples had a narrower variability spanning the lower and upper quadrants by approximately 2 μm . By contrast the chilling treated samples spanned a wider 3.5 μm , however the median indicates no significant difference in cuticle thickness between treatments. Plants were measured immediately following chilling treatments within 8 hours of sample collection.

Table 4.4 Two-way ANOVA comparing means of cuticle thickness of leaf (V6; adaxial side) ‘mild’ chilling condition, mature corn across genotypes (884, 959) and treatment (chilling treated, non-chilled); n=120.

	Sum of Squares	df	Mean Square	F	p- value
Treatment	0.32	1	0.3163	0.627	0.429
Genotypes	0.01	1	0.0082	0.016	0.899
Residuals	240.51	477	0.5042		

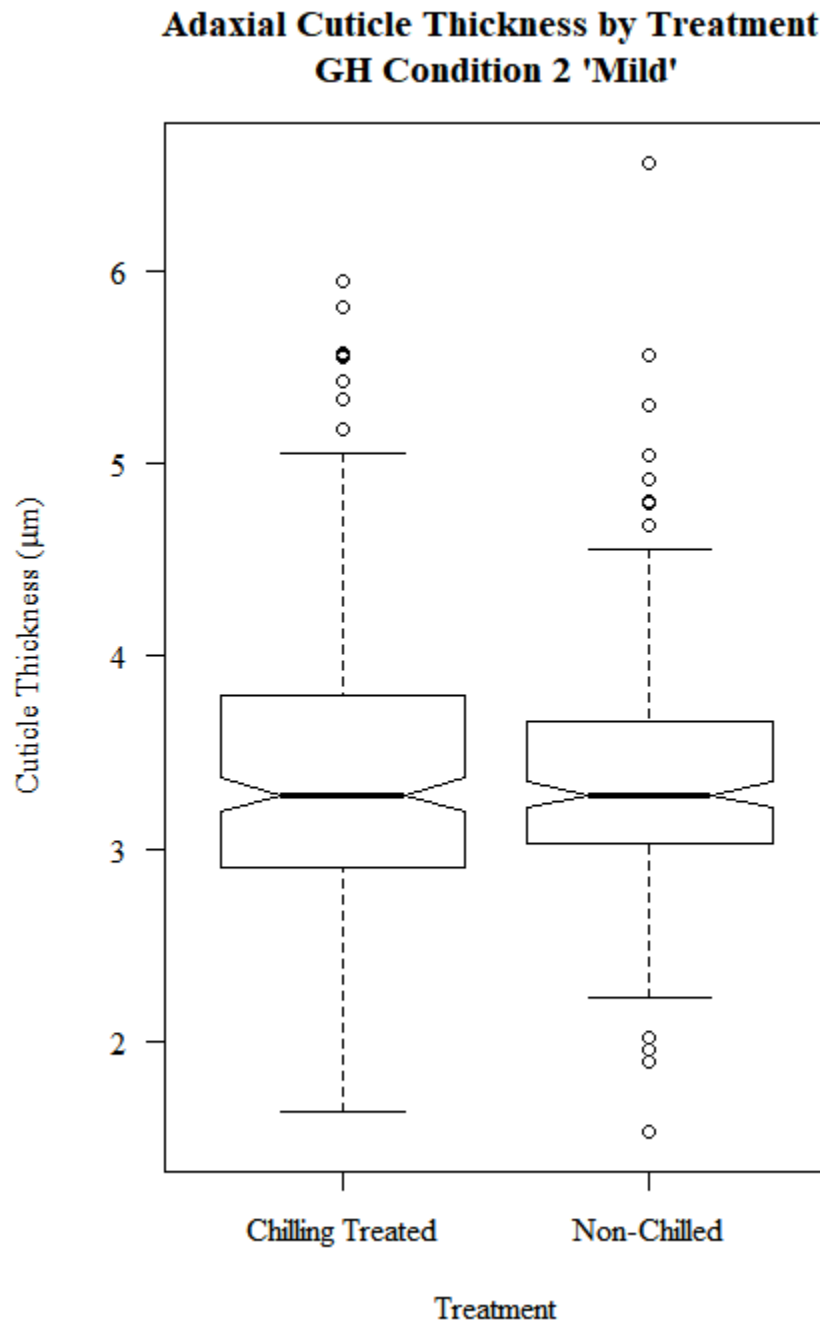


Figure 4.8 Cuticle thickness of leaf (V6; adaxial side) of mature corn plants under 'mild' chilling conditions by treatment by combined genotypes (884, 959) averaged results using CLSM, n=240; o = represents outliers.

4.3.3 ‘Mild’ Controlled Environment Chilling Conditions – Integrations by Genotype

Unlike cuticular thickness, under ‘mild’ chilling conditions, the CH₃ (region 1) demonstrated increased absorption in the chilling treated samples (higher integration areas). This finding was consistent across all genotypes tested except for 675, which showed no change in response to chilling treatment while all other treatments increased in wax concentration prevalence of detectable lipid compounds following chilling treatment. Genotype 256 was the only genotype to experience significant ($p < 0.05$) lipid increase following chilling treatment.

The lack of responsiveness of genotype 675 is consistent with the previous findings in both thermal and hydrophobic measurements. Although not significant, the asymmetrical (Figure 4.10) and symmetrical (Figure 4.11) broad band integration have the same trend of genotype 675 to show an inverse and limited response compared with the other genotypes. Genotypes 884 and 959 showed a stable and slight reduction in integration area. By contrast, genotype 256 had a more reduction in region 2 and 3 than the other genotypes. In all regions, the results indicated that the two more resistant varieties (884 and 959) have a consistent stability of response to chilling treatment with a slight reduction of integration areas following exposure.

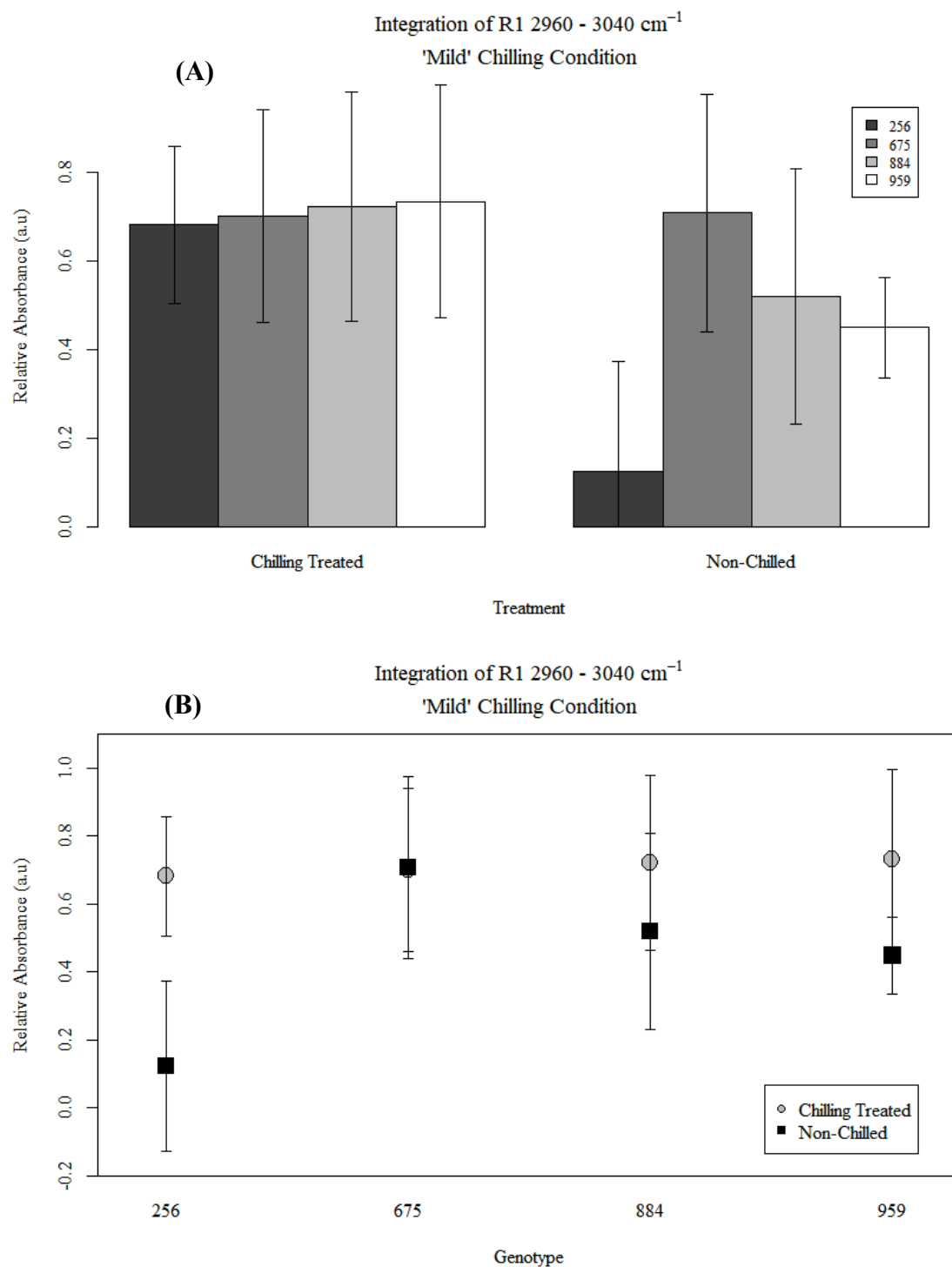


Figure 4.9 Peak area integration (a.u.) of CH_3 (region 1) 2960-3040 cm^{-1} of leaf (V6; adaxial side) 'mild' chilling condition mature corn by genotype (256, 675, 884, 959) and treatment (chilling treated, non-chilled) using ATR-FTIR. spectra scan average 512; 18 spectra replicates **(A)** Barplot demonstrates difference between genotypes; **(B)** Interaction plot illustrating the response of the area beneath integration region one to different combinations of factors (genotype, treatment).

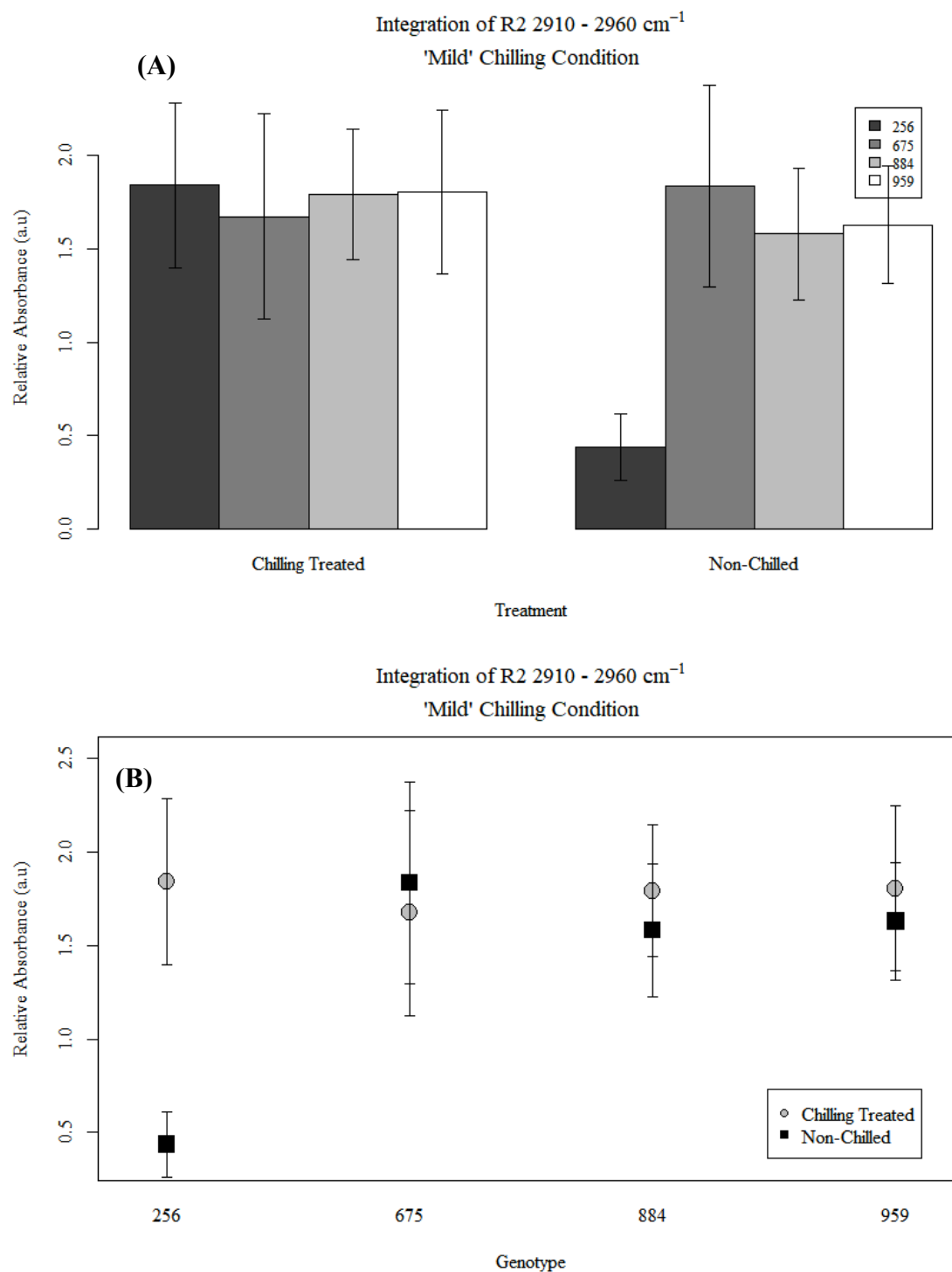


Figure 4.10 Peak area integration (a.u.) of asymmetrical CH_2 bend (region 2; $2910\text{-}2960\text{cm}^{-1}$) of leaf (V6; adaxial side) 'mild' chilling condition mature corn by genotype (256, 675, 884, 959) and treatment (chilling treated, non-chilled) using ATR-FTIR; spectra scan average 512; 18 spectra replicates (A) Barplot demonstrates difference between genotypes; (B) Interaction plot illustrating the response of the area beneath integration region two to different combinations of factors (genotype, treatment).

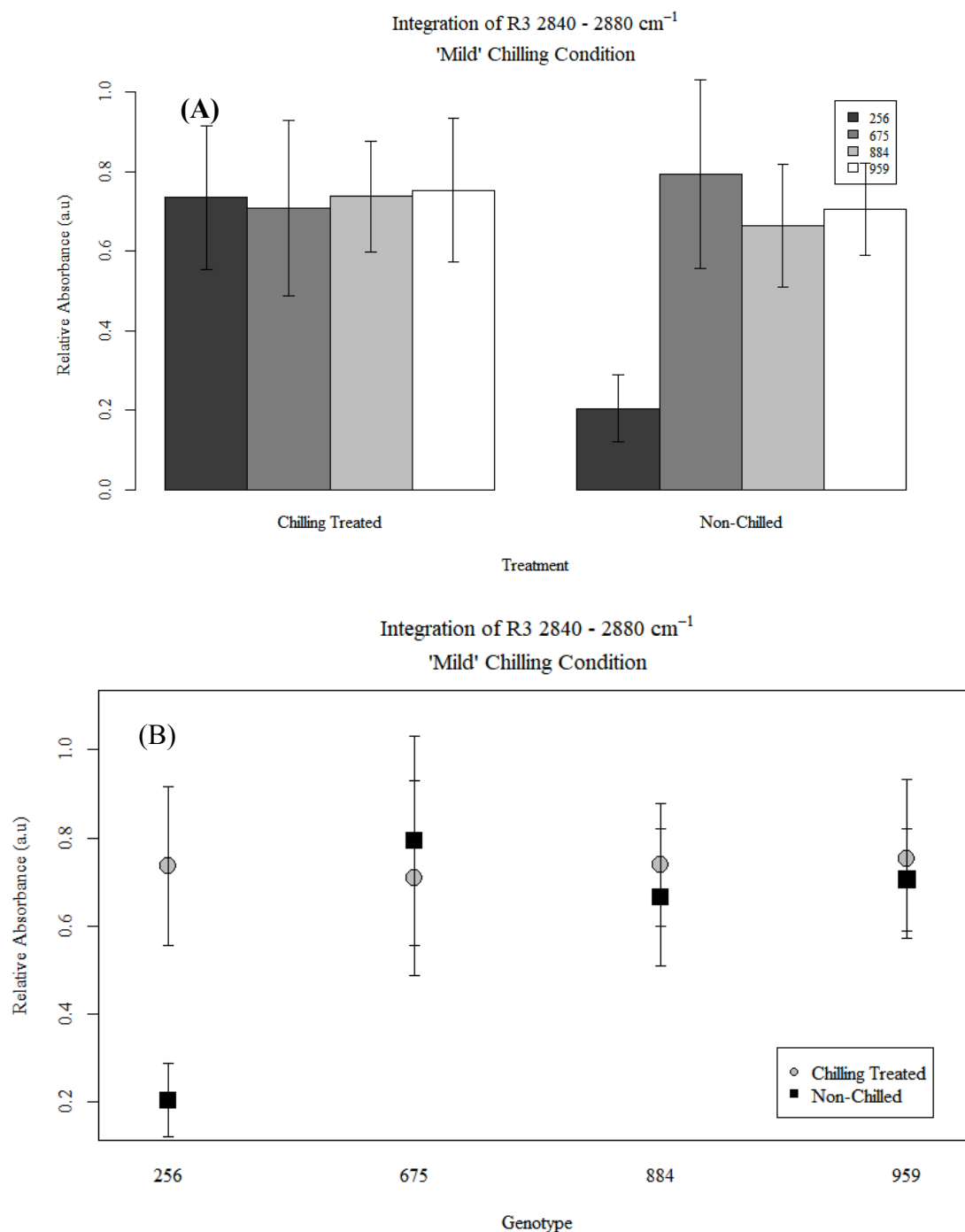


Figure 4.11 Peak area integration (a.u.) of symmetrical CH_2 bend (region 3; 2840-2880 cm^{-1}) of leaf (V6; adaxial side) 'mild' chilling condition mature corn by genotype (256, 675, 884, 959) and treatment (chilling treated, non-chilled) using ATR-FTIR; spectra scan average 512; 18 spectra replicates (A) Barplot demonstrates difference between genotypes; (B) Interaction plot illustrating the response of the area beneath integration region two to different combinations of factors (genotype, treatment).

4.3.4 ‘Mild’ Controlled Environment Chilling Condition – Integrations by Treatment

We observed a treatment effect across the asymmetrical CH_2 bending groups, with a strong effect ($P < 0.05$) across the CH_3 demonstrated by an increase in peak area intensity following chilling treatment. There was a moderate effect ($P < 0.10$) of chilling treatment, indicated by peak area increase, across the asymmetrical bend (Figure 4.12). There was no effect of chilling treatment to the symmetrical bend (Figure 4.13). Increase in peak area intensity of these CH_2 functional groups has been attributed to an increase in cutin and waxes (Ramirez et al. 1992, España et al. 2014, Heredia-Guerrero et al. 2014).

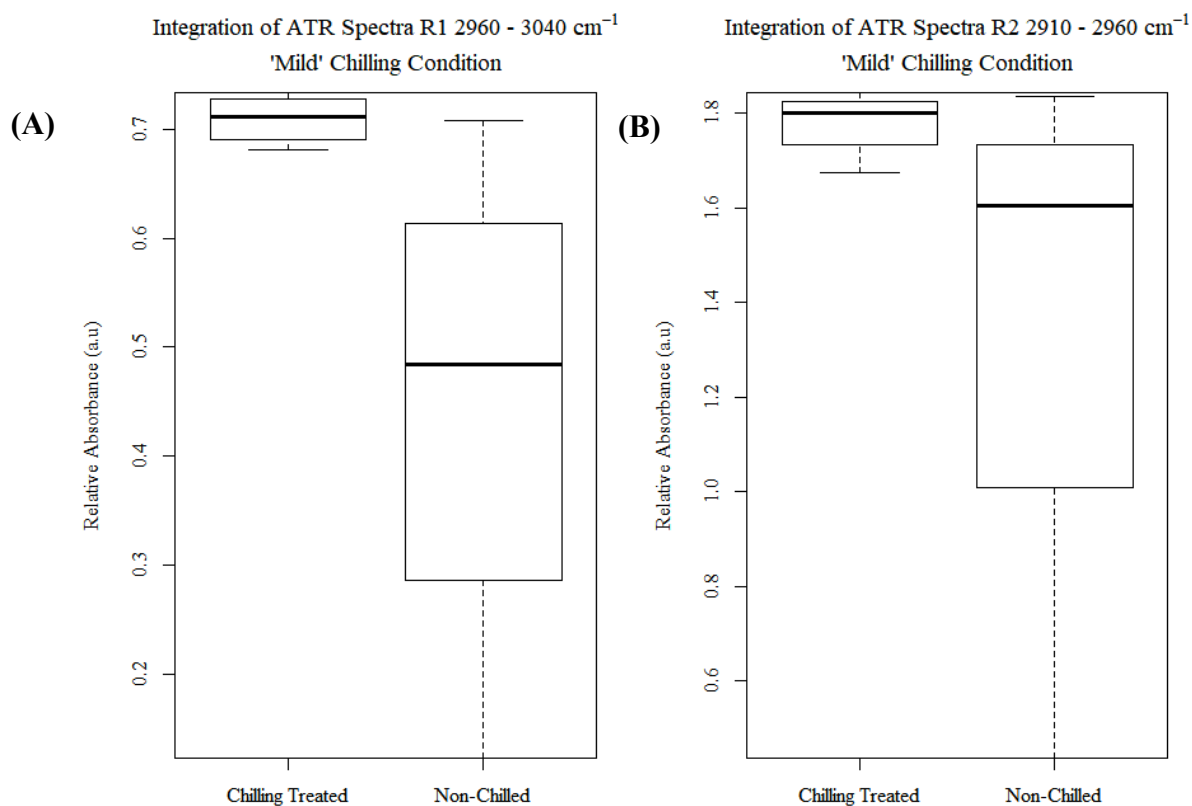


Figure 4.12 Boxplot of peak area integration (a.u.) of asymmetrical CH_2 bending groups of leaf (V6; adaxial side) ‘mild’ chilling condition mature corn by treatment (chilling treated, non-chilled) using ATR-FTIR; spectra scan average 512; **(A)** Bar plot of CH_3 (region 1; 2960-3040 cm^{-1}) by treatment; Total $F_{0.05}(1,6) = 6.856$, $p = 0.0397$; NC $\mu = 0.54$, $\sigma = 0.13$; CT $\mu = 0.714$, $\sigma = 0.025$; **(B)** Bar plot asymmetrical CH_2 bend (region 2; 2910-2960 cm^{-1}) by treatment; Total $F_{0.05}(1,6) = 2.976$, $p = 0.135$; NC $\mu = 1.63$, $\sigma = 0.18$; CT $\mu = 1.793$, $\sigma = 0.070$;

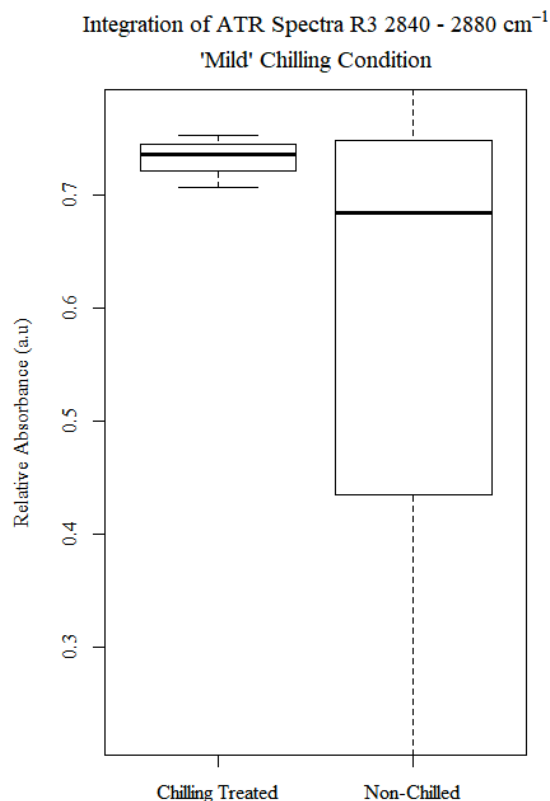


Figure 4.13 Boxplot of peak area integration (a.u.) of symmetrical CH_2 bending group (region 3; $2840\text{-}2880\text{cm}^{-1}$) of leaf (V6; adaxial side) 'mild' chilling condition mature corn by treatment (chilling treated, non-chilled) using ATR-FTIR; spectra scan average 512; Total $F_{0.05}(1,6) = 0.819$, $p=0.4$; NC $\mu=0.683$ $\sigma=0.077$; CT $\mu=0.719$, $\sigma=0.017$;

4.3.7 'Field' Chilling Conditions – CH_2 Regions Defined

The spectra for each treatment (F1-F6) were plotted across the lipid fingerprint region ($2800\text{-}3000\text{cm}^{-1}$), separately for each genotype, (Figure 4.14, 4.15, 4.16, 4.17) and indicate a decrease in lipid intensity over five week outdoor field conditions from 2016-08-16 to 2016-09-14 .

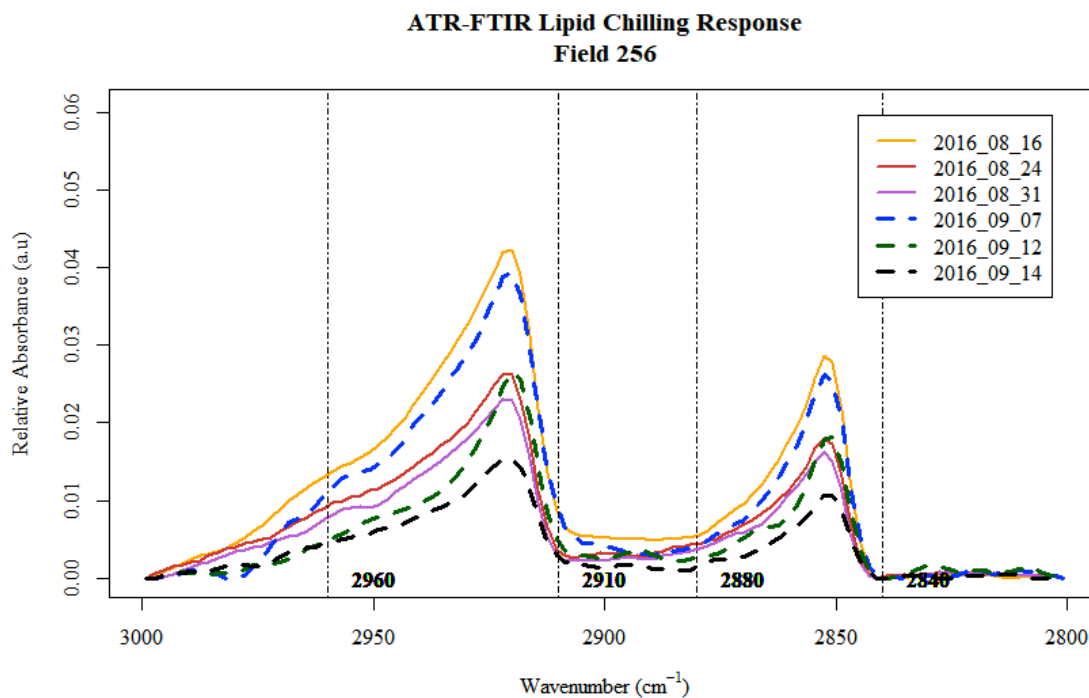


Figure 4.14 Lipid fingerprint ($2840\text{-}3040\text{cm}^{-1}$) average spectra of genotype 256 with band regions (region 1, $2960\text{-}3040\text{cm}^{-1}$; region 2, $2910\text{-}2960\text{cm}^{-1}$; region 3, $2840\text{-}2880\text{cm}^{-1}$) assigned to the CH_2 groups of field produced mature corn leaf V6 (adaxial side) over a five-week outdoor period spanning 2016-08-16 to 2016-09-14 (Table 4.1); Using ATR-FTIR, separate leaf samples collected weekly; spectra scan average 512.

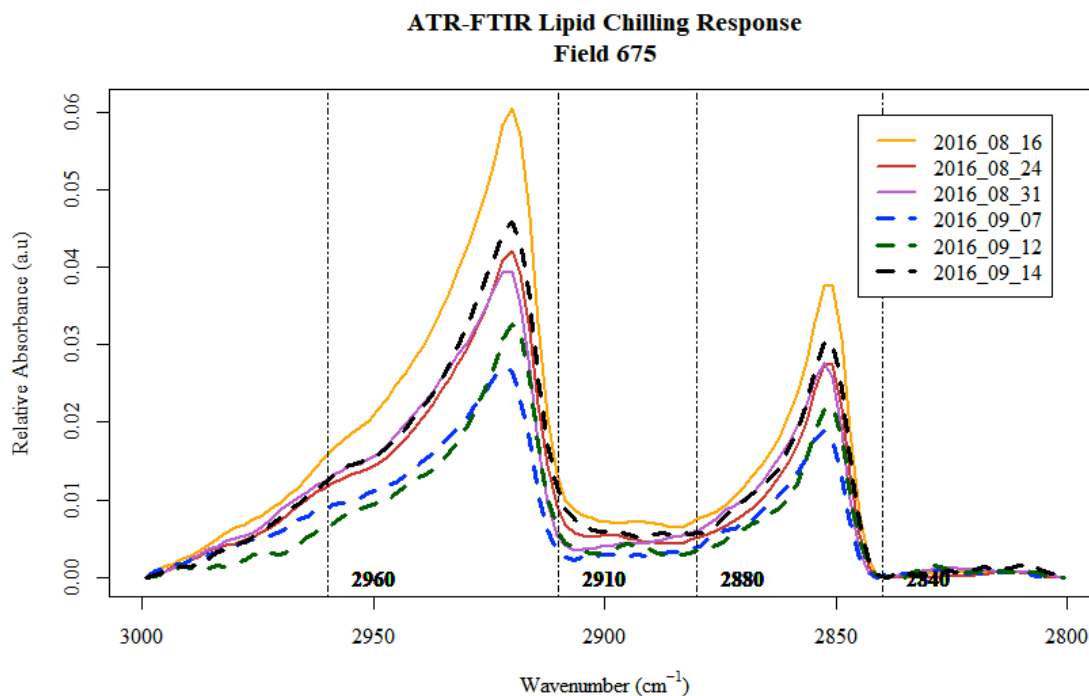


Figure 4.15 Lipid fingerprint ($2840\text{-}3040\text{cm}^{-1}$) average spectra of genotype 675 with band regions (region 1, $2960\text{-}3040\text{cm}^{-1}$; region 2, $2910\text{-}2960\text{cm}^{-1}$; region 3, $2840\text{-}2880\text{cm}^{-1}$) assigned to the CH₂ groups of field produced mature corn leaf V6 (adaxial side) over a five-week outdoor period spanning 2016-08-16 to 2016-09-14 (Table 4.1); Using ATR-FTIR, separate leaf samples collected weekly; spectra scan average 512.

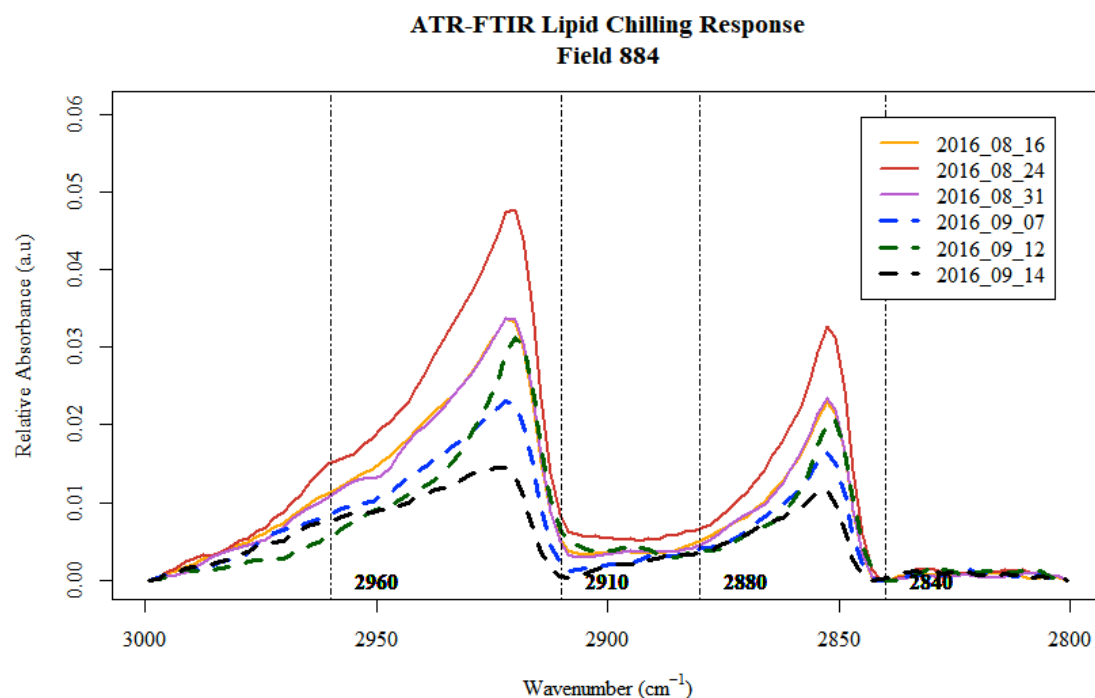


Figure 4.16 Lipid fingerprint ($2840\text{-}3040\text{cm}^{-1}$) average spectra of genotype 884 with band regions (region 1, $2960\text{-}3040\text{cm}^{-1}$; region 2, $2910\text{-}2960\text{cm}^{-1}$; region 3, $2840\text{-}2880\text{cm}^{-1}$) assigned to the CH_2 groups of field produced mature corn leaf V6 (adaxial side) over a five-week outdoor period spanning 2016-08-16 to 2016-09-14 (Table 4.1); Using ATR-FTIR, separate leaf samples collected weekly; spectra scan average 512.

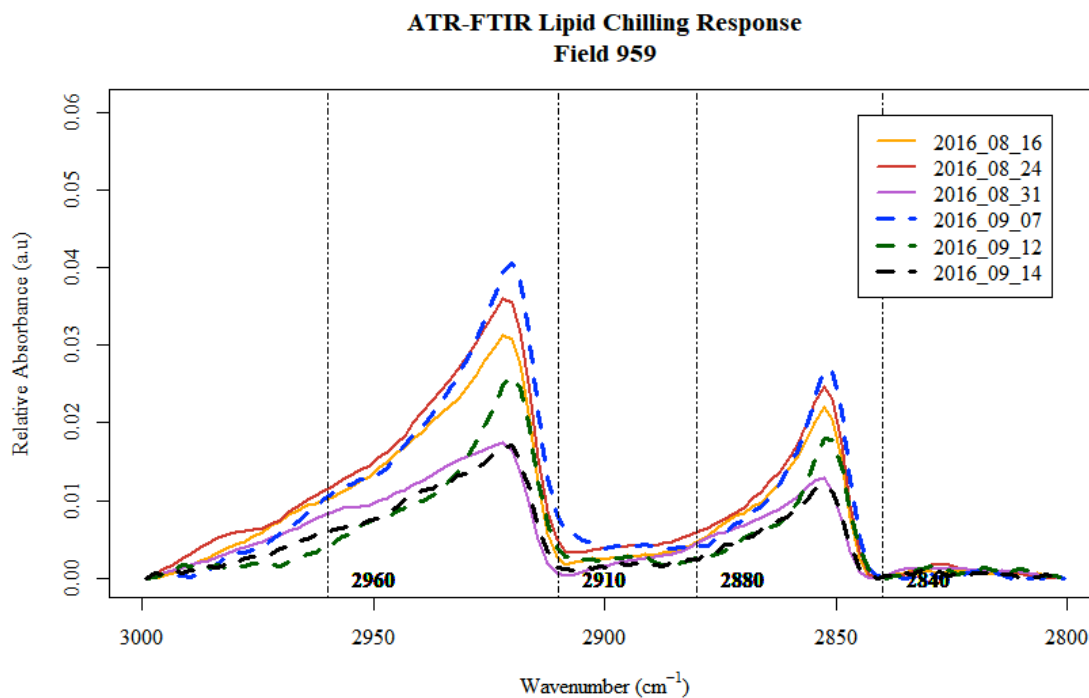


Figure 4.17 Lipid fingerprint ($2840\text{-}3040\text{cm}^{-1}$) average spectra of genotype 959 with band regions (region 1, $2960\text{-}3040\text{cm}^{-1}$; region 2, $2910\text{-}2960\text{cm}^{-1}$; region 3, $2840\text{-}2880\text{cm}^{-1}$) assigned to the CH_2 groups of field produced mature corn leaf V6 (adaxial side) over a five-week outdoor period spanning 2016-08-16 to 2016-09-14 (Table 4.1); Using ATR-FTIR, separate leaf samples collected weekly; spectra scan average 512.

4.3.8 'Field' Chilling Conditions – Integrations by Genotype

All genotypes expressed a general depreciation of intensity in lipid response over time (Figure 4.21, 4.22, 4.23) which would indicate a reduction in cuticular wax concentration. In genotypes 256 (Figure 4.14) and 675 (Figure 4.15), the early measurement period (F1 - Table 4.1) had the highest peak intensity. By contrast genotypes 884 (Figure 4.16) and 959 (Figure 4.17) showed increasing intensity between 24-08-2016 and 07-09-2016. Genotype 675 had the highest initial (relative absorbance) intensity of 0.06 (a.u.) at the asymmetrical CH₂ bend (region 2).

Absorbance Units (a.u) are a measure of the absorbance of light through the material. It is used as the measure for spectroscopy because as concentrations of a compound increase, the a.u. increases linearly. Genotypes 256, 884, and 959 had lower initial intensities of approximately 0.035 (a.u.). In the CH₃ region (region 1), genotype 675 was again non-responsive to stress treatment under natural outdoor conditions over periods 2016-08-24 to 2016-09-09 (F2, F3, F4- Figure 4.18) whereas the remainder of genotypes 256, 884 and 959 expressed a progressive and consistent reduction in asymmetrical bend intensity over this period.

Figure 4.19 and 4.20 indicate a significant increase in lipid peak integration intensity in genotype 675 in the final reporting period (2016-09-14; F6), five weeks after the initial measurement (2016-08-14; F1). The spike of genotype 675 in the final reporting period is largely influencing the treatment averages (across all genotypes) (Figure 4.21, 4.22, 4.23) in the final reporting period.

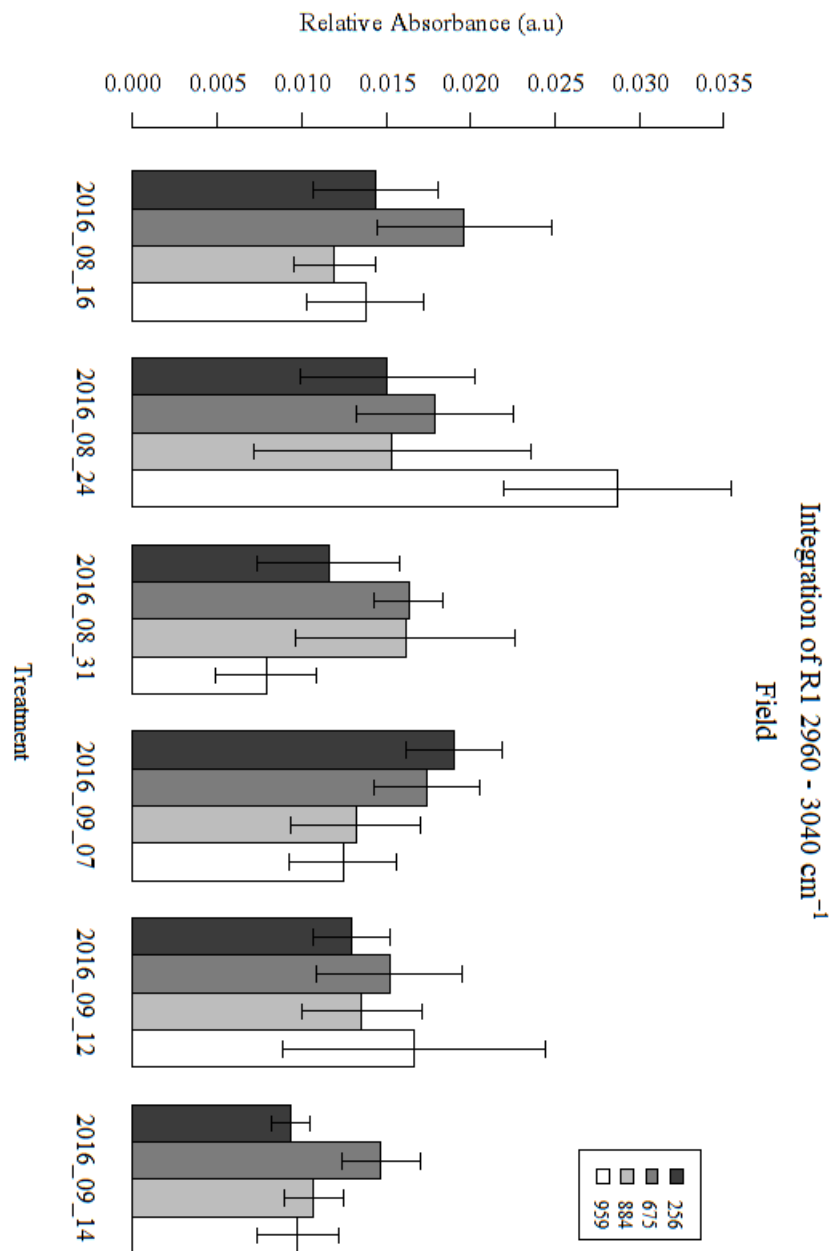


Figure 4.18 Peak area integration (a.u.) of CH₃ (region 1; 2960-3040 cm⁻¹) of leaf (adaxial side). V6 field produced mature corn by genotype (256, 675, 884 and 959) and treatment (field conditions- Table 4.1) using ATR-FTIR; spectra scan average 512; six replicates (two technical reps; three biological reps; per genotype; per period).

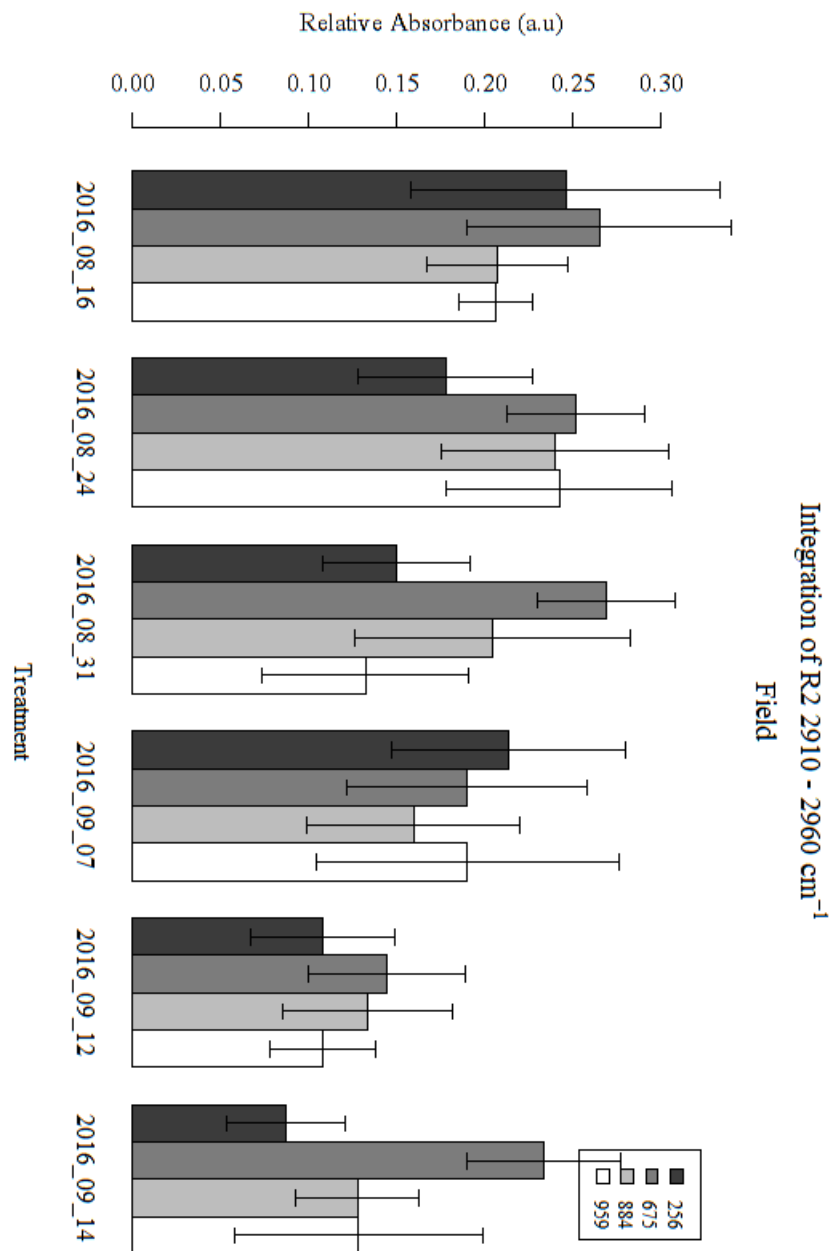


Figure 4.19 Peak area integration (a.u.) of the asymmetrical CH₂ bend (region 2; 2910-2960cm⁻¹) of leaf (adaxial side). V6 field produced mature corn by genotype (256, 675, 884 and 959) and treatment (field conditions- Table 4.1) using ATR-FTIR; spectra scan average 512; six replicates (two technical reps; three biological reps; per genotype; per period)

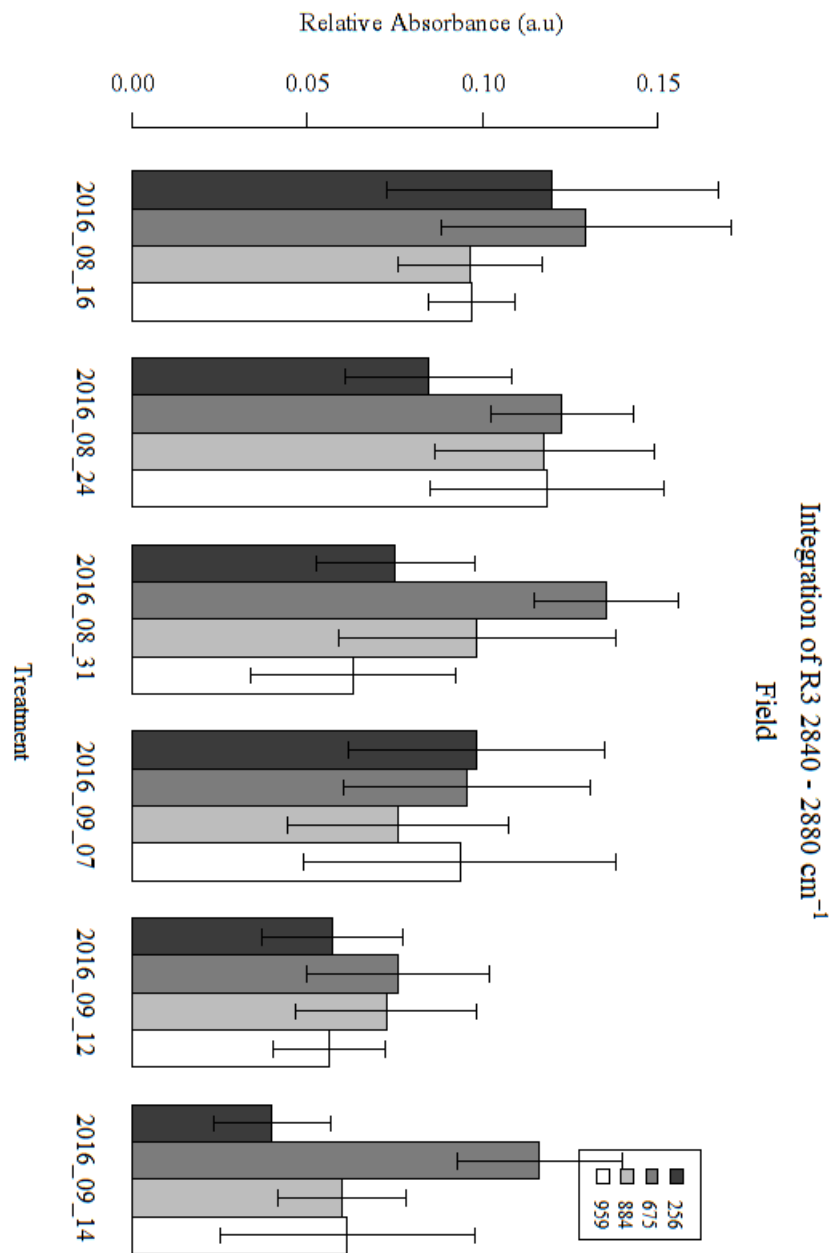


Figure 4.20 Peak area integration (a.u.) of the symmetrical CH₂ bend, (region 3; 2840-2880cm⁻¹) of leaf (adaxial side). V6 field produced mature corn by genotype (256, 675, 884 and 959) and treatment (field conditions- Table 4.1) using ATR-FTIR; spectra scan average 512; six replicates (two technical reps; three biological reps; per genotype; per period).

4.3.9 ‘Field’ Chilling Conditions – Integrations by Treatment

Under field conditions, according to the ATR findings, the asymmetrical and symmetrical CH₂ bending groups show a trend in overall wax reduction measured by peak area integrations (Figures 4.22, 4.23). The final reporting period 2016-09-14 (F6) has approximately half the intensity of the initial reporting period 2016-08-16 (F1) in all regions following natural outdoor conditions (Figure 4.21, Figure 4.22, Figure 4.23). This is additionally verified with a comparison of means of peak area integration, between the measurement periods where early (F1, F2) and late (F5, F6) are significantly reduced over time ($P < 0.05$) (Table 4.5).

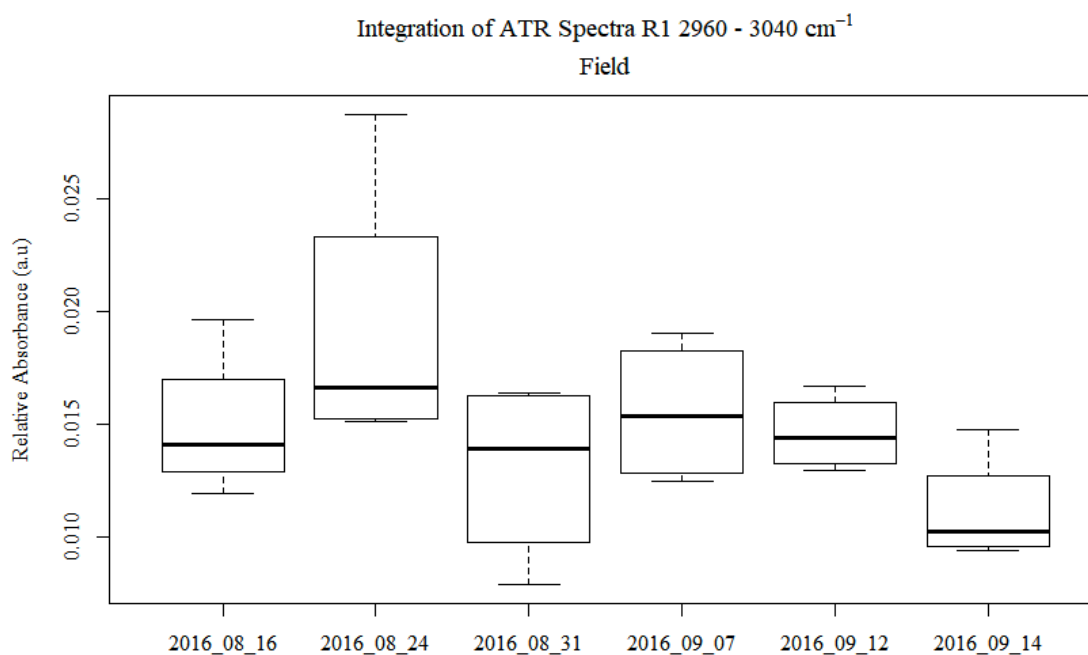


Figure 4.21 Boxplot of peak area integration (a.u.) of the CH_3 group average across all genotypes, region 1, 2960-3040 cm^{-1} of leaf (adaxial side). V6 field produced mature corn over five-week field conditions spanning 2016-08-16 to 2016-09-14 (Table 4.1) using ATR-FTIR, separate leaf samples collected weekly; spectra scan average 512.

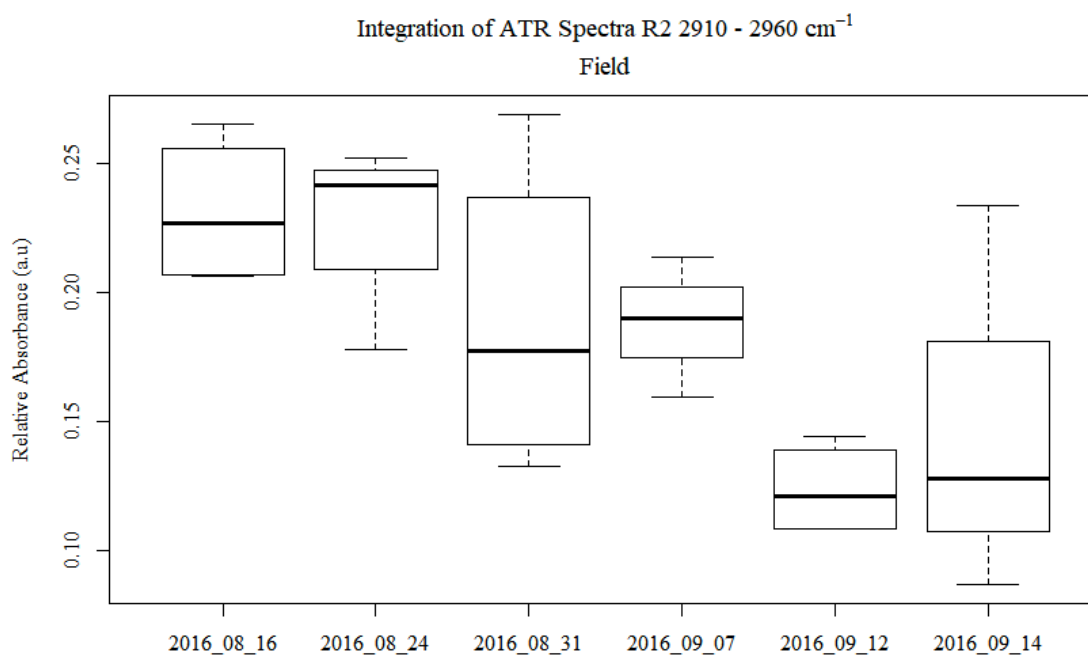


Figure 4.22 Boxplot of peak area integration (a.u.) of asymmetrical CH_2 bending group average across all genotypes, region 2, $2910\text{-}2960\text{cm}^{-1}$ of leaf (adaxial side). V6 field produced mature corn over five-week outdoor conditions spanning 2016-08-16 to 2016-09-14 (Table 4.1) using ATR-FTIR, separate leaf samples collected weekly; spectra scan average 512.

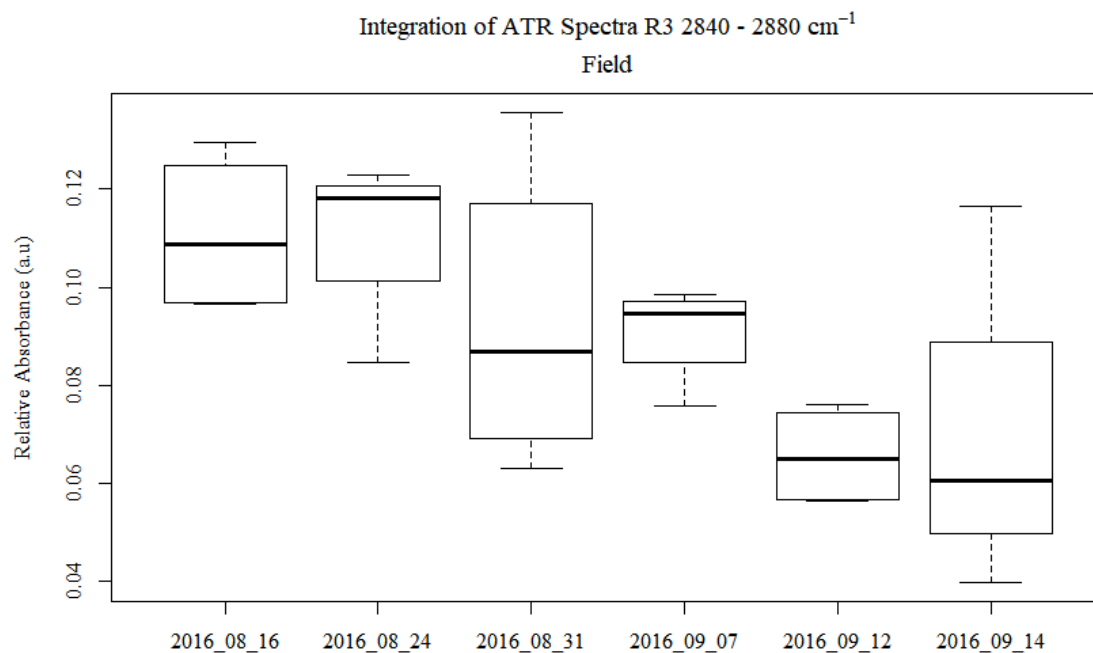


Figure 4.23 Boxplot of peak area integration (a.u.) of symmetrical CH_2 bending group average across all genotypes, region 3, $2840\text{-}2880\text{cm}^{-1}$ of leaf (adaxial side). V6 field produced mature corn over five-week outdoor conditions spanning 2016-08-16 to 2016-09-14 (Table 4.1) using ATR-FTIR, separate leaf samples collected weekly; spectra scan average 512.

Table 4.5 Comparison of Means (HSD Tukey Method) of combined (Regions 1, 2 and 3) peak area integration of field produced from leaf (V6; adaxial side) of mature corn by treatment (F1 to F6; Table 4.1), average across all genotypes with 95% confidence interval around the lower and upper range.

TUKEY POST HOC TEST				
MEASUREMENT PERIOD	diff	lwr	upr	p-value
2016_08_24-2016_08_16	-0.0537	-0.2446	0.1371	0.9610
2016_08_31-2016_08_16	-0.1783	-0.3691	0.0125	0.0801
2016_09_07-2016_08_16	-0.1563	-0.3472	0.0345	0.1689
2016_09_12-2016_08_16	-0.2741	-0.4649	-0.0833	0.0011
2016_09_14-2016_08_16	-0.2752	-0.4660	-0.0844	0.0010
2016_08_31-2016_08_24	-0.1246	-0.3154	0.0662	0.3997
2016_09_07-2016_08_24	-0.1026	-0.2934	0.0882	0.6135
2016_09_12-2016_08_24	-0.2204	-0.4112	-0.0295	0.0146
2016_09_14-2016_08_24	-0.2214	-0.4123	-0.0306	0.0139
2016_09_07-2016_08_31	0.0220	-0.1688	0.2128	0.9994
2016_09_12-2016_08_31	-0.0958	-0.2866	0.0950	0.6799
2016_09_14-2016_08_31	-0.0969	-0.2877	0.0940	0.6696
2016_09_12-2016_09_07	-0.1178	-0.3086	0.0730	0.4634
2016_09_14-2016_09_07	-0.1189	-0.3097	0.0720	0.4530
2016_09_14-2016_09_12	-0.0011	-0.1919	0.1897	1.0000

4.3.10 Identification of Adaxial Cuticular Composition in ‘Mild’ Chilling Treatment and Field Produced Corn

The cuticular wax composition of one hundred and forty-two known compounds were identified through peak area integrations of chromatograms from the adaxial lipid cuticle extract under ‘mild’ chilling conditions and field produced mature corn leaves using the in-house Maize GC-MS library of W.M. Keck Metabolomics Research Laboratory (Iowa State University, Ames, Iowa, USA). The cuticular wax composition represents both cutin and wax originating from the cuticular layer extract. From the false-color heat map, it was observed that within the treatments the highest abundance across the cuticular components was found within large grouped clades in both resistant types ‘mild’ condition 884 (chilling treated and non-chilled) and 959 (non-chilled)(Figure 4.24). The dendrogram which was produced using a divisive hierarchical cluster analysis (HCA), demonstrates many small clusters, indicating a large degree of dissimilarity amongst the groups (Figure 4.24).

Twenty-five out of one hundred and forty-two, cuticular compounds were found to have significant ($p < 0.05$) contribution to the differential between chilling treated and non-chilled samples in genotypes 884 and 959 under ‘mild’ chilling conditions.

The cuticular composition of ten compounds were selected with significant ($p < 0.05$) contribution to the differential between early 2016-08-22 and late 2016-09-30 field samples in genotypes 675, 884 and 959. Of the cuticular wax compounds identified, seven were common between both the ‘mild’ condition and field produced sets across all sampling dates, therefore they were amalgamated to form a superset of 28 cuticular wax compounds (Table 4.6).

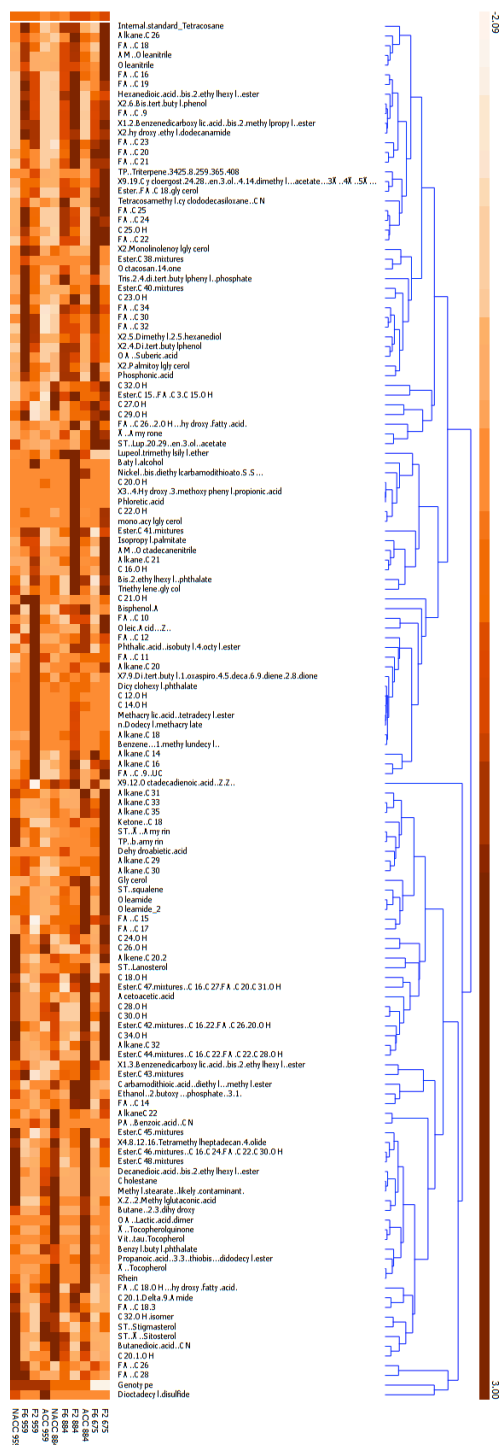


Table 4.6 Cuticular wax composition, localized by multiple linear regression to 28 key compounds, identified through GC-MS of chilling treatment differential between treatments under ‘Mild’ chilling (chilling treated[884, 959]; non-chilled [884, 959]) and Field produced (early 2016-08-22 [675, 884, 959], late 2016-09-30 [675, 884, 959]) conditions of adaxial wax extracts of leaf (V6) from mature grain corn. Chemicals of significance ($p < 0.05$) from both conditions were compounded to create a union set of compounds. Union set is the set of elements found in either A (‘mild’) or B (field) or both identifying their degree of contribution ($p < 0.05$) to the set.

Cuticular Wax Composition of Adaxial Leaf Surface	Union Set
A. Tocopherol	‘Mild’ Condition
Alkane.C29	BOTH
Alkane.C31	BOTH
Alkane.C33	BOTH
Alkane.C35	‘Mild’ Condition
C26.OH	‘Mild’ Condition
C28.OH	‘Mild’ Condition
C30.OH	‘Mild’ Condition
C32.OH.isomer	‘Mild’ Condition
Cholestane	‘Mild’ Condition
Dicyclohexyl phthalate	‘Mild’ Condition
Ester.C42.mixtures.C16.22.FA.C26.20.OH	‘Mild’ Condition
Ester.C44.mixtures.C16.C22.FA.C22.C28.OH	BOTH
Ester.C46.mixtures.C16.C24.FA.C22.C30.OH	BOTH
Ester.C48.mixtures	‘Mild’ Condition
FA.C16	‘Mild’ Condition
FA.C18	‘Mild’ Condition
FA.C26	‘Mild’ Condition
FA.C28	‘Mild’ Condition
FA.C30	‘Mild’ Condition
FA.C32	‘Mild’ Condition
Methacrylic acid tetradecyl ester	Field
n-Dodecyl methacrylate	Field
Oleamide	‘Mild’ Condition
A.Amyrin	‘Mild’ Condition
β.amyrin	BOTH
Triterpene.3425.8.259.365.408	BOTH
X.Z..2.Methylglutaconic.acid	Field

4.3.11 ‘Mild’ Chilling Condition – Identification of Lipid Compounds under Controlled Environment conditions in Genotype 884 and 959

The composition of 28 cuticular wax compounds were identified with significant variation of concentrations between chilling treated and non-chilled samples. Two chemical classes, alcohols and fatty acids (Table 5.1) were found to be of high ranking importance ($P < 0.05$) in the ‘Mild’ chilling condition. There is a strong genotype effect based on metabolic signatures across the heat map over the composition of the 28 identified cuticular wax compounds between 884 and 959 in response to chilling treatment. The heatmap identified four, third-order clades indicating dissimilarity between those groups. Within each clade there was a moderate level of like-compound similarity, based on chemical makeup although the lowest order clade groupings do not seem to be exclusively ordered by chemical composition (Figure 4.25). The alkanes group well into near partner clades whereas the fatty acid and alcohol groups dispersed among the matrix as small groups.

There was an increase in prevalence of the concentration of the cuticular wax composition in 26 of the 28 compounds in genotype 884 in response to chilling with the exceptions of C32.OH isomer and the methacrylic acid tetradecyl ester (Figure 4.26). In genotype 884, the largest increase occurred in the dendrogram cluster containing: C28.OH, AlkaneC35, FA.C18, Oleamide, C30.OH and AlkaneC33. The percent abundance of each chemical classification for 884 was not modified by chilling treatment (Figure 4.29).

Chilling treatment induced a reduction of 24 of the 28 compounds in genotype 959; four compounds increased (n-Dodecyl methacrylate, FA.C16, A. Tocopherol, and Methacrylic acid tetradecyl ester) and one remained unchanged (C26.OH) (Figure 4.28). The percent abundance of each chemical class showed changes in alcohols modified by chilling treatment from 17% (chilling treated) to 13% (non-chilled) and in triterpenes from 13% (chilling treated) to 17% (non-chilled). The only notable change in abundance between genotypes 884 and 959 was in the ‘other’ group class containing A-Tocopherol, Oleamide, and X.Z.2.Methylglutaconic acid 10%(884) and 3%(959).

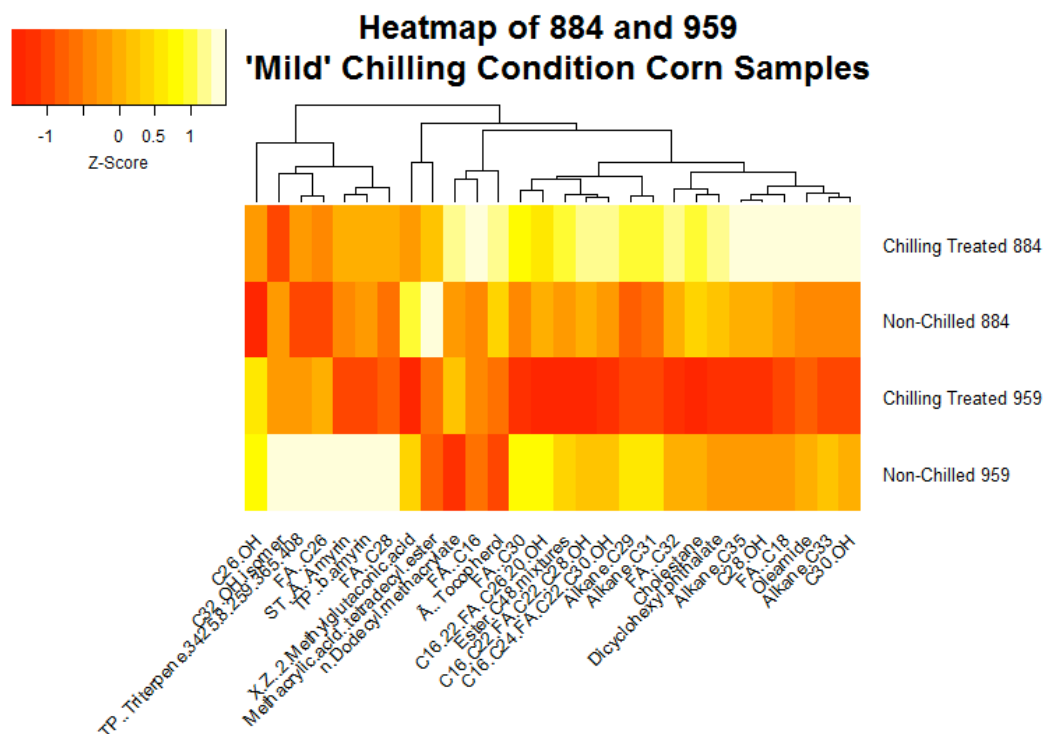


Figure 4.25 Heat Map and Dendrogram of 'Mild' chilling treated (884, 959) showing z-scores of adjusted metabolites mean-centered and scaled by mean and standard deviation (warm, lower abundance; cool, higher abundance) as indicated in the legend, across the cuticular composition of 28 key compounds from mature corn leaf (V6; adaxial side) surface lipid extracts.

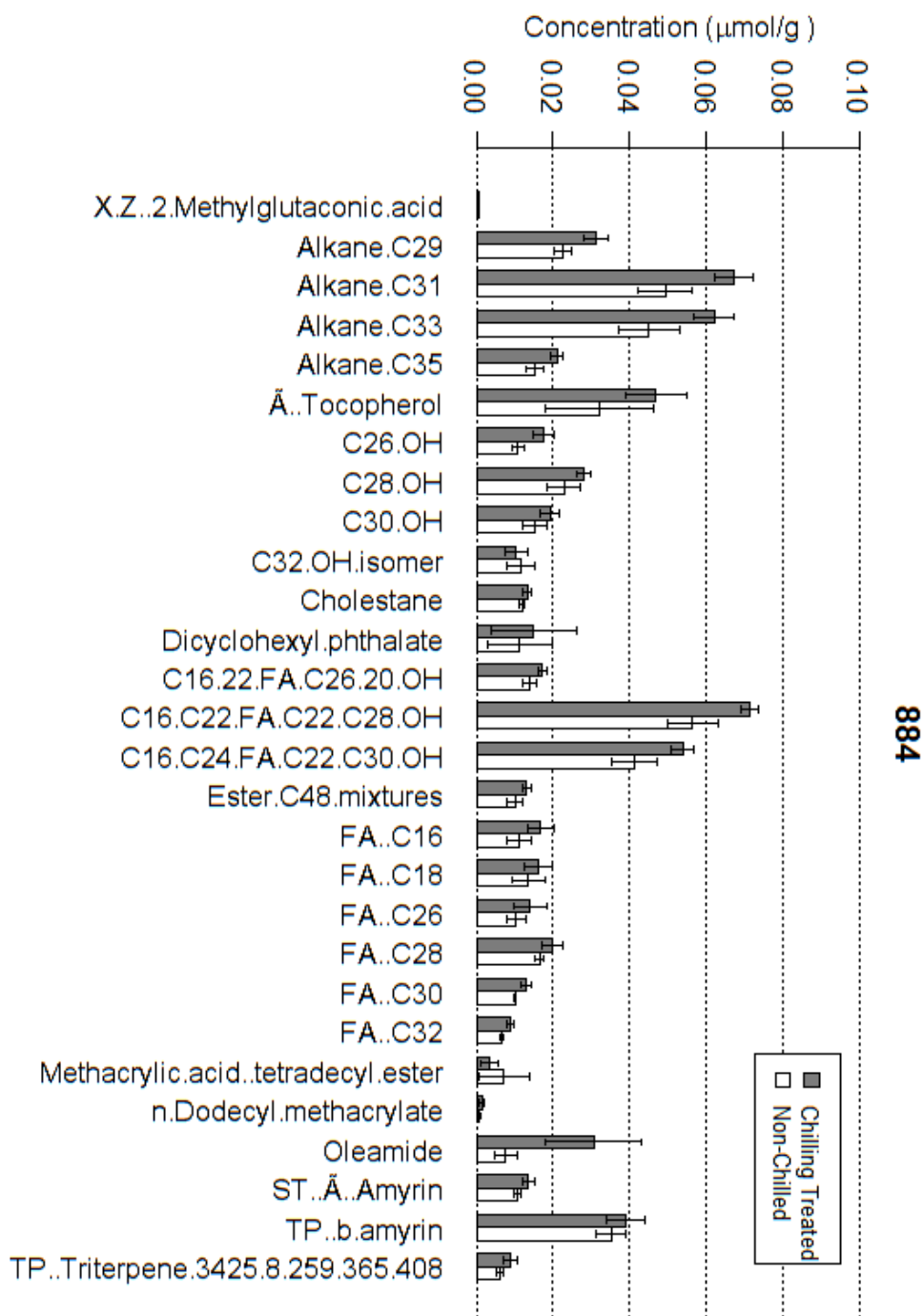


Figure 4.26 Cuticular wax composition of chilling treatment on the concentration of 28 compounds of the cuticular wax extracted and analyzed from leaf (V6; adaxial side) surface of mature corn leaves in genotype 884 under 'Mild' chilling condition Three replicates. Error bars denote standard error.

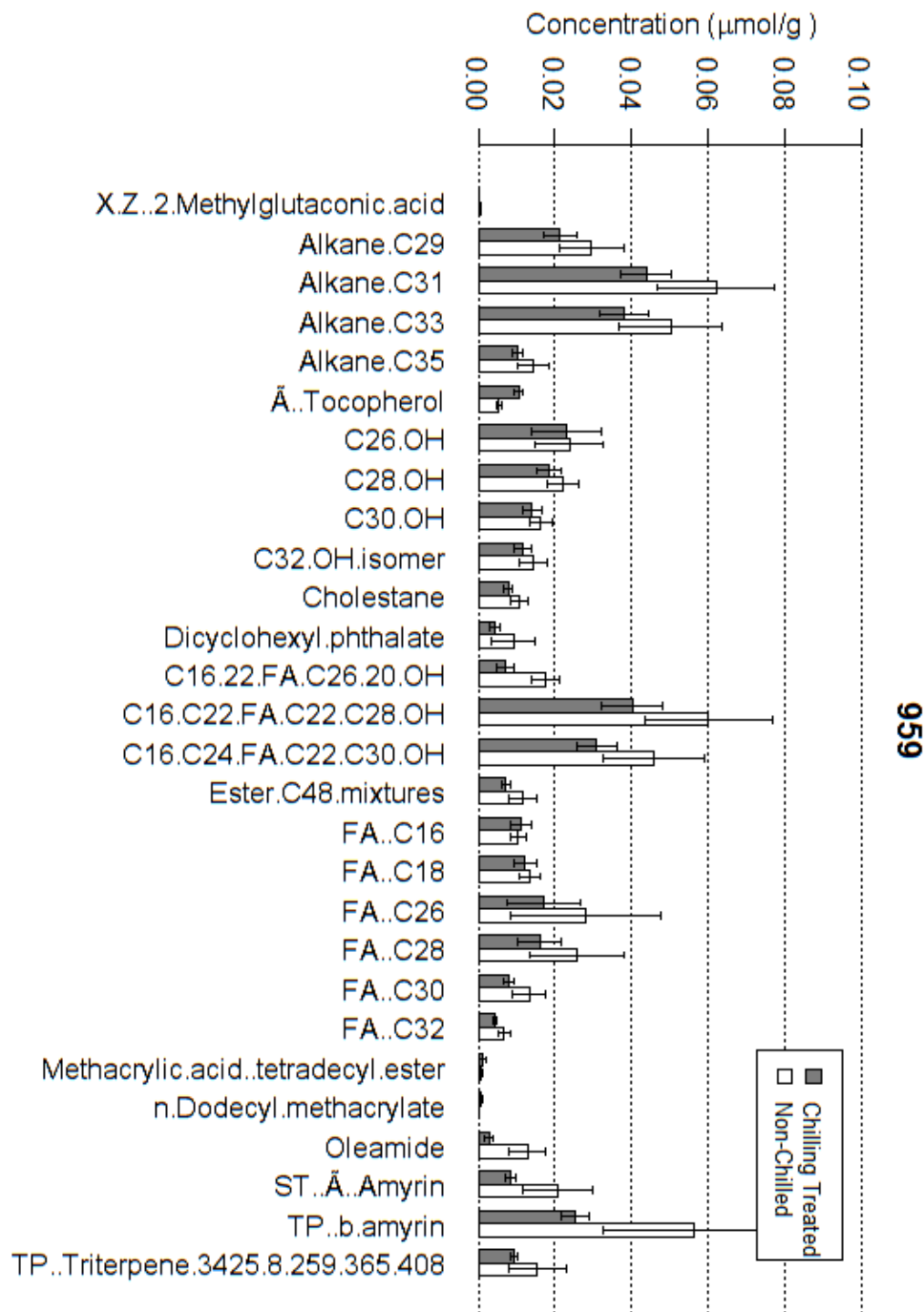


Figure 4.27: Cuticular wax composition of chilling treatment on the concentration of 28 compounds of the cuticular wax extracted and analyzed from leaf (V6; adaxial side) surface of mature corn leaves in genotype 959 under 'Mild' chilling condition. Three replicates. Error bars denote standard error.

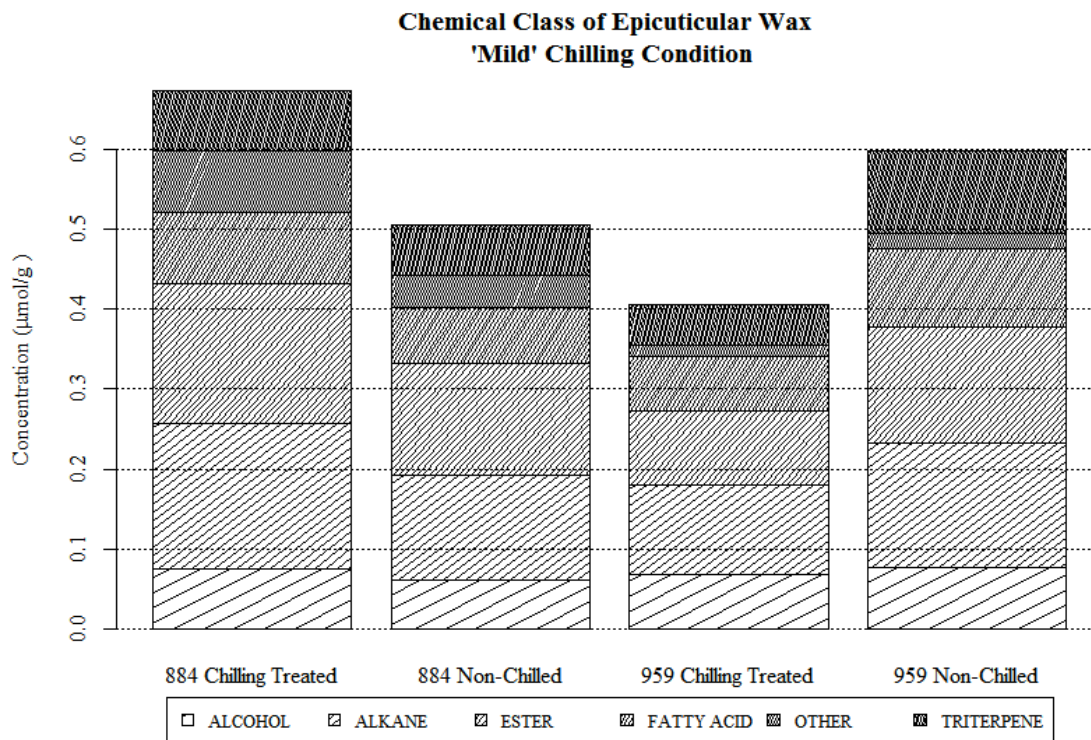


Figure 4.28 Cuticular wax composition of chilling treatment on the concentration of 28 compounds of the cuticular wax extracted and analyzed from leaf (V6; adaxial side) surface of mature corn leaves in genotypes (884, 959) under 'Mild' chilling condition Three replicates. Error bars denote standard error.

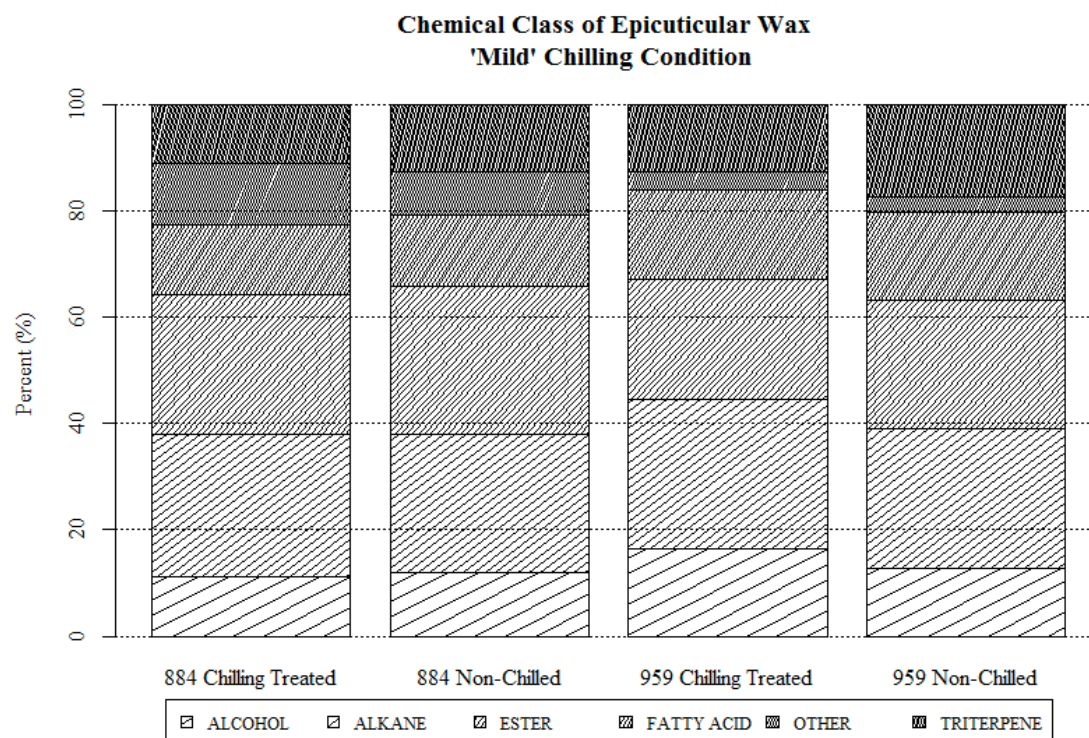


Figure 4.29. Percentage abundance of chemical classes (alcohol, alkane, ester, fatty acid, other and triterpene) of two 'mild' chilling condition genotypes (884, 959) across two treatments (chilling treated, non-chilled) of the cuticular wax extracted and analyzed from mature corn leaf (V6; adaxial). Three replicates.

4.3.12 Field Condition – Identification of Lipid Compounds in Genotype 675, 884 and 959

Across all genotypes (675, 884, 959), the dendrogram cluster containing very long chain Fatty Acids (VLCFA)(C26-C32) increased in response to late (2016-09-30) season conditions (Figure 4.30), with the most significant VLCFA response in genotype 959 (Figure 4.35B). Dendrogram cluster (rows 22-27) shows a decrease in prevalence of compounds for genotypes 675 and 884 in response to late season conditions and by contrast genotype 959 increased in all compounds except EsterC46 Mixture, which remained constant. Genotypes 884 and 959 had a large (>4X) spike in two ester groups (Methacrylic acid tetradecyl ester and n-Dodecyl methacrylate) at the late season measurement (Figure 4.32, 4.34) and 675 had a very low prevalence of these compounds (Figure 4.31). Genotype 675 had a large decrease in the concentration of alkanes C28 (-0.018 $\mu\text{m/g}$), C31(-0.03 $\mu\text{m/g}$), C33(-0.038 $\mu\text{m/g}$), C35(-0.02 $\mu\text{m/g}$)

(Figure 4.31) by comparison 884 and 959 had no change in alkanes (

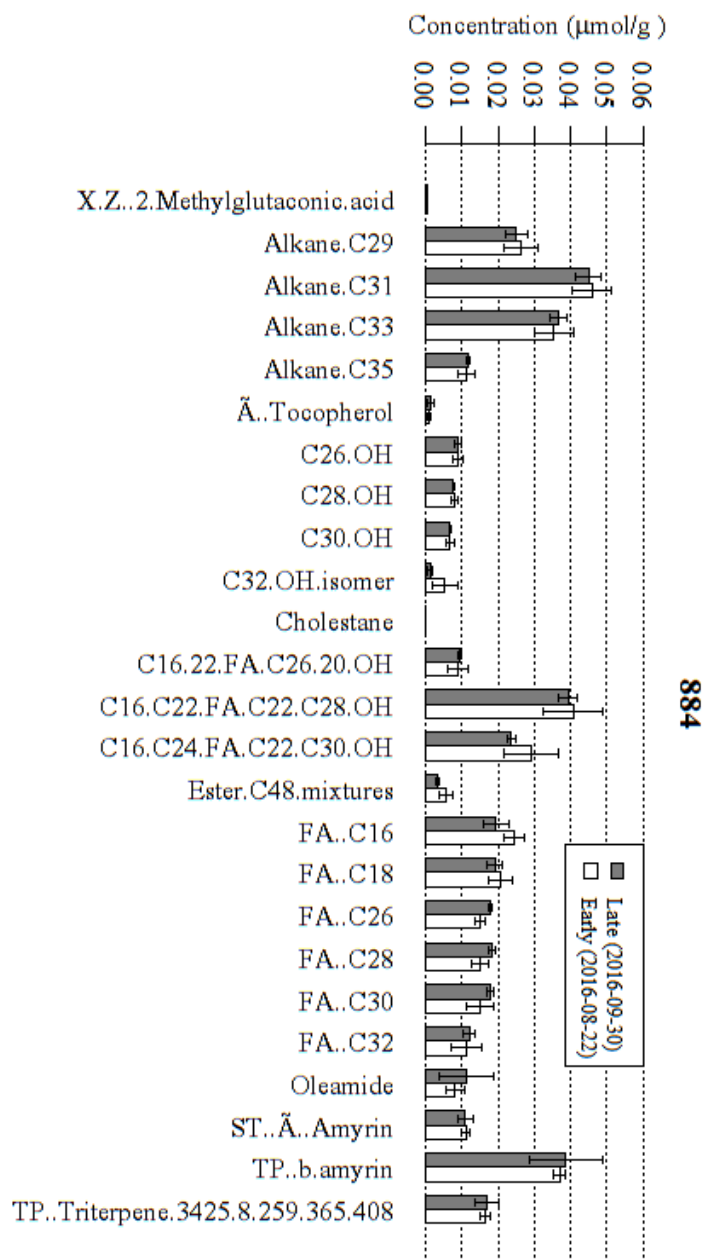


Figure 4.33, 4.35).

Unlike the results from the ‘mild’ conditions, there were large changes in the percentage abundance of chemical classes of the field produced samples between early (2016-08-22) and

late (2016-09-30) measurements across all three genotypes. As was noted in the concentration changes, there was no change in percentage of alkane in 675, while 884 and 959 expressed large percentage concentration increases in late season, +12% and 22%, respectively (Figure 4.36). A large negative ester shift was measured in 884 (-34%) and 959(-60%) with a strong decrease in field produced samples following late (2016-09-30) period measurement (Figure 4.36).

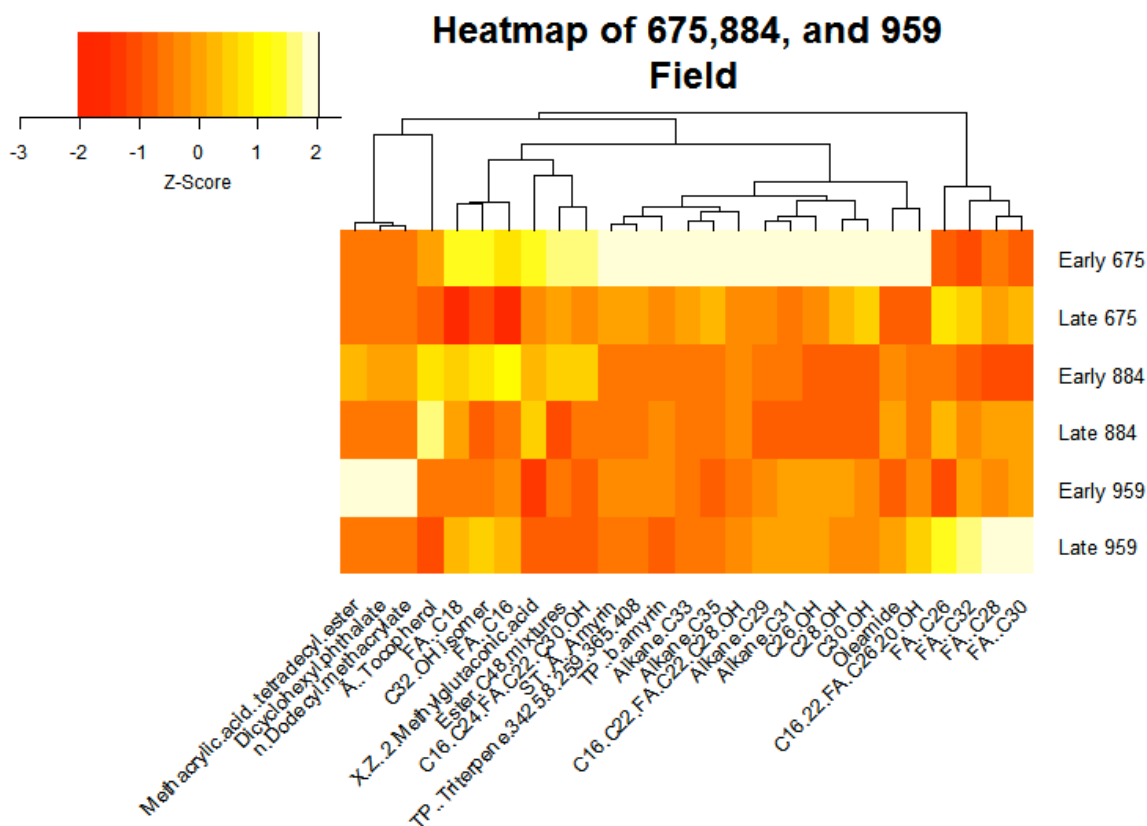


Figure 4.30 Heat Map and Dendrogram of three field produced genotypes (675, 884, 959) by two treatments (early; 2016-08-22, late; 2016-09-30), showing z-scores of adjusted metabolites, mean-centered and scaled by mean and standard deviation (light, lower abundance; dark, higher abundance) as indicated in the legend, across the cuticular composition of 28 key compounds from mature corn of leaf (V6; adaxial side) surface lipid extracts.

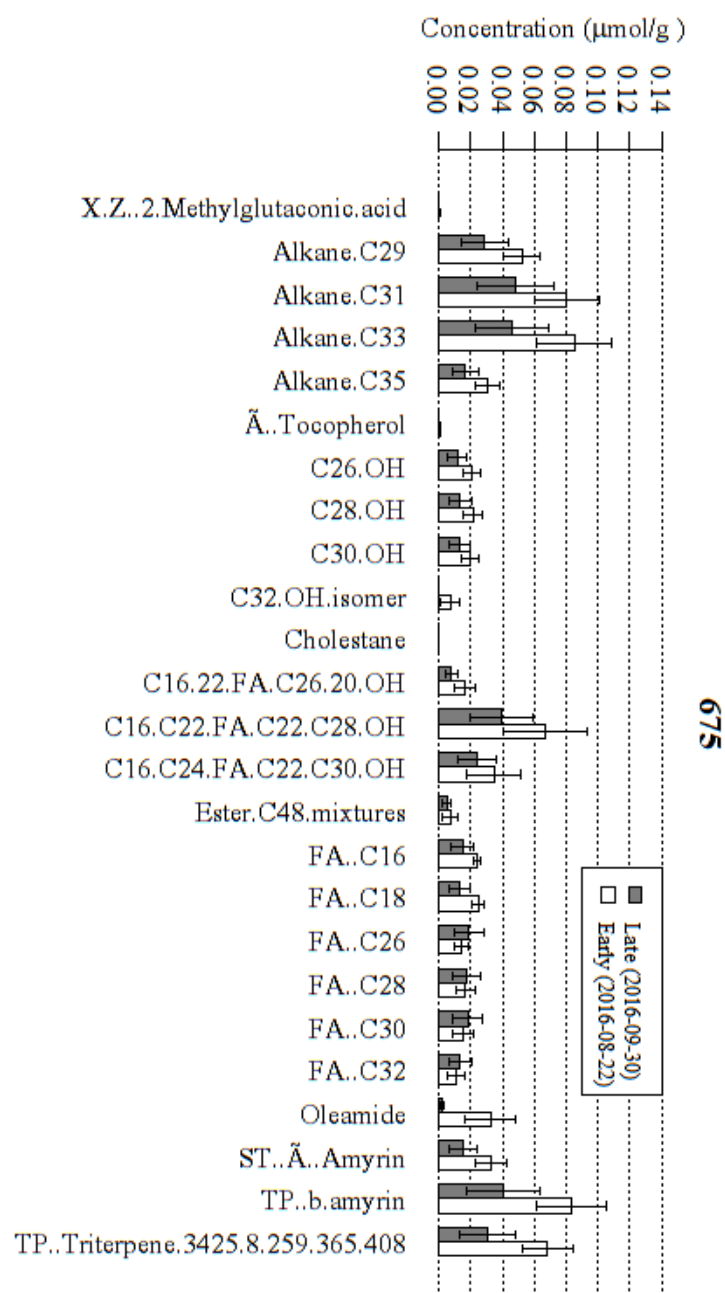


Figure 4.31 Field produced cuticular wax composition of two treatments (early; 2016-08-22, late; 2016-09-30) on the concentration of 28 compounds of the cuticular wax extracted and analyzed from adaxial surface of mature corn leaf (V6) in genotype 675Three replicates. Error bars denote standard error.

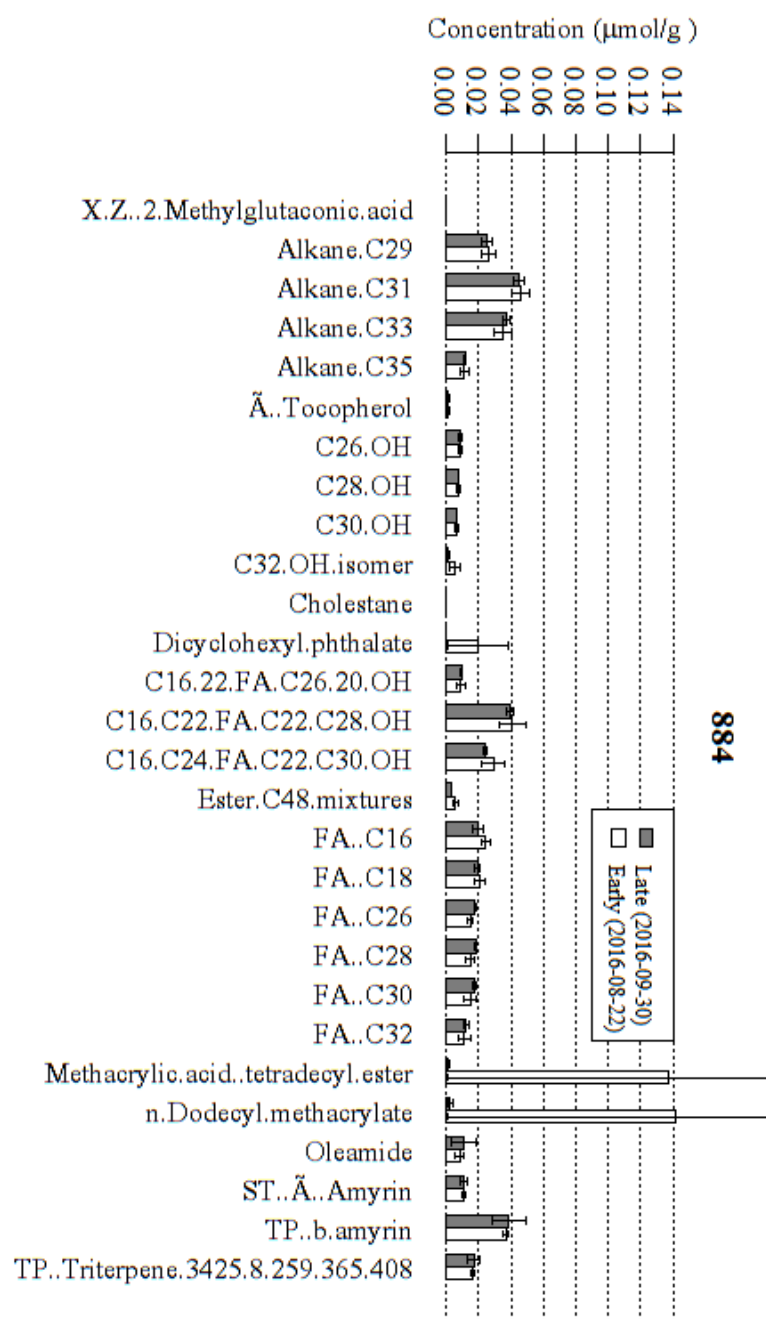


Figure 4.32 Field produced cuticular wax composition of two treatments (early; 2016-08-22, late; 2016-09-30) on the concentration of 28 compounds of the cuticular wax extracted and analyzed from adaxial surface of mature corn leaf (V6) in genotype 884. Three replicates. Error bars denote standard error.

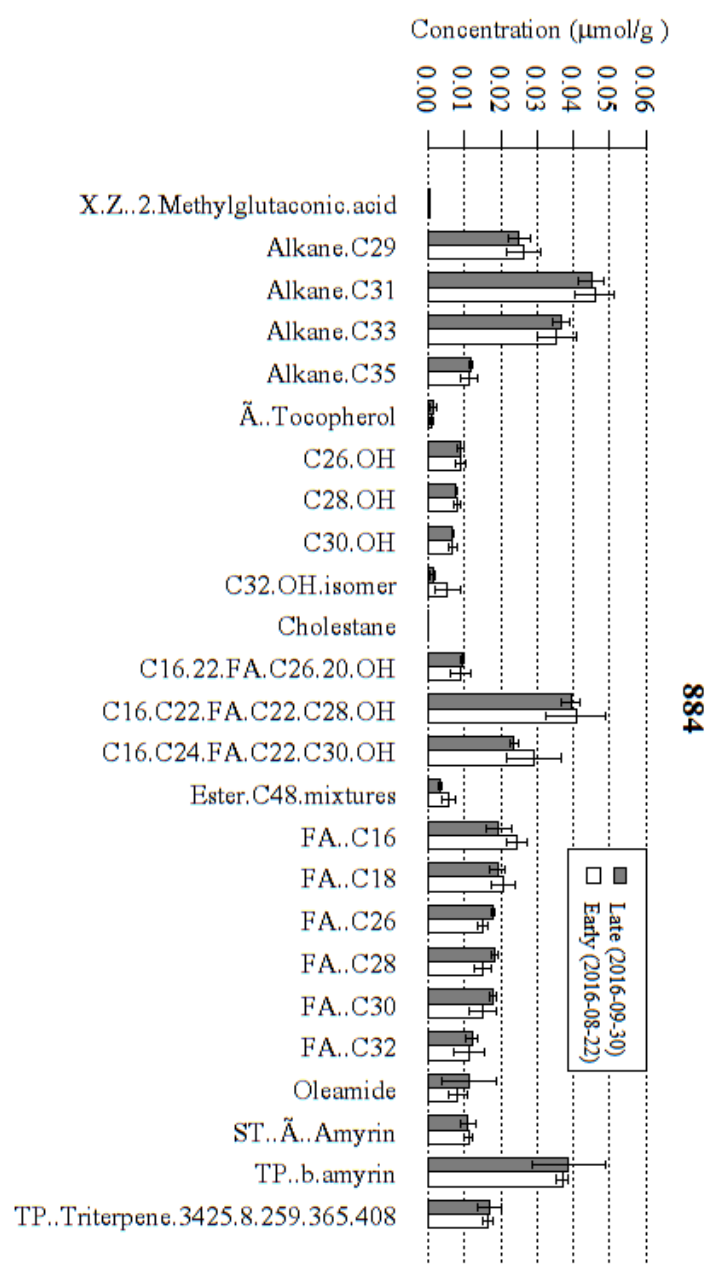


Figure 4.33 Field produced cuticular wax composition of two treatments (early; 2016-08-22, late; 2016-09-30) on the concentration of 26 compounds (Methacrylic acid tetradecyl ester, n-Dodecyl methacrylate removed) of the cuticular wax extracted and analyzed from adaxial surface of mature corn leaf (V6) in genotype 884. Three replicates. Error bars denote standard error.

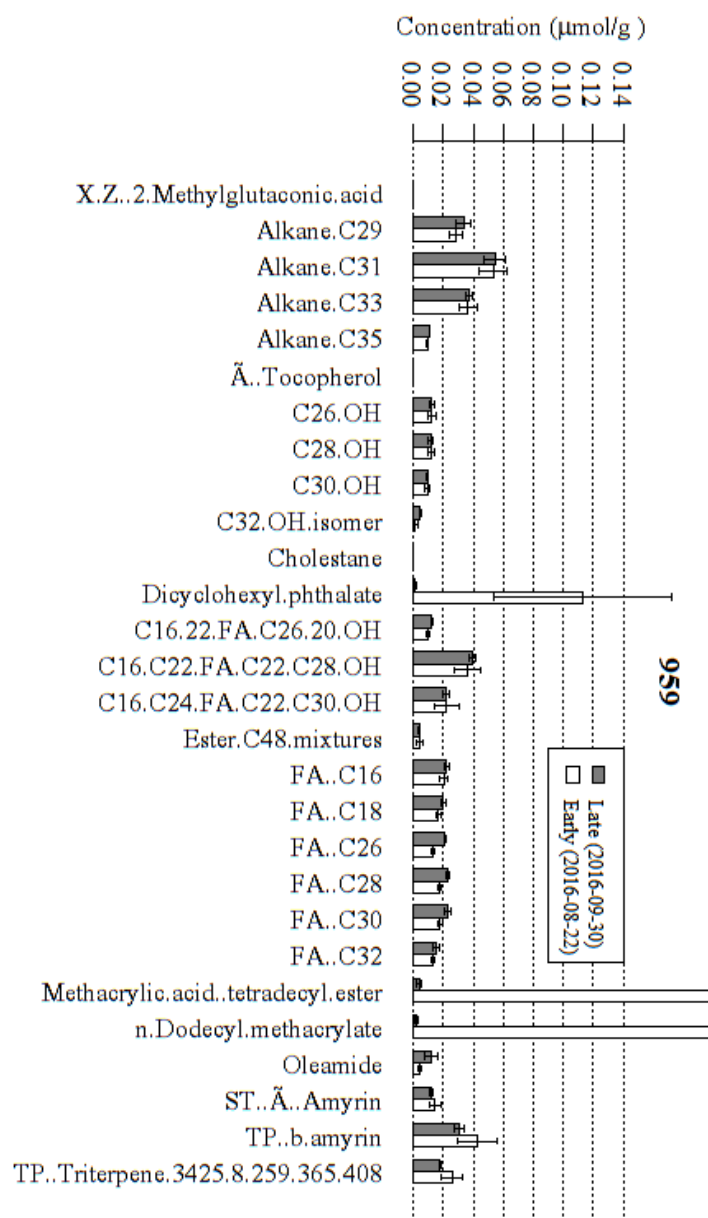


Figure 4.34 Field produced cuticular wax composition of two treatments (early; 2016-08-22, late; 2016-09-30) on the concentration of 28 compounds of the cuticular wax extracted and analyzed from adaxial surface of mature corn leaf (V6) in genotype 959. Three replicates. Error bars denote standard error.

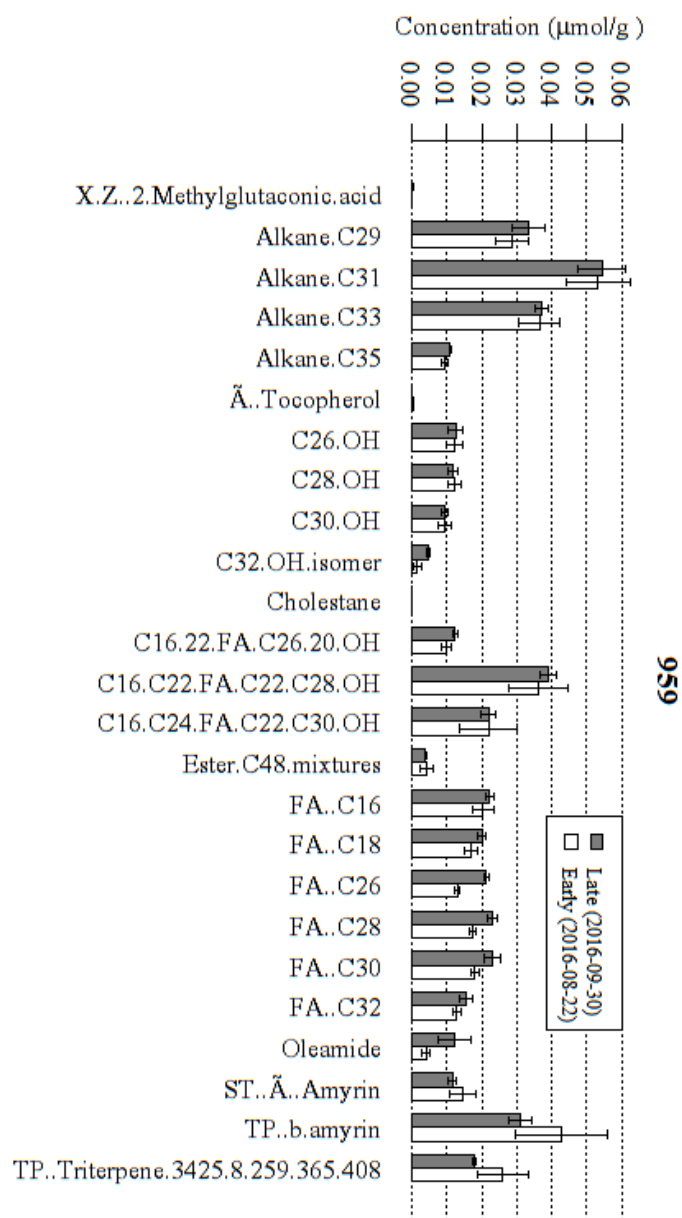


Figure 4.35 Field produced cuticular wax composition of two treatments (early; 2016-08-22, late; 2016-09-30) on the concentration of 26 compounds (Methacrylic acid tetradecyl ester, n-Dodecyl methacrylate removed) of the cuticular wax extracted and analyzed from adaxial surface of mature corn leaf (genotype 959). Three replicates. Error bars denote standard error.

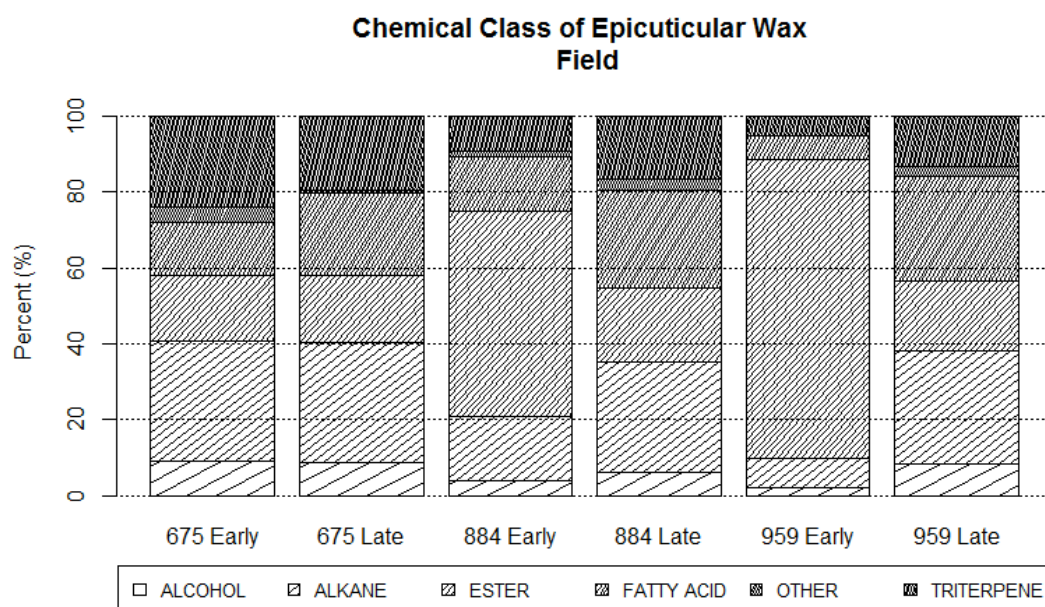


Figure 4.36 Percentage abundance of chemical classes (alcohol, alkane, ester, fatty acid, other and triterpene) of three Field produced genotypes (675, 884, 959) across two treatments (early; 2016-08-22, late; 2016-09-30) of the cuticular wax extracted and analyzed from adaxial leaf (V6) surface of mature corn leaves. Three replicates.

4.4 Discussion

This study continues to evaluate potential physical markers indicative of freezing avoidance by investigation into ice nucleation avoidance and cuticular alterations following chilling treatment through physical and biochemical modifications. Linking trait modification of cuticular wax to freezing avoidance works towards the objective of addressing the need for increased global food production, specifically expansion opportunities into cool temperate regions with abundance of arable land such as the Canadian prairies, for grain corn. The cuticle is essential to support plant life (Kerstiens 1996). The prevalence of the cuticle on all terrestrial land plants may make cuticular waxes one of the most high abundance sources for very long chain fatty acids (VLCFA)(Perera 2005). VLCFA are classified as 20 carbon chain length and greater. These compounds are found in cuticular waxes and cutin on the surface of aerial plant parts. Utilization of a variety of complementary techniques was used to identify physical and biochemical markers linked to freezing avoidance for relative high-throughput screening of cuticular modifications for pre-existing germplasm.

The study utilized techniques, such as confocal laser scanning microscopy coupled with mid-IR spectroscopy and gas chromatography mass spectrometry, to evaluate physical (cuticular thickness), biochemical composition (lipid fingerprint region spectra) and biochemical localization and quantification (GC-MS). The purpose of a combined technique approach was to identify markers linked to freezing avoidance using mature hybrid grain corn leaf samples of four contrasting chilling resistant genotypes.

The results indicate that under ‘mild’ chilling conditions (ten day) the cuticular thickness remains unchanged, by contrast, however, longer duration (five weeks) field conditions indicate a statistically significant increase ($p < 0.05$) in the thickness of the cuticle. In addition to cuticle thickness there were also genotypic differences detectable. Freezing sensitive genotype (256) was found to have a significantly ($p < 0.05$) thinner cuticle compared with all other genotypes. The integrity of the cuticular wax membrane is known to change under varied environmental parameters (Sherrick et al. 1986). Differences in controlled environment chamber and field results could be explained by the variability between environments. Factors such as direct sunlight (Skoss 1955, Hull et al. 1975), temperature and water stress (Skoss 1955), relative humidity (Sutter 1979) and photoperiod (von Wettstein-Knowles 1982) are possible confounding

factors. Fluctuations in these environmental factors would be more severe under field production compared with ‘mild’ chilling condition produced and may have contributed to the differences in our findings. In addition to environmental factors, there is potential for duration effect to modify the cuticular thickness. For example, a five-week period under field conditions was subject to a longer period to synthesize wax than the ten days under ‘mild’ chilling treated. In leek (*Allium purrum* L.), previous late stage wax synthesis occurred beyond cell expansion stage (Rhee et al. 1998) and it has been observed that the distribution of chemical compounds in the cuticle to differ based on developmental age (Jetter and Schäffer 2001). Aside from known environmental modifiers, we did observe significant late season affect with a comparable time period (2 weeks) to ‘mild’ condition results as observed in the field between 24-08-2016 and 12-09-2017 (Table 4.5).

Although there were no significant cuticular thickness modifications under ‘mild’ chilling treatment, it is notable that cuticle thickness has been shown in an array of species to not correlate with water permeability and surface interaction (Riederer and Schreiber 2001) while in other studies a thicker cuticle was shown to be effective in avoiding ice nucleation (Wisniewski and Fuller 1999, Workmaster et al. 1999) however generally in herbaceous plants the cuticle alone was not enough to prevent ice nucleation (Wisniewski et al. 2002). The ATR-FTIR spectroscopy results during this period indicate that, biochemically, there are significant modifications occurring in the CH₃ region of the lipid fingerprint. The CH₃ group is indicative methyl groups rather than methylene as are found within the band. The methyl groups are an extension of aliphatic compounds and aromatic residuals most closely associated to cutan (Heredia-Guerrero et al. 2014). The aliphatic hydrocarbon functional group combined with its derivatives (alcohols, alkanes, ketones, and esters) comprise plant waxes and cutin and are hydrophobic (Koch and Ensikat 2008). Aromatic residuals are known for their influence over protein regulation and stability in addition to their hydrophobic characteristics (Howell et al. 1999, Dougherty 2007). Adam and Elliott (1962) demonstrated the strong hydrophobic characteristics of methyl over methylene (~30% greater). The differences found through FTIR-ATR would suggest that FTIR-ATR is a more sensitive measurement and is detectable at lower limits than CLSM cuticle thickness measurements. In previous gas chromatography on cuticle isolation in tomato and apple (Chen et al. 2008), as well as corn and *Arabidopsis thaliana* (Kunst and Samuels 2003) aliphatic carbon compounds were found to be an important component of the

chemical makeup (Chen et al. 2008). The ATR-FTIR study indicated over a ten day ‘mild’ chilling treatment, chilling treated samples have higher cuticular wax content. The exception to this being genotype 675, which was once again found to be non-responsive to chilling treatment.

Under field conditions, the ATR-FTIR findings across all three regions of interest demonstrated a tendency to decrease wax intensity over the five-week treatment period. This is to be expected as Region 2 and 3, the asymmetrical and symmetrical CH₂ groups, respectively, represent identical groups of compounds, only with varying geometric conformations. The symmetrical group represents biomolecules in-phase and more non-polar than asymmetrical groups which have uneven molecule bond bending. Non-polar groups are more hydrophobic as water is a polar molecule and would be attracted to polarity in a molecule. Symmetric non-polar molecules typically have a higher melting point and lower solubility (Pinal 2004) also leading to improved hydrophobicity. This decrease in wax intensity could be attributed to the modification of percentage of classes of compounds as outlined in the GC-MS results for the field conditions indicating that the prevalence of longer chain fatty acids and larger biomolecules were preferentially synthesized over time. This preferential synthesis would be advantageous from both an energy savings and physiological barrier perspective.

There are two distinct pathways for VLCFA synthesis: acyl reduction and decarbonylation. The pathway for ester synthesis (acyl reduction) seems to have slowed greatly in the field grown resistant genotypes (884,959) and it has been found in maize for the reduction pathway to occur in lower levels as the tissue matures (Perera 2005) Ester-cutin has been shown to be converted into both cutan and non-ester cutin after cell expansion stages (Schreiber and Schonherr 2009). In sorghum (*Sorghum bicolor*) and *Arabidopsis*, indicate a likelihood for increased chain length in wax accumulation over time (Atkin and Hamilton 1982, Jenks et al. 1996). Riederer and Schneider (1990) found that warm day/night temperature modify wax composition percentages and most constituents respond with increase to warm days with the exception of esters. Esters were found to preferentially increase with warm night temperatures (Riederer and Schneider 1990). In our studies, the night temperatures were drastically getting cooler during the late period (Appendix A), and this may account for the drop in ester production within the field conditions despite an increase in the alcohols which act as the building blocks for ester groups.

Further, the modifications of the distribution and chemical composition expected are only to a moderate degree (Baker et al. 1982, Prasad and Gölz 1990, Maier and Post-Beittenmiller 1998, Jetter and Schäffer 2001). This may explain the subtle differences observed in the ten day ‘mild’ treatment. As the resultant spectra are a measure of specific vibrational signatures of the atoms in the molecule (Türker-Kaya and Huck 2017), a shift towards an increased prevalence of alkanes and long chain fatty acids, as was observed in the field sample percent abundance chemical shift, may in part explain the reduction in the intensity in the spectra in the lipid fingerprint; rather the biochemical makeup of larger molecules is modifying the spectra response. Lastly the limitation of the penetration of the IR light into the thicker field produced cuticle could represent a biased sampling of the upper surface of the wax. The upper surface of the wax will degrade overtime due to environmental impact and new deposition occurs on the innermost side adjacent to the epidermis and may not have been adequately excited by the light to measure true accumulation.

The lipidomics work using GC-MS indicate under ‘mild’ chilling conditions the genotypic differences were strong compared with chilling treatment induced modifications. These findings were not expected as genotypic variation was not discernable from the spectra collected using ATR-FTIR, demonstrating the necessity of combined techniques. GC-MS is commonly preferentially used in lipid analysis due to superior quantification and high accuracy for identification of compounds (Heredia-Guerrero et al. 2014). However, based on the findings of differing response to freezing avoidance following chilling treatment between 884 and 959, it was suspected that they may have different freezing avoidance contributors. Significant shifts ($p < 0.05$) in percentage abundance of groups of compounds in the field samples induced by the chilling treatment were observed. Notable increases were identified in alkanes and fatty acid groups. These long chain carbon compounds are known contributors to the hydrophobic properties of the cuticular surface (Nadiminti et al. 2015). In addition to these larger group percentage shifts, in genotype 884 a significant increase ($p < 0.05$) was observed in oleamide. Oleamide is an extremely hydrophobic compound and has been indicated in thermoregulation and sensitivity (Laws et al. 2001) as well as signaling systems and plant defense (Chatterjee et al. 2010). As a percentage composition change we observed a strong decrease in triterpenes. Pentacyclic triterpenoids are found in many wax species (Jetter et al. 2007) and they tend to

accumulate in the intracuticular wax (Buschhaus and Jetter 2012). In 959, a significant decrease ($p < 0.05$) in amyirin was observed. In work by Buschhaus and Jetter (2012), they found that B-amyirin was detrimental to the integrity of the water barrier. A decrease in amyirin would be a beneficial survival mechanism to maintain a strong barrier during ice propagation. Previous works have established gas chromatography as a valuable tool to understand the multifaceted nature of the cuticle, as a complicated hydrophobic layer (Jetter et al. 2007, Nadiminti et al. 2015).

In response to our sub-hypothesis, that chilling treatment will cause contrasting chilling resistant genotypes to modify cuticular thickness or biochemical composition, we conclude that chilling treatment increases cuticular thickness over time and that the chemical makeup is changed in the aliphatic region with a shift toward decreased intensity in the CH_3 of ‘mild’ produced samples and a consistent decrease across the lipid region over the 5-week field produced samples. The variability induced by the chilling treatment can be represented by 28 compounds identified through gas chromatography mass spectrometry.

In future studies, investigation of the physical and biochemical cuticular modifications occurring in other economically important crops with contrasting chilling resistance, both in field and controlled environment conditions, would further the understanding and ability to map the link between chemical makeup and the spectral signatures for a more high-throughput approach. Another area of interest would be to track the modifications from seedling to maturation to establish early season traits that may correlate to late fall season freezing avoidance.

In summary, characteristics linked to the cuticular layer as a barrier indicates importance to freezing avoidance such as: a thinner cuticle associated with more freezing sensitive genotype (256) and agreeance with the previous chapter, chilling treatment in the field tends to demonstrate a negative effect on the total wax production and favors longer chain carbon aliphatic compounds. Longer chain fatty acids have a low polarity, compared with short and medium chain fatty acids, making them well suited to create a hydrophobic moisture barrier (Gunstone 2006). A highly hydrophobic barrier, made of long chain, and unsaturated fatty acids (Ivanov 2015) seems to be effective in freezing avoidance through delay of ice nucleation into the intracellular space (Wisniewski and Fuller 1999, Fuller et al. 2003, Wisniewski et al. 2009). This study reinforces the evidence that the cuticular layer is a critical region of interest to

improve freezing avoidance to move corn into new geographies for increased acreage and consistent production.

CHAPTER 5

GENERAL DISCUSSION

Cuticular modifications following chilling treatment were demonstrated using a complementary suite of techniques. The impact of fall conditions on freezing avoidance has not been well studied. Freezing avoidance is of critical importance in chilling and freezing sensitive crops, such as corn. Once ice enters the intracellular space in these plants it is always lethal. Chilling treatment appears to signal both physical and biochemical modifications within the cuticle in both controlled growth environment and field studies. The overall hypothesis that chilling treatment will alter cuticular characteristics that are linked to ice nucleation avoidance, was supported by the research findings as is described in the visual model below (Figure 5.1).

The cuticle has been long proposed as a critical barrier to biotic and abiotic stresses, including freezing avoidance. The modifications which occur prior to the first freezing event, during the fall frost-free period, specifically the non-lethal pre-chilling temperatures have not been widely investigated. The ability to avoid freezing was significantly reduced in all genotypes following chilling treatment. This caused the plants to be less able to tolerate freezing temperatures. The deterioration in freezing avoidance following chilling treatment, indicated that these genotypes at physiological maturity were not able to acclimate. By contrast, other comparable locally produced grain crops are more resistant and can avoid and tolerate similar stress. Typically when plants are exposed to chilling treatment, an acclimation response is exhibited and subsequent freezing resistance (avoidance + tolerance) is improved. To trigger

these kinds of responses in a sub-tropically originated species such as corn, it may be necessary to tap into ancestral and diversity panel materials. One of the limitations of this study was the limited diversity within our materials to respond to cold treatment. A key limitation of this study was the infrared light sample penetration depth, especially into the thicker field produced cuticle. The cuticle is synthesized in the plastid by de novo fatty acid biosynthesis of C16 or C18 and transported into the endoplasmic reticulum (ER) with chain extension of 2 carbons per cycle by fatty acid elongase (FAE) to generate VLCFA's (von Wettstein-Knowles 1993, Kunst and Samuels 2003, Kunst et al. 2005, Perera 2005). The wax is transported by lipid transfer proteins to the epidermal surface (Pyee et al. 1994) with heterogenous deposition in layers (Jetter and Schäffer 2001).

The inability of this material to cold acclimate led into an additional investigation of how the cuticle was acting as a barrier in the protection of ice nucleation and characterization of modifications which were occurring during chilling treatment. Although both physical and biochemical modifications were observed it appeared that the impact of the cuticular modification was greater in biochemical measurements. It is unclear whether biochemical modifications are occurring more quickly or if the detection limits are simply substantially better. However, it is clear that FTIR and GC-MS provide complementary feedback. In field studies, it was found that the cuticle thickness increased significantly over time. The controlled environment studies did not observe that same degree of change. This indicated that both outdoor environmental shift and duration play a critical role in wax deposition. Field studies provide great value and insight into how materials will perform in a multi-variate environment however they also come with some challenges. Field studies add a great deal of complication into the analysis, but they provide invaluable insight into true performance metrics. Aligning chamber

and field studies remains difficult. Chamber studies allow for the utmost control of variables, year-round production, and intensive growing. By contrast field studies allow for extreme and fluctuating realistic conditions to draw out intensified and additive factor results. These differences create a challenge to correlate and draw conclusions between chamber and field results.

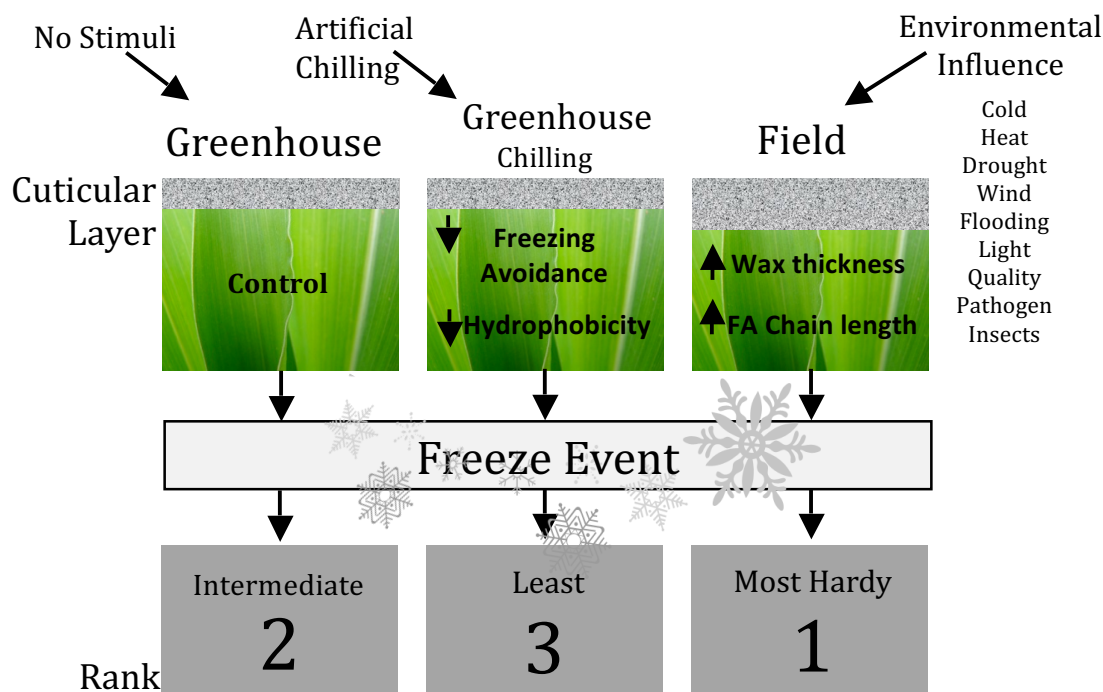


Figure 5.1: Ultrastructural and Biochemical Cuticle Model Flowchart

Using mature corn, with contrasting chilling resistant genotypes for understanding modifications to the adaxial cuticular layer has shown to be a useful model. This system enabled investigation of the physiological mechanisms within the cuticle, acting as a barrier, between the plant and environment to control and prevent ice nucleation. Continued development of an understanding for implications of the cuticular influence on freezing avoidance has widespread potential. It will impact the development and expansion of underutilized crops into temperate regions abundant in arable land. In order to meet the needs of the demand to move the cornbelt

northward, this crop will need to be more frost avoidant. Global warming will necessitate new production regions due to reduced snow cover and deacclimation. Adequate freezing avoidance may allow increased distribution of freezing resistant trait-tailored annual crops into new geographies as the need for world food security soars.

5.1 Future Research Directions

Future work to build upon this study could include a wider diversity panel as well as testing the system on other Western Canadian grain crops. Development of protocols to sample the entire wax thickness would enable higher-throughput of materials with more precise data feedback. This system could also reduce costs and time through the reduction in the need to use GC-MS. In order to displace the GC-MS, an cuticular wax specific library would need to be developed to localize more specific compounds within the spectra. Other future work could include correlation analysis of the carbohydrates and proteins within the spectra, to provide a more complete picture of leaf level changes.

5.2 Novel Findings

The key novel finding of this work was of the reduced plasticity to respond to temperature changes of the plant in a mature stage. In addition, the finding for both hydrophobicity and temperature to ice nucleation to be impaired following chilling treatment was unexpected and did not follow the typical acclimation response. Lastly, the lipid region modifications especially in region 1 (CH₃ functional group) provide evidence for the very hydrophobic alkane groups' important contribution towards the cuticle layer as a barrier for ice nucleation. This finding was reinforced by the GC-MS increase in alkanes and other hydrophobic VLCFA's following chilling treatment.

5.2 Conclusions

- Chilling Treated Plants Freeze at Significantly Warmer Temperature
- Hydrophobicity is significantly reduced following chilling exposure
- Cuticular thickness does not change in the 'mild' condition
- Cuticular thickness increases over time in the Field
- 'mild' chilling treatment indicated increasing cutan, cutin, & epicuticular wax in Region 1
- Field treatment indicated reduction in cutan, cutin, and epicuticular wax in Region 1, 2 &3
- 142 Known Compounds Found were identified
- 28 Compounds were found to represent variation between CT and NC in 'Mild' and field
- 5 Classes of compounds identified of the 28 key

LIST OF REFERENCES

- Adam, N. and G. Elliott (1962). "Contact angles of water against saturated hydrocarbons." Journal of the Chemical Society(JUN): 2206-&.
- Albersheim, P., et al. (2010). Plant cell walls, Garland Science.
- Alexandratos, N. and J. Bruinsma (2012). World agriculture towards 2030/2050: the 2012 revision, ESA Working paper Rome, FAO.
- Allen, D. J. and D. R. Ort (2001). "Impacts of chilling temperatures on photosynthesis in warm-climate plants." Trends in plant science **6**(1): 36-42.
- Anderson, M. D., et al. (1994). "Differential gene expression in chilling-acclimated maize seedlings and evidence for the involvement of abscisic acid in chilling tolerance." Plant physiology **105**(1): 331-339.
- Araus, J., et al. (2002). "Plant breeding and drought in C3 cereals: what should we breed for?" Annals of Botany **89**(7): 925-940.
- Arbuckle, J. G., et al. (2013). "Climate change beliefs, concerns, and attitudes toward adaptation and mitigation among farmers in the Midwestern United States." Climatic Change **117**(4): 943-950.
- Ashraf, M. and L. Wu (1994). "Breeding for salinity tolerance in plants." Critical Reviews in Plant Sciences **13**(1): 17-42.
- Ashworth, E., et al. (1988). "Ice formation and tissue response in apple twigs." Plant, cell & environment **11**(8): 703-710.
- Ashworth, E. and T. Kieft (1995). "Ice nucleation activity associated with plants and fungi." Biological ice nucleation and its applications. APS Press, St. Paul, Minn: 137-162.
- Ashworth, E. N. and R. S. Pearce (2002). "Extracellular freezing in leaves of freezing-sensitive species." Planta **214**(5): 798-805.
- ASTM Compass C813 (2014). Standard Test Method for Hydrophobic Contamination on Glass by Contact Angle Measurement. ASTM C813. West Conshohocken, Pennsylvania, United States, ASTM International.
- Atkin, D. and R. Hamilton (1982). "The changes with age in the epicuticular wax of Sorghum bicolor." Journal of Natural Products **45**(6): 697-703.
- Audisio, G., et al. (1987). "CGC- MS determination of mixtures of long chain aliphatic esters." Journal of Separation Science **10**(11): 594-597.

Avato, P., et al. (1990). "Chemosystematics of surface lipids from maize and some related species." Phytochemistry **29**(5): 1571-1576.

Avato, P., et al. (1987). Ontogenetic Variations in the Chemical Composition of Maize Surface Lipids. The Metabolism, Structure, and Function of Plant Lipids. P. Stumpf, J. B. Mudd and W. D. Nes, Springer New York: 549-551.

Azócar, A., et al. (1988). "Freezing tolerance in *Draba chionophila*, a 'miniature' caulescent rosette species." Oecologia **75**(1): 156-160.

Baker, E. (1974). "The influence of environment on leaf wax development in *Brassica oleracea* var. *gemmifera*." New Phytologist **73**(5): 955-966.

Baker, E., et al. (1982). Composition of tomato fruit cuticle as related to fruit growth and development. Linnean Society symposium series.

Bakhsh, A. and T. Hussain (2015). "Engineering crop plants against abiotic stress: current achievements and prospects." Emirates Journal of Food and Agriculture **27**(1): 24.

Bargel, H., et al. (2004). "Plant cuticles: multifunctional interfaces between plant and environment." Evolution of plant physiology. Academic, London: 171-194.

Bargel, H., et al. (2006). "Evans Review No. 3: Structure–function relationships of the plant cuticle and cuticular waxes—a smart material?" Functional Plant Biology **33**(10): 893-910.

Barron, C. (2011). "Prediction of relative tissue proportions in wheat mill streams by Fourier transform mid-infrared spectroscopy." Journal of agricultural and food chemistry **59**(19): 10442-10447.

Beck, E., et al. (1984). "Equilibrium freezing of leaf water and extracellular ice formation in Afroalpine 'giant rosette' plants." Planta **162**(3): 276-282.

Benitez, J. J., et al. (2004). "Plant biopolyester cutin: a tough way to its chemical synthesis." Biochimica et Biophysica Acta (BBA)-General Subjects **1674**(1): 1-3.

Bianchi, A., et al. (1985). "Biosynthetic pathways of epicuticular wax of maize as assessed by mutation, light plant age inhibitor studies." Maydica **30**: 179-198.

Bianchi, G., et al. (1989). "Composition and structure of maize epicuticular wax esters." Phytochemistry **28**(1): 165-171.

Biel, E. R. (1961). "Microclimate, bioclimatology, and notes on comparative dynamic climatology." American Scientist **49**(3): 326-357.

Bird, S. M. and J. E. Gray (2003). "Signals from the cuticle affect epidermal cell differentiation." New Phytologist **157**(1): 9-23.

Bornman, C. H. and E. JANSSON (1980). "Nicotiana tabacum callus studies. X. ABA increases resistance to cold damage." Physiologia Plantarum **48**(4): 491-493.

Boyer, J. S. (1982). "PLANT PRODUCTIVITY AND ENVIRONMENT." Science **218**(4571): 443-448.

Brongniart, A. T. (1834). Nouvelles recherches sur la structure de l'épiderme des végétaux.

Brown, R. A. and N. J. Rosenberg (1999). "Climate change impacts on the potential productivity of corn and winter wheat in their primary United States growing regions." Climatic Change **41**(1): 73-107.

Buda, G. J., et al. (2009). "Three- dimensional imaging of plant cuticle architecture using confocal scanning laser microscopy." The Plant Journal **60**(2): 378-385.

Budke, J. M., et al. (2012). "The cuticle on the gametophyte calyptra matures before the sporophyte cuticle in the moss *Funaria hygrometrica* (Funariaceae)." American Journal of Botany **99**(1): 14-22.

Burke, M., et al. (1976). "Freezing and injury in plants." Annual Review of Plant Physiology **27**(1): 507-528.

Buschhaus, C. and R. Jetter (2012). "Composition and physiological function of the wax layers coating *Arabidopsis* leaves: β -amyirin negatively affects the intracuticular water barrier." Plant physiology **160**(2): 1120-1129.

Buttner, K. (1934). "Die Übertragung durch Leitung und Konvektion, Verdunstung und Strahlung in Bioklimatologie und meteorologie (Abh. preuss.). meteorol." Institut **10**: 37.

Canada. Agriculture Agri-Food Canada issuing body (2015). Corn. Agriculture and Agri-Food Canada. Ottawa, Canada.

Cannell, M. and R. Smith (1986). "Climatic warming, spring budburst and forest damage on trees." Journal of Applied Ecology: 177-191.

Carter, J., et al. (1999). "Low-temperature tolerance of blackcurrant flowers." HortScience **34**(5): 855-859.

Carter, J., et al. (2001). "Patterns of ice formation and movement in blackcurrant." HortScience **36**(6): 1027-1032.

Casado, C. G. and A. Heredia (2001). "Specific heat determination of plant barrier lipophilic components: biological implications." Biochimica et Biophysica Acta (BBA)-Biomembranes **1511**(2): 291-296.

Castiglioni, P., et al. (2008). "Bacterial RNA chaperones confer abiotic stress tolerance in plants and improved grain yield in maize under water-limited conditions." Plant physiology **147**(2): 446-455.

Catalá, R., et al. (2011). "Integration of low temperature and light signaling during cold acclimation response in Arabidopsis." Proceedings of the National Academy of Sciences **108**(39): 16475-16480.

Ceccardi, T. L., et al. (1995). "Low-temperature exotherm measurement using infrared thermography." HortScience **30**(1): 140-142.

Celler, K., et al. (2016). "Microtubules in plant cells: strategies and methods for immunofluorescence, transmission electron microscopy, and live cell imaging." Cytoskeleton methods and protocols: methods and protocols: 155-184.

Chatterjee, S., et al. (2010). "Bioactive lipid constituents of fenugreek." Food chemistry **119**(1): 349-353.

Chefetz, B. (2007). "Decomposition and sorption characterization of plant cuticles in soil." Plant and soil **298**(1-2): 21-30.

Chen, B., et al. (2008). "Role of the extractable lipids and polymeric lipids in sorption of organic contaminants onto plant cuticles." Environmental science & technology **42**(5): 1517-1523.

Chen, H.-H. and P. H. Li (1982). Potato Cold Acclimation. Plant Cold Hardiness and Freezing Stress. P. H. L. Sakai, Academic Press: 5-22.

Chen, T. H.-H., et al. (1983). "Freezing injury and root development in winter cereals." Plant physiology **73**(3): 773-777.

Chen, T. H. and L. V. Gusta (1983). "Abscisic acid-induced freezing resistance in cultured plant cells." Plant physiology **73**(1): 71-75.

Chéné, Y., et al. (2012). "On the use of depth camera for 3D phenotyping of entire plants." Computers and Electronics in Agriculture **82**: 122-127.

Chhetri, N. B., et al. (2010). "Modeling path dependence in agricultural adaptation to climate variability and change." Annals of the Association of American Geographers **100**(4): 894-907.

Chibnall, A. C., et al. (1934). "The constitution of the primary alcohols, fatty acids and paraffins present in plant and insect waxes." Biochemical Journal **28**(6): 2189.

- Chichester, C. O. (1979). Advances in Food Research. London, Academic Press, Inc.
- Clawson, K. L. and B. L. Blad (1982). "Infrared thermometry for scheduling irrigation of corn." Agronomy journal **74**(2): 311-316.
- Dietrich, C. R., et al. (2005). "Characterization of two GL8 paralogs reveals that the 3- ketoacyl reductase component of fatty acid elongase is essential for maize (*Zea mays* L.) development." The Plant Journal **42**(6): 844-861.
- Dilcher, D. L. (1974). "Approaches to the identification of angiosperm leaf remains." The botanical review **40**(1): 1-157.
- Dolgin, E. (2009). "Maize genome mapped." Nature News **1098**.
- Dougherty, D. A. (2007). "Cation- π interactions involving aromatic amino acids." The Journal of nutrition **137**(6): 1504S-1508S.
- DuPont Pioneer (2017). "Corn in Western Canada." from https://www.pioneer.com/home/site/ca/products/corn/western_canada_corn/?site=saskatoon.
- Eagles, H. and A. Hardacre (1979). "Genetic variation in maize for early seedling growth in a low temperature environment." New Zealand journal of agricultural research **22**(4): 553-559.
- Edwards, D. (1993). "Cells and tissues in the vegetative sporophytes of early land plants." New Phytologist **125**(2): 225-247.
- Ellenson, J. L. and R. G. Amundson (1982). "Delayed light imaging for the early detection of plant stress." Science **215**(4536): 1104-1106.
- Ensikat, H., et al. (2010). "Scanning electron microscopy of plant surfaces: simple but sophisticated methods for preparation and examination." Microscopy: Science, technology, applications and education **1**(13): 248-255.
- Environment and Climate Change Canada (1981-2010). "Canadian Climate Normals." from http://climate.weather.gc.ca/climate_normals/index_e.html.
- España, L., et al. (2014). "Biomechanical properties of the tomato (*Solanum lycopersicum*) fruit cuticle during development are modulated by changes in the relative amounts of its components." New Phytologist **202**(3): 790-802.
- Esteve Agelet, L., et al. (2012). "Feasibility of near infrared spectroscopy for analyzing corn kernel damage and viability of soybean and corn kernels." Journal of Cereal Science **55**(2): 160-165.
- Evert, R. F. (2006). Esau's plant anatomy: meristems, cells, and tissues of the plant body: their structure, function, and development, John Wiley & Sons.

- Eyre-Walker, A., et al. (1998). "Investigation of the bottleneck leading to the domestication of maize." Proceedings of the National Academy of Sciences **95**(8): 4441-4446.
- Fahlgren, N., et al. (2015). "Lights, camera, action: high-throughput plant phenotyping is ready for a close-up." Current opinion in plant biology **24**: 93-99.
- Fernández, S., et al. (1999). "Monitoring and visualising plant cuticles by confocal laser scanning microscopy." Plant Physiology and Biochemistry **37**(10): 789-794.
- Fernández, V., et al. (2011). "New insights into the properties of pubescent surfaces: peach fruit as a model." Plant physiology **156**(4): 2098-2108.
- Food and Agriculture Organization of the United Nations (2013). "Crop Water Information: Maize." Retrieved 07/07/2015, from http://www.fao.org/nr/water/cropinfo_maize.html.
- Franks, F. (1985). Biophysics and biochemistry at low temperatures, Cambridge University Press.
- Freeling, M. and V. Walbot (2013). The maize handbook, Springer Science & Business Media.
- Fujikawa, S., et al. (1999). "Freezing behavior of xylem ray parenchyma cells in softwood species with differences in the organization of cell walls." Protoplasma **206**(1): 31-40.
- Fuller, M., et al. (2003). "Protection of plants from frost using hydrophobic particle film and acrylic polymer." Annals of applied biology **143**(1): 93-98.
- Ganie, A. H., et al. (2015). "Metabolite profiling of low-P tolerant and low-P sensitive maize genotypes under phosphorus starvation and restoration conditions." PloS one **10**(6): e0129520.
- Gao, C., et al. (2009). "Association of polyamines in governing the chilling sensitivity of maize genotypes." Plant Growth Regulation **57**(1): 31-38.
- Gardner, B. L. (2009). American agriculture in the twentieth century: How it flourished and what it cost, Harvard University Press.
- George, M. F. (1982). FREEZING AVOIDANCE BY SUPERCOOLING OF TISSUE WATER IN VEGETATIVE AND REPRODUCTIVE STRUCTURES OF *Juniperus virginiana*. Plant Cold Hardiness and Freezing Stress. P. H. L. Sakai, Academic Press: 367-377.
- George, M. F., et al. (1974). "Supercooling in overwintering azalea flower buds." Plant physiology **54**(1): 29-35.
- Gibson, A. C. (1996). Special topics in water relations. Structure-Function Relations of Warm Desert Plants, Springer: 143-168.

Gillooly, J. F., et al. (2001). "Effects of size and temperature on metabolic rate." Science **293**(5538): 2248-2251.

Girard, A.-L., et al. (2012). "Tomato GDSL1 is required for cutin deposition in the fruit cuticle." The Plant Cell **24**(7): 3119-3134.

Glenn, D. M., et al. (2001). Method for enhanced supercooling of plants to provide frost protection, Google Patents.

Glover, B. J. (2000). "Differentiation in plant epidermal cells." Journal of Experimental Botany **51**(344): 497-505.

Gobin, A., et al. (2013). "" Weather-related hazards and risks in agriculture"." Natural Hazards & Earth System Sciences **13**(10).

Goddard, J. M. and J. Hotchkiss (2007). "Polymer surface modification for the attachment of bioactive compounds." Progress in polymer science **32**(7): 698-725.

Goldstein, G., et al. (1985). "Cold hardiness and supercooling along an altitudinal gradient in Andean giant rosette species." Oecologia **68**(1): 147-152.

Goodwin, S. M. and M. A. Jenks (2005). "Plant cuticle function as a barrier to water loss." Plant abiotic stress: 14-36.

Government of Canada (2016). "Daily Data Report." from http://climate.weather.gc.ca/climate_data/daily_data_e.html?StationID=47707.

Griffith, M. and M. Antikainen (1996). "Extracellular ice formation in freezing-tolerant plants." Adv Low-Temp Biol **3**: 107-139.

Grogan, C. (1970). Genetic variability in maize (Zea mays L.) for germination and seedling vigor at low temperatures. Proc Ann Corn Sorghum Res Conf.

Gu, L., et al. (2008). "The 2007 Eastern US spring freeze: Increased cold damage in a warming world?" BioScience **58**(3): 253-262.

Guan, Y., et al. (2015). ""On-Off" Thermoresponsive Coating Agent Containing Salicylic Acid Applied to Maize Seeds for Chilling Tolerance." PloS one **10**(3): e0120695.

Gunstone, F. D. (2006). Modifying lipids for use in food, Woodhead Publishing.

Gusta, L., et al. (1978). "A system for freezing biological materials [Plants]." HortScience.

Gusta, L. V., et al. (1982). FACTORS INFLUENCING HARDENING AND SURVIVAL IN WINTER WHEAT. Plant Cold Hardiness and Freezing Stress. P. H. L. Sakai, Academic Press: 23-40.

- Gusta, L. V., et al. (2009). Plant Cold Hardiness: from the laboratory to the field. Oxfordshire, UK, CABI.
- Guy, C. L. (1990). "Cold acclimation and freezing stress tolerance: role of protein metabolism." Annual review of plant biology **41**(1): 187-223.
- Hashimoto, Y., et al. (1984). "Dynamic analysis of water stress of sunflower leaves by means of a thermal image processing system." Plant physiology **76**(1): 266-269.
- Heredia-Guerrero, J. A., et al. (2014). "INFRARED AND RAMAN SPECTROSCOPIC FEATURES OF PLANT CUTICLES: A REVIEW." Frontiers in Plant Science **5**.
- Heuberger, A. L., et al. (2014). "Evaluating plant immunity using mass spectrometry-based metabolomics workflows." Frontiers in Plant Science **5**: 291.
- Heydari, G., et al. (2013). "Hydrophobic surfaces: topography effects on wetting by supercooled water and freezing delay." The Journal of Physical Chemistry C **117**(42): 21752-21762.
- Hincha, D. K. and E. Zuther (2014). Introduction: Plant Cold Acclimation and Freezing Tolerance. Plant Cold Acclimation, Springer: 1-6.
- Holmes, M. G. and D. R. Keiller (2002). "Effects of pubescence and waxes on the reflectance of leaves in the ultraviolet and photosynthetic wavebands: a comparison of a range of species." Plant, cell & environment **25**(1): 85-93.
- Howden, S. M., et al. (2007). "Adapting agriculture to climate change." Proceedings of the National Academy of Sciences **104**(50): 19691-19696.
- Howell, N. K., et al. (1999). "Raman spectral analysis in the C–H stretching region of proteins and amino acids for investigation of hydrophobic interactions." Journal of agricultural and food chemistry **47**(3): 924-933.
- Huang, L., et al. (2012). "Effect of contact angle on water droplet freezing process on a cold flat surface." Experimental Thermal and Fluid Science **40**: 74-80.
- Huber, B. (1935). "Die physiologische Bedeutung der Ring-und Zerstreutporigkeit." Ber. dtsh. bot. Ges **53**: 711-719.
- Hull, H., et al. (1975). "Environmental influences on cuticle development and resultant foliar penetration." The botanical review **41**(4): 421-452.
- Inouye, D. W. (2000). "The ecological and evolutionary significance of frost in the context of climate change." Ecology Letters **3**(5): 457-463.

Inouye, D. W. (2008). "EFFECTS OF CLIMATE CHANGE ON PHENOLOGY, FROST DAMAGE, AND FLORAL ABUNDANCE OF MONTANE WILDFLOWERS." Ecology **89**(2): 353-362.

Ishikawa, M. and A. Sakai (1982). CHARACTERISTICS OF FREEZING AVOIDANCE IN COMPARISON WITH FREEZING TOLERANCE: A DEMONSTRATION OF EXTRAORGAN FREEZING. Plant Cold Hardiness and Freezing Stress. P. H. L. Sakai, Academic Press: 325-340.

Ivanov, V. (2015). Environmental microbiology for engineers, CRC press.

Jain, S. M. and S. C. Minocha (2013). Molecular biology of woody plants, Springer Science & Business Media.

Jansen, M., et al. (2009). "Simultaneous phenotyping of leaf growth and chlorophyll fluorescence via GROWSCREEN FLUORO allows detection of stress tolerance in Arabidopsis thaliana and other rosette plants." Functional Plant Biology **36**(11): 902-914.

Jeffree, C. E. (1996). "Structure and ontogeny of plant cuticles." Plant cuticles: an integrated functional approach. BIOS Scientific Publishers Ltd.: Oxford, UK: 33-82.

Jenks, M. A. and E. N. Ashworth (1999). "Plant epicuticular waxes: function, production, and genetics." Horticultural reviews **23**: 1-68.

Jenks, M. A. and P. M. Hasegawa (2008). Plant abiotic stress, John Wiley & Sons.

Jenks, M. A., et al. (1996). "Changes in epicuticular waxes on wildtype and eceriferum mutants in Arabidopsis during development." Phytochemistry **42**(1): 29-34.

Jetter, R., et al. (2007). "Composition of plant cuticular waxes." Annual Plant Reviews Volume 23: Biology of the Plant Cuticle: 145-181.

Jetter, R. and S. Schäffer (2001). "Chemical composition of the Prunus laurocerasus leaf surface. Dynamic changes of the epicuticular wax film during leaf development." Plant physiology **126**(4): 1725-1737.

Jian, L., et al. (2004). "Increment of chilling tolerance and its physiological basis in chilling-sensitive corn sprouts and tomato seedlings after cold-hardening at optimum temperatures." Zuo wu xue bao **31**(8): 971-976.

Jung, S., et al. (2011). "Are superhydrophobic surfaces best for icephobicity?" Langmuir **27**(6): 3059-3066.

Kaku, S. (1971). "Changes in supercooling and freezing processes accompanying leaf maturation in Buxus." Plant and Cell Physiology **12**(1): 147-155.

- Kaku, S. (1975). "Analysis of freezing temperature distribution in plants." Cryobiology **12**(2): 154-159.
- Kasuga, M., et al. (1999). "Improving plant drought, salt, and freezing tolerance by gene transfer of a single stress-inducible transcription factor." Nature biotechnology **17**(3): 287-291.
- Kazarian, S. G. and K. A. Chan (2010). "Micro-and macro-attenuated total reflection Fourier transform infrared spectroscopic imaging." Applied spectroscopy **64**(5): 135A-152A.
- KB Storey and JM Storey (2005). Freezing Tolerance. Gerday C, Glansdorff N (eds) Extremophiles encyclopedia of life support systems (EOLSS). developed under the auspices of the UNESCO. EOLSS, Oxford.
- Kerstiens, G. (1996). "Cuticular water permeability and its physiological significance." Journal of Experimental Botany **47**(12): 1813-1832.
- Koch, K. and H.-J. Ensikat (2008). "The hydrophobic coatings of plant surfaces: epicuticular wax crystals and their morphologies, crystallinity and molecular self-assembly." Micron **39**(7): 759-772.
- Kolaksazov, M., et al. (2013). "Effect of chilling and freezing stresses on jasmonate content in *Arabis alpina*." Bulg. J. Agric. Sci. **19**: 15-17.
- Kolattukudy, P. (1980). "Biopolyester membranes of plants: cutin and suberin." Science **208**(4447): 990-1000.
- Kolattukudy, P. (1996). "Biosynthetic pathways of cutin and waxes, and their sensitivity to environmental stresses." Plant cuticles: an integrated functional approach. BIOS Scientific Publishers Ltd.: Oxford, UK: 83-108.
- Kolattukudy, P. E. and T. J. Walton (1973). "The biochemistry of plant cuticular lipids." Progress in the Chemistry of Fats and other lipids **13**: 119-175.
- Konoshima, M. (1962). Laboratory manual of botany. [In Japanese.]. Tokyo.
- Kourounioti, R. L. A., et al. (2013). "Buckling as an origin of ordered cuticular patterns in flower petals." Journal of The Royal Society Interface **10**(80): 20120847.
- Kucharik, C. J. and S. P. Serbin (2008). "Impacts of recent climate change on Wisconsin corn and soybean yield trends." Environmental Research Letters **3**(3): 034003.
- Kulinich, S., et al. (2010). "Superhydrophobic surfaces: are they really ice-repellent?" Langmuir **27**(1): 25-29.
- Kumar, S., et al. (2016). "Infrared spectroscopy combined with imaging: A new developing analytical tool in health and plant science." Applied Spectroscopy Reviews **51**(6): 466-483.

Kunst, L. and A. Samuels (2003). Biosynthesis and secretion of plant cuticular wax. Progress in lipid research. **42**: 51-80.

Kunst, L., et al. (2005). The plant cuticle: formation and structure of epidermal surfaces. Plant Lipids—Biology, Utilisation and Manipulation, D. Murphy, ed (Oxford, UK: Blackwell): 270-302.

Lahlali, R., et al. (2014). "ATR–FTIR spectroscopy reveals involvement of lipids and proteins of intact pea pollen grains to heat stress tolerance." Frontiers in Plant Science **5**.

Lang, P., et al. (2005). "Identification of cold acclimated genes in leaves of Citrus unshiu by mRNA differential display." Gene **359**: 111-118.

Larcher, W. (2003). Physiological plant ecology: ecophysiology and stress physiology of functional groups, Springer Science & Business Media.

Largo-Gosens, A., et al. (2014). "Fourier transform mid infrared spectroscopy applications for monitoring the structural plasticity of plant cell walls." Frontiers in Plant Science **5**.

Laws, D., et al. (2001). Editorial II: Fatty acid amides are putative endogenous ligands for anaesthetic recognition sites in mammalian CNS, Oxford University Press.

Leugers, A., et al. (2003). "High-throughput analysis in catalysis research using novel approaches to transmission infrared spectroscopy." Journal of combinatorial chemistry **5**(3): 238-244.

Leung, W. (2012). Early thaw and late freeze lay waste to Ontario's orchards. The Globe and Mail. Toronto, Ontario.

Leuning, R. (1988). "Leaf temperatures during radiation frost part II. A steady state theory." Agricultural and Forest Meteorology **42**(2-3): 135-155.

Leuning, R. and K. Cremer (1988). "Leaf temperatures during radiation frost Part I. Observations." Agricultural and Forest Meteorology **42**(2-3): 121-133.

Levitt, J. (1958). Frost, drought, and heat resistance. Frost, Drought, and Heat Resistance, Springer: 1-85.

Levitt, J. (1972). Responses of plants to environmental stresses, Academic Press, New York.

Levitt, J. (1980). Responses of plants to environmental stresses. Volume II. Water, radiation, salt, and other stresses, Academic Press.

Levitt, J. and G. Scarth (1936). "FROST-HARDENING STUDIES WITH LIVING CELLS: II. PERMEABILITY IN RELATION TO FROST RESISTANCE AND THE SEASONAL CYCLE." Canadian Journal of Research **14**(8): 285-305.

Li, L., et al. (2014). "A review of imaging techniques for plant phenotyping." Sensors **14**(11): 20078-20111.

Li, P. H. (2012). Plant cold hardiness and freezing stress: Mechanisms and crop implications, Elsevier.

Lindow, S. (1983). "The role of bacterial ice nucleation in frost injury to plants." Annual review of phytopathology **21**(1): 363-384.

Lucas, J. W. (1954). "Subcooling and ice nucleation in lemons." Plant physiology **29**(3): 245.

Mahmoud, R. S. and K. Narisawa (2013). "A new fungal endophyte, *Scolecobasidium humicola*, promotes tomato growth under organic nitrogen conditions." PloS one **8**(11): e78746.

Maier, C. G.-A. and D. Post-Beittenmiller (1998). "Epicuticular wax on leek in vitro developmental stages and seedlings under varied growth conditions." Plant Science **134**(1): 53-67.

Masuka, B., et al. (2012). "Phenotyping for abiotic stress tolerance in maize." Journal of integrative plant biology **54**(4): 238-249.

Matos, D. A., et al. (2014). "Daily changes in temperature, not the circadian clock, regulate growth rate in *Brachypodium distachyon*." PloS one **9**(6): e100072.

May, T., et al. (2007). "Mid-infrared spectromicroscopy beamline at the Canadian Light Source." Nuclear Instruments and Methods in Physics Research Section A: Accelerators, Spectrometers, Detectors and Associated Equipment **582**(1): 111-113.

Mazur, P. (1969). "Freezing injury in plants." Annual Review of Plant Physiology **20**(1): 419-448.

Melillo, J. M., et al. (2014). "Climate change impacts in the United States." Third National Climate Assessment.

Monsanto Canada (2013). "Monsanto Canada embarks on bold plan to bring new crop options to western Canadian farmers." Retrieved 14/07/2015, from <http://www.monsanto.ca/newsviews/Pages/NR-2013-06-24.aspx>.

Moose, S. P. and P. H. Sisco (1994). "Glossy15 controls the epidermal juvenile-to-adult phase transition in maize." The Plant Cell **6**(10): 1343-1355.

Mutka, A. M. and R. S. Bart (2015). "Image-based phenotyping of plant disease symptoms." Frontiers in Plant Science **5**: 734.

Nadiminti, P. P., et al. (2015). "Confocal laser scanning microscopy elucidation of the micromorphology of the leaf cuticle and analysis of its chemical composition." Protoplasma **252**(6): 1475-1486.

Neuner, G. and J. Hacker (2012). Ice formation and propagation in alpine plants. Plants in Alpine Regions, Springer: 163-174.

Nielsen, B. and E. Christmas (2001). "Frost and low temperature injury to corn and soybean." Purdue Pest Management and Crop Production Newsletter. Purdue Univ **20**.

Nosonovsky, M. and V. Hejazi (2012). "Why superhydrophobic surfaces are not always icephobic." ACS nano **6**(10): 8488-8491.

Olien, C. R. (1961). "A method of studying stresses occurring in plant tissue during freezing." Crop Science **1**(1): 26-28.

Palta, J. P. (2014). "Merging Physiological and Genetic Approaches to Improve Abiotic Stress Resistance." Journal of Crop Improvement **28**(2): 260-304.

Palva, E. T. (1994). "Gene expression under low temperature stress." Stress induced gene expression in plants: 103-130.

Papagiannaki, K., et al. (2014). "Agricultural losses related to frost events: use of the 850 hPa level temperature as an explanatory variable of the damage cost." Natural Hazards and Earth System Sciences **14**(9): 2375.

Pearce, R. (1988). "Extracellular ice and cell shape in frost-stressed cereal leaves: a low-temperature scanning-electron-microscopy study." Planta **175**(3): 313-324.

Pearce, R. and E. Ashworth (1992). "Cell shape and localisation of ice in leaves of overwintering wheat during frost stress in the field." Planta **188**(3): 324-331.

Pearce, R. S. (2001). "Plant Freezing and Damage." Annals of Botany **87**(4): 417-424.

Pearce, R. S. and M. P. Fuller (2001). "Freezing of barley studied by infrared video thermography." Plant physiology **125**(1): 227-240.

Pellett, H. (1971). "Comparison of cold hardiness levels of root and stem tissue." Canadian journal of plant science **51**(3): 193-195.

Perera, M. (2005). "Molecular and chemical characterization of genes involved in maize cuticular wax biosynthesis."

Pinal, R. (2004). "Effect of molecular symmetry on melting temperature and solubility." Organic & biomolecular chemistry **2**(18): 2692-2699.

Prasad, R. and P.-G. Giilz (1990). "Developmental and Seasonal Variations in the Epicuticular W axes of Beech Leaves (*Fagus sylvatica* L.)." Zeitschrift für Naturforschung C **45**(7-8): 805-812.

Prasad, T. K., et al. (1994). "Evidence for chilling-induced oxidative stress in maize seedlings and a regulatory role for hydrogen peroxide." The Plant Cell **6**(1): 65-74.

Pyee, J., et al. (1994). "Identification of a lipid transfer protein as the major protein in the surface wax of broccoli (*Brassica oleracea*) leaves." Archives of Biochemistry and Biophysics **311**(2): 460-468.

Rada, F., et al. (1987). "Supercooling along an altitudinal gradient in *Espeletia schultzei*, a caulescent giant rosette species." Journal of Experimental Botany **38**(3): 491-497.

Ramirez, F., et al. (1992). "Fourier transform IR study of enzymatically isolated tomato fruit cuticular membrane." Biopolymers **32**(11): 1425-1429.

Raschke, K. (1960). "Heat transfer between the plant and the environment." Annual Review of Plant Physiology **11**(1): 111-126.

Rhee, Y., et al. (1998). "Epicuticular wax accumulation and fatty acid elongation activities are induced during leaf development of leeks." Plant physiology **116**(3): 901-911.

Riederer, M. and C. Markstadter (1996). "Cuticular waxes: a critical assessment of current knowledge." Plant cuticles: an integrated functional approach. BIOS Scientific Publishers Ltd.: Oxford, UK: 189-200.

Riederer, M. and G. Schneider (1990). "The effect of the environment on the permeability and composition of Citrus leaf cuticles." Planta **180**(2): 154-165.

Riederer, M. and L. Schreiber (2001). "Protecting against water loss: analysis of the barrier properties of plant cuticles." Journal of Experimental Botany **52**(363): 2023-2032.

Roesch-McNally, G. E., et al. (2017). "What would farmers do? Adaptation intentions under a Corn Belt climate change scenario." Agriculture and Human Values **34**(2): 333-346.

Rojas, C. M., et al. (2014). "Regulation of primary plant metabolism during plant-pathogen interactions and its contribution to plant defense." Frontiers in Plant Science **5**.

Rosenberg, N. J., et al. (1983). Microclimate: the biological environment, John Wiley & Sons.

Rossini, M., et al. (2016). "Multiple abiotic stresses on maize grain yield determination: Additive vs multiplicative effects." Field Crops Research **198**: 280-289.

- S. Sanghera, G., et al. (2011). "Engineering cold stress tolerance in crop plants." Current genomics **12**(1): 30.
- Safar, M., et al. (1994). "Characterization of edible oils, butters and margarines by Fourier transform infrared spectroscopy with attenuated total reflectance." Journal of the American Oil Chemists' Society **71**(4): 371.
- Sakai, A. (1960). "Survival of the twig of woody plants." Nature, London **185**(4710): 393-394.
- Sakai, A. (1979). "Freezing avoidance mechanism of primordial shoots of conifer buds." Plant and Cell Physiology **20**(7): 1381-1390.
- Sakai, A. and W. Larcher (1987). Frost Survival of Plants. Eco-logical Studies 62, Springer, Berlin Heidelberg New York.
- Sanchez-Martin, J., et al. (2015). "A metabolomic study in oats (*Avena sativa*) highlights a drought tolerance mechanism based upon salicylate signalling pathways and the modulation of carbon, antioxidant and photo- oxidative metabolism." Plant, cell & environment **38**(7): 1434-1452.
- Saskatchewan Ministry of Agriculture (2010). "Corn Production." Retrieved 14/07/2015, from <http://www.agriculture.gov.sk.ca>.
- Scallan, N. (2012). Fruit industry in Ontario devastated by extreme weather. The Star. Toronto, Ontario, Toronto Star Newspapers Ltd. .
- Schindelin, J., et al. (2012). "Fiji: an open-source platform for biological-image analysis." Nature methods **9**(7): 676-682.
- Schreiber, L. and J. Schonherr (2009). Water and solute permeability of plant cuticles, Springer.
- Sevilla, R. (2006). "Use of native and introduced maize diversity to improve cold tolerance in Andean maize." Enhancing the use of crop genetic diversity to manage abiotic stress in agricultural production systems. Pags: 84-91.
- Sharma, R., et al. (2015). "Particle films and their applications in horticultural crops." Applied Clay Science **116**: 54-68.
- Sherrick, S. L., et al. (1986). "Effects of adjuvants and environment during plant development on glyphosate absorption and translocation in field bindweed (*Convolvulus arvensis*)." Weed Science: 811-816.
- Shi, H., et al. (2014). "Comparative proteomic and metabolomic analyses reveal mechanisms of improved cold stress tolerance in bermudagrass (*Cynodon dactylon* (L.) Pers.) by exogenous calcium." Journal of integrative plant biology **56**(11): 1064-1079.

- Shinozaki, K., et al. (2003). "Regulatory network of gene expression in the drought and cold stress responses." Current opinion in plant biology **6**(5): 410-417.
- Single, W. and H. Marcellos (1974). "Studies on frost injury to wheat. IV.* Freezing of ears after emergence from the leaf sheath." Australian journal of agricultural research **25**(5): 679-686.
- Skoss, J. D. (1955). "Structure and composition of plant cuticle in relation to environmental factors and permeability." Botanical Gazette **117**(1): 55-72.
- Smith, B. D. (1989). "Origins of Agriculture in Eastern Noh America."
- Smith, C. W. and J. Betrán (2004). Corn: origin, history, technology, and production, John Wiley & Sons.
- Snyder, R. and J. De Melo-Abreu (2005). "Frost Protection: Fundamentals, Practice and Economics. Vol. I.: United Nations." Food and Agriculture Organization, Rome.
- Stamp, P. (1984). "Chilling tolerance of young plants demonstrated on the example of maize (*Zea mays* L.)." Fortschritte im Acker-und Pflanzenbau (Germany).
- Statistics Canada (2015, 18/02/2015). "Corn: Canada's third most valuable crop." from <http://www.statcan.gc.ca/pub/96-325-x/2014001/article/11913-eng.htm#n3>.
- Steinfath, M., et al. (2010). "Discovering plant metabolic biomarkers for phenotype prediction using an untargeted approach." Plant biotechnology journal **8**(8): 900-911.
- Steponkus, P. L. (1984). "Role of the plasma membrane in freezing injury and cold acclimation." Annual Review of Plant Physiology **35**(1): 543-584.
- Steponkus, P. L., et al. (1983). "Destabilization of the plasma membrane of isolated plant protoplasts during a freeze-thaw cycle: the influence of cold acclimation." Cryobiology **20**(4): 448-465.
- Storey, K. B. and K. K. Tanino (2012). Temperature adaptation in a changing climate: nature at risk, CABI.
- Strable, J. and M. J. Scanlon (2009). "Maize (*Zea mays*): A Model Organism for Basic and Applied Research in Plant Biology." Cold Spring Harbor Protocols **2009**(10): pdb.emo132.
- Sturaro, M., et al. (2005). "Cloning and characterization of GLOSSY1, a maize gene involved in cuticle membrane and wax production." Plant physiology **138**(1): 478-489.
- Sutter, E. (1979). "Epicuticular wax formation on carnation plantlets regenerated from shoot tip culture." J. am. Soc. hort. Sci. **104**: 493-496.

- Tanaka, Y., et al. (2005). "Ethylene inhibits abscisic acid-induced stomatal closure in *Arabidopsis*." Plant physiology **138**(4): 2337-2343.
- Taylor, F. (1971). "SOME ASPECTS OF THE GROWTH OF MANGO (*MANGIFERA INDICA* L) LEAVES." New Phytologist **70**(5): 911-922.
- Thomas, D. and H. Barber (1974). "Studies on leaf characteristics of a cline of *Eucalyptus urnigera* from Mount Wellington, Tasmania. I. Water repellency and the freezing of leaves." Australian journal of Botany **22**(3): 501-512.
- Thomashow, M. F. (1999). "Plant cold acclimation: freezing tolerance genes and regulatory mechanisms." Annual review of plant biology **50**(1): 571-599.
- Tumanov, I. and O. Krasavtsev (1959). "Hardening of northern woody plants by temperatures below zero." Sov. Plant Physiol **6**: 663-673.
- Türker-Kaya, S. and C. W. Huck (2017). "A Review of mid-infrared and near-infrared imaging: principles, concepts and applications in plant tissue analysis." Molecules **22**(1): 168.
- Urban, M. A., et al. (2016). "Cuticle and subsurface ornamentation of intact plant leaf epidermis under confocal and superresolution microscopy." Microscopy Research and Technique: n/a-n/a.
- Viant, M. R. (2008). "Recent developments in environmental metabolomics." Molecular BioSystems **4**(10): 980-986.
- Vijayan, P., et al. (2015). "Synchrotron radiation sheds fresh light on plant research: The use of powerful techniques to probe structure and composition of plants." Plant and Cell Physiology: pcv080.
- Villena, J. F., et al. (1999). "Characterization and biosynthesis of non-degradable polymers in plant cuticles." Planta **208**(2): 181-187.
- Vivek, B. (2008). Breeding quality protein maize (QPM): Protocols for developing QPM cultivars, CIMMYT.
- von Wettstein-Knowles, P. (1982). "Elongase and epicuticular wax biosynthesis." Physiol. Veg **20**(4): 797-809.
- von Wettstein-Knowles, P. (1993). Waxes, cutin and suberin. In 'Lipid metabolism in plants'. (Ed. TS Moore) pp. 127–166, CRC Press: Boca Raton, FL.
- Vose, P. B. and S. G. Blixt (2012). Crop breeding: a contemporary basis, Elsevier.
- Waltz, E. (2014). "Beating the heat." Nature biotechnology **32**(7): 610.
- Wang, C. Y. (1990). Chilling injury of horticultural crops, CRC Press.

Weatherwax, P. (1955). "History and origin of corn. I. Early history of corn and theories as to its origin." Corn and corn improvement **1**: 1-16.

Weiser, C. (1970). "Cold resistance and injury in woody plants knowledge of hardy plant adaptations to freezing stress may help us to reduce winter damage." Science **169**(3952): 1269-1278.

Welti, R., et al. (2007). "Plant lipidomics: discerning biological function by profiling plant complex lipids using mass spectrometry."

Whitaker, S. (2013). Fundamental principles of heat transfer, Elsevier.

Wildung, D., et al. (1973). "Temperature and moisture effects on hardening of apple roots." HortScience.

Wisniewski, M. and M. Fuller (1999). Ice nucleation and deep supercooling in plants: new insights using infrared thermography. Cold-Adapted Organisms, Springer: 105-118.

Wisniewski, M., et al. (2002). Extrinsic Ice Nucleation in Plants. Plant Cold Hardiness. P. Li and E. T. Palva, Springer US: 211-221.

Wisniewski, M., et al. (2002). "Use of a hydrophobic particle film as a barrier to extrinsic ice nucleation in tomato plants." Journal of the American Society for Horticultural Science **127**(3): 358-364.

Wisniewski, M., et al. (2009). "Ice nucleation, propagation and deep supercooling: the lost tribes of freezing studies." Plant Cold Hardiness: from the Laboratory to the Field: 1-11.

Wisniewski, M., et al. (1997). "Observations of ice nucleation and propagation in plants using infrared video thermography." Plant physiology **113**(2): 327-334.

Wisniewski, M., et al. (2014). "The Use of High-resolution Infrared Thermography (HRIT) for the Study of Ice Nucleation and Ice Propagation in Plants." Journal of visualized experiments: JoVE(99).

Wisniewski, M., et al. (2015). "The use of high-resolution infrared thermography (HRIT) for the study of ice nucleation and ice propagation in plants." Journal of visualized experiments: JoVE(99): e52703-e52703.

Workmaster, B. (2001). Cold hardiness, ice nucleation, and growth modeling in the cranberry plant (*Vaccinium macrocarpon*), The University of Wisconsin - Madison. **Ph.D.**

Workmaster, B. A. A., et al. (1999). "Ice nucleation and propagation in cranberry uprights and fruit using infrared video thermography." Journal of the American Society for Horticultural Science **124**(6): 619-625.

Xiong, L. and J. K. Zhu (2001). "Abiotic stress signal transduction in plants: molecular and genetic perspectives." Physiologia Plantarum **112**(2): 152-166.

Xu, S., et al. (2016). "Metabolomic prediction of yield in hybrid rice." The Plant Journal **88**(2): 219-227.

Yeats, T. H. and J. K. Rose (2013). "The formation and function of plant cuticles." Plant physiology **163**(1): 5-20.

Zhu, J.-K. (2002). "Salt and drought stress signal transduction in plants." Annual review of plant biology **53**(1): 247-273.

Zhu, J., et al. (2007). "Interplay between cold-responsive gene regulation, metabolism and RNA processing during plant cold acclimation." Current opinion in plant biology **10**(3): 290-295.

Zia, K. M., et al. (2016). "Lipid functionalized biopolymers: A review." International journal of biological macromolecules **93**: 1057-1068.

Zia, S., et al. (2013). "Infrared Thermal Imaging as a Rapid Tool for Identifying Water- Stress Tolerant Maize Genotypes of Different Phenology." Journal of Agronomy and Crop Science **199**(2): 75-84.

APPENDIX A 2016 GROWING SEASON DAILY TEMPERATURES

MAX, MIN AND MEAN DAILY TEMPERATURES JUNE TO SEPTEMBER 2016

Daily maximum, minimum and mean daily temperatures at Saskatoon RCS station
monthly reports from June 2016 to September 2016 (Government of Canada 2016)

Latitude: 52.17

Longitude: -106.72

Elevation: 504.1

2016 June Temperatures by Day			
Date/Time	Max Temp (°C)	Min Temp (°C)	Mean Temp (°C)
2016-06-01	22.3	4.6	13.5
2016-06-02	28.2	9.2	18.7
2016-06-03	25	10.6	17.8
2016-06-04	27.1	6.8	17
2016-06-05	25.4	8.8	17.1
2016-06-06	24.3	5.3	14.8
2016-06-07	28.7	13.3	21
2016-06-08	29.2	14.3	21.8
2016-06-09	30.2	16.6	23.4
2016-06-10	17.7	7.7	12.7
2016-06-11	20.6	5.3	13
2016-06-12	23.5	11.4	17.5
2016-06-13	26.2	10	18.1
2016-06-14	29.2	7.8	18.5
2016-06-15	21.8	9.1	15.5
2016-06-16	21.7	7.1	14.4
2016-06-17	21.5	7.2	14.4
2016-06-18	25.4	5.9	15.7
2016-06-19	20.5	10	15.3
2016-06-20	24.8	6.6	15.7
2016-06-21	23.4	9.2	16.3
2016-06-22	25.8	11	18.4
2016-06-23	29.7	14.1	21.9
2016-06-24	26.7	15.2	21
2016-06-25	20.8	12.5	16.7
2016-06-26	19.4	12.4	15.9
2016-06-27	25.8	12.3	19.1
2016-06-28	26.9	12.6	19.8
2016-06-29	25.4	12.5	19
2016-06-30	24	10.1	17.1

2016 July Temperatures by Day			
Date/Time	Max Temp (°C)	Min Temp (°C)	Mean Temp (°C)
2016-07-01	22.1	13.6	17.9
2016-07-02	23.4	13.8	18.6
2016-07-03	26.6	14.1	20.4
2016-07-04	23.5	11.6	17.6
2016-07-05	22.7	8.8	15.8
2016-07-06	22.5	11.1	16.8
2016-07-07	24.5	10	17.3
2016-07-08	24.1	11.8	18
2016-07-09	27.1	16.8	22
2016-07-10	25.1	15.7	20.4
2016-07-11	19.5	14.7	17.1
2016-07-12	21.7	15.1	18.4
2016-07-13	23.9	12.3	18.1
2016-07-14	23	11.2	17.1
2016-07-15	23.6	7.7	15.7
2016-07-16	25.2	8	16.6
2016-07-17	25.3	13.4	19.4
2016-07-18	27.3	11.2	19.3
2016-07-19	29.3	14.4	21.9
2016-07-20	28.3	15.2	21.8
2016-07-21	27.5	12.9	20.2
2016-07-22	28	10	19
2016-07-23	24.9	13.6	19.3
2016-07-24	26.4	9	17.7
2016-07-25	27	11.1	19.1
2016-07-26	26	7.9	17
2016-07-27	27.4	8.3	17.9
2016-07-28	28.6	10.3	19.5
2016-07-29	25.9	16.2	21.1
2016-07-30	28.4	14	21.2
2016-07-31	24.7	11.6	18.2

2016 August Temperatures by Day			
Date/Time	Max Temp (°C)	Min Temp (°C)	Mean Temp (°C)
2016-08-01	23.7	11.2	17.5
2016-08-02	27.7	11.5	19.6
2016-08-03	18.8	12.6	15.7
2016-08-04	24	11.2	17.6
2016-08-05	24.3	8	16.2
2016-08-06	25.6	10.6	18.1
2016-08-07	24.5	11.1	17.8
2016-08-08	17.9	14.1	16
2016-08-09	23.6	12.9	18.3
2016-08-10	22.6	14.3	18.5
2016-08-11	20.6	13.8	17.2
2016-08-12	24.7	11.9	18.3
2016-08-13	25.8	8.9	17.4
2016-08-14	26.5	14.7	20.6
2016-08-15	26.8	13.1	20
2016-08-16	28.8	11.6	20.2
2016-08-17	23.7	12.9	18.3
2016-08-18	20.6	9.2	14.9
2016-08-19	18.9	8.6	13.8
2016-08-20	23.7	9.8	16.8
2016-08-21	27.9	12.4	20.2
2016-08-22	29	14.3	21.7
2016-08-23	17.3	9.6	13.5
2016-08-24	19	8.5	13.8
2016-08-25	23.2	5.4	14.3
2016-08-26	19.4	9.8	14.6
2016-08-27	25.2	7.7	16.5
2016-08-28	19	6.2	12.6
2016-08-29	19.8	1.8	10.8
2016-08-30	22.9	6.2	14.6
2016-08-31	26.4	11.3	18.9

2016 September Temperatures by Day			
Date/Time	Max Temp (°C)	Min Temp (°C)	Mean Temp (°C)
2016-09-01	28.7	16.2	22.5
2016-09-02	25	11.5	18.3
2016-09-03	21.5	7.2	14.4
2016-09-04	16	3.1	9.6
2016-09-05	13.9	2.9	8.4
2016-09-06	19.8	0.8	10.3
2016-09-07	20.6	4.9	12.8
2016-09-08	21.3	3.3	12.3
2016-09-09	19.9	5.1	12.5
2016-09-10	23.2	5.1	14.2
2016-09-11	14.6	5.8	10.2
2016-09-12	9.9	1.8	5.9
2016-09-13	17.5	-0.2	8.7
2016-09-14	24.2	4.8	14.5
2016-09-15	24	4	14
2016-09-16	23.9	2.4	13.2
2016-09-17	22.7	7.6	15.2
2016-09-18	17.7	8.3	13
2016-09-19	17.7	3.8	10.8
2016-09-20	17.7	-0.6	8.6
2016-09-21	16.9	-1.3	7.8
2016-09-22	18.4	-1.8	8.3
2016-09-23	11.5	8.3	9.9
2016-09-24	13.4	5	9.2
2016-09-25	17.7	1.5	9.6
2016-09-26	20.4	-0.6	9.9
2016-09-27	24.4	6.4	15.4
2016-09-28	15.7	-0.5	7.6
2016-09-29	17.5	6.7	12.1
2016-09-30	20.9	5.6	13.3

APPENDIX B 'EXTREME' CHILLING CONDITION ATR-FTIR RESULTS

Results

B.1.1 'Extreme' Chilling Conditions – CH₂ Regions Defined

Three regions (as defined 4.2.14 Spectra CH₂ Regions Defined) define the limits of the lipid peak integration area (Figure B.1)

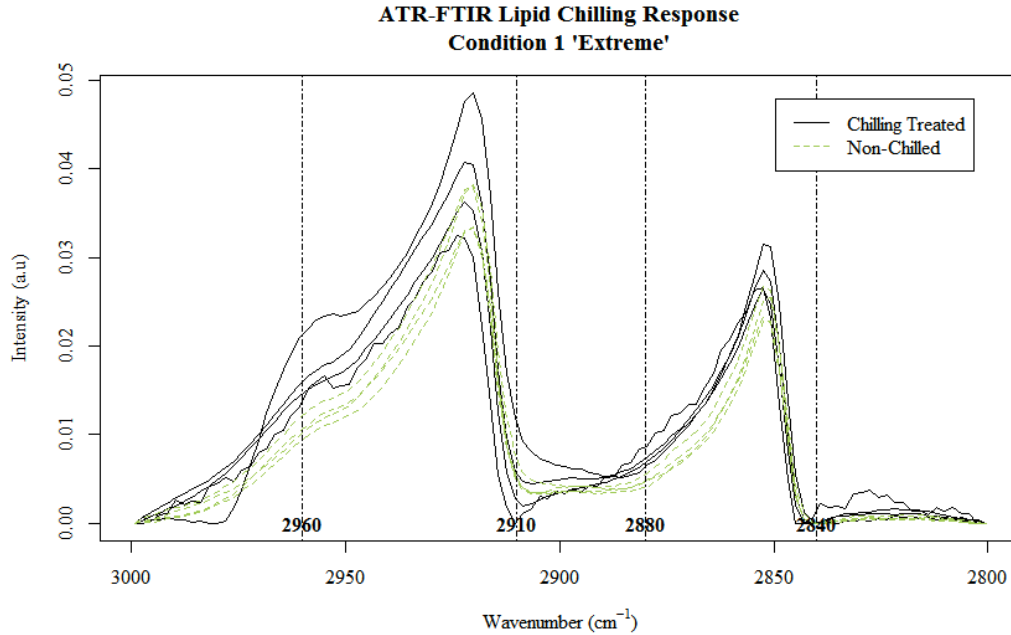


Figure B.1 Chilling treated and non-chilled average spectra by genotype with band regions (region 1, 2960-3040cm⁻¹; region 2, 2910-2960cm⁻¹; region 3, 2840-2880cm⁻¹) assigned to the CH₂ groups under 'extreme' chilling conditions of mature corn leaf (V6; adaxial side).

B.1.2 'Extreme' Chilling Conditions – Integrations by Genotype

No significant genotypic differences were observed across the three regions in these genotypes, however consistent with 'mild' condition findings, genotype 884 and 959 were most responsive to chilling treatment in the CH₃ group(Figure B.2). There was a data interpolation issue for the X-coordinates along the spectrum, due to a setting malfunction, with genotype 256 (Figure B.1) which has artifacts evident in both region 1 and 2 of genotype 256 (Figures .20 and .30)

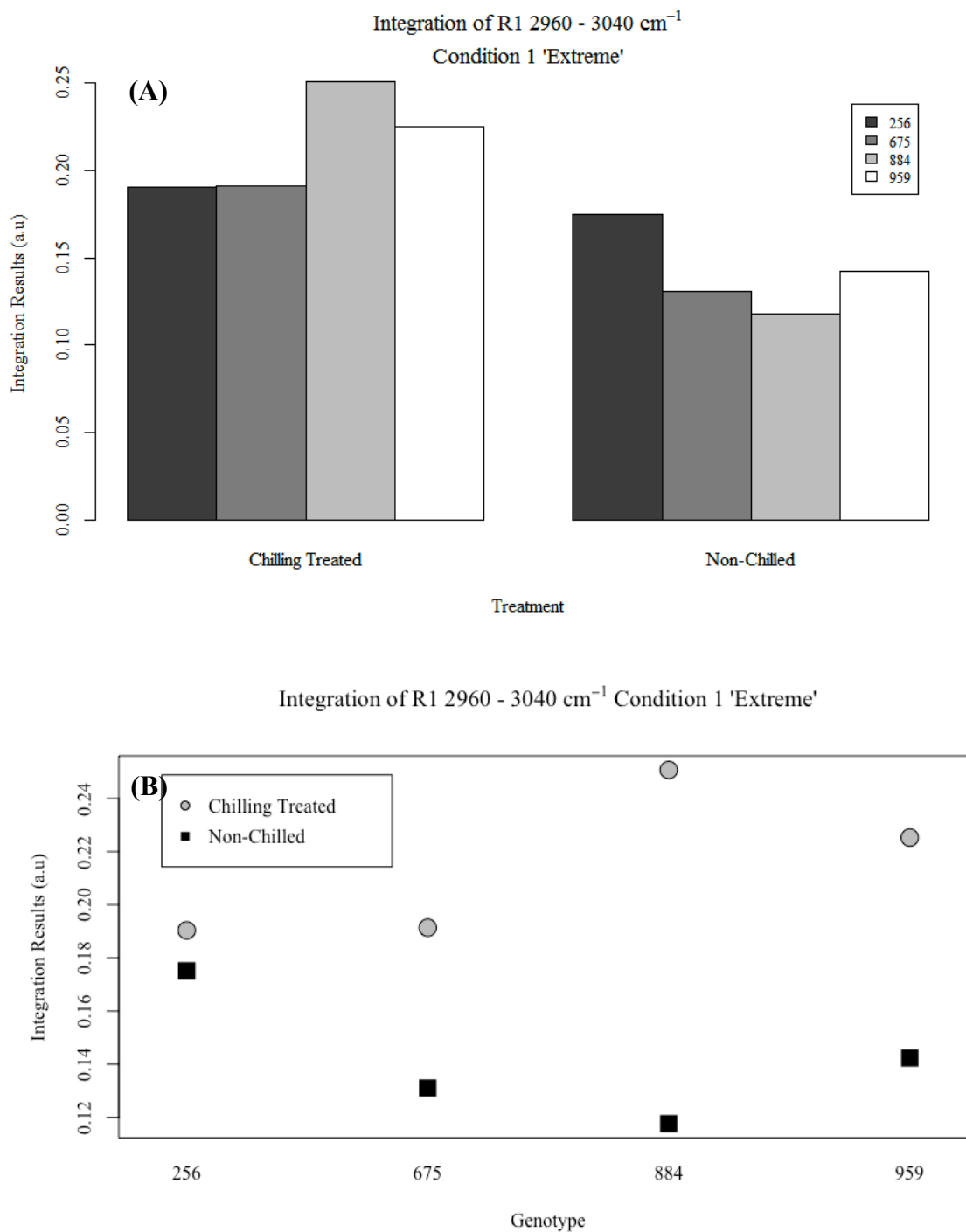


Figure B.2 Peak area integration (a.u.) of CH_3 group (region 1; 2960-3040 cm^{-1}) of leaf (V6; adaxial side) 'extreme' chilling condition mature corn by genotype (256, 675, 884, 959) and treatment (chilling treated, non-chilled) using ATR-FTIR; spectra scan average 512; min. five spectra replicates (A) Barplot demonstrates difference between genotypes; (B) Interaction plot illustrating the response of the area beneath integration region one to different combinations of factors (genotype, treatment).

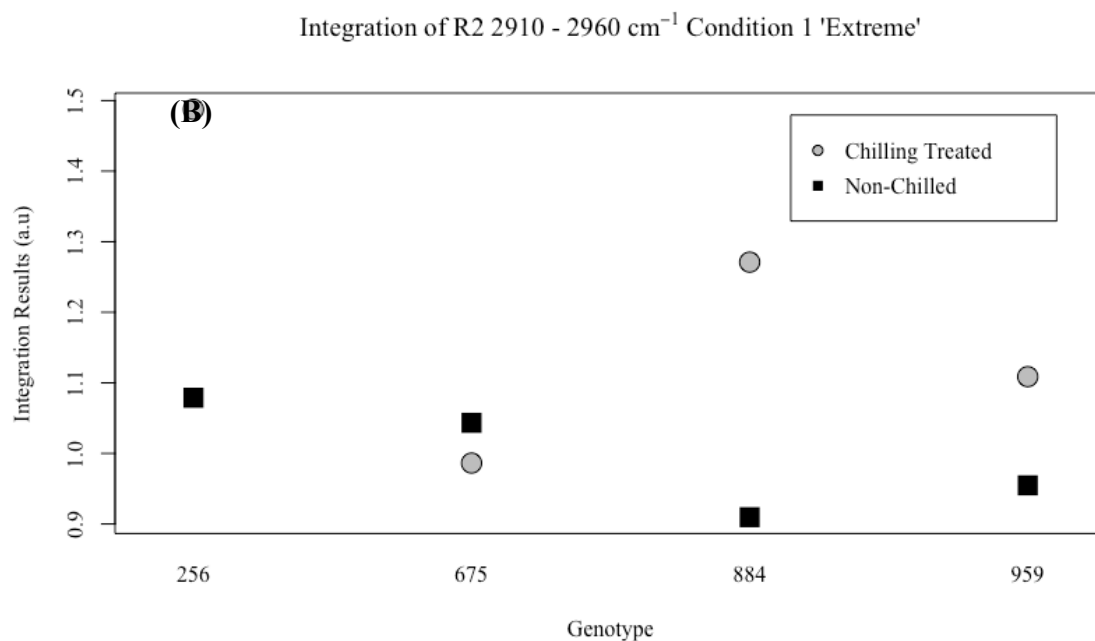
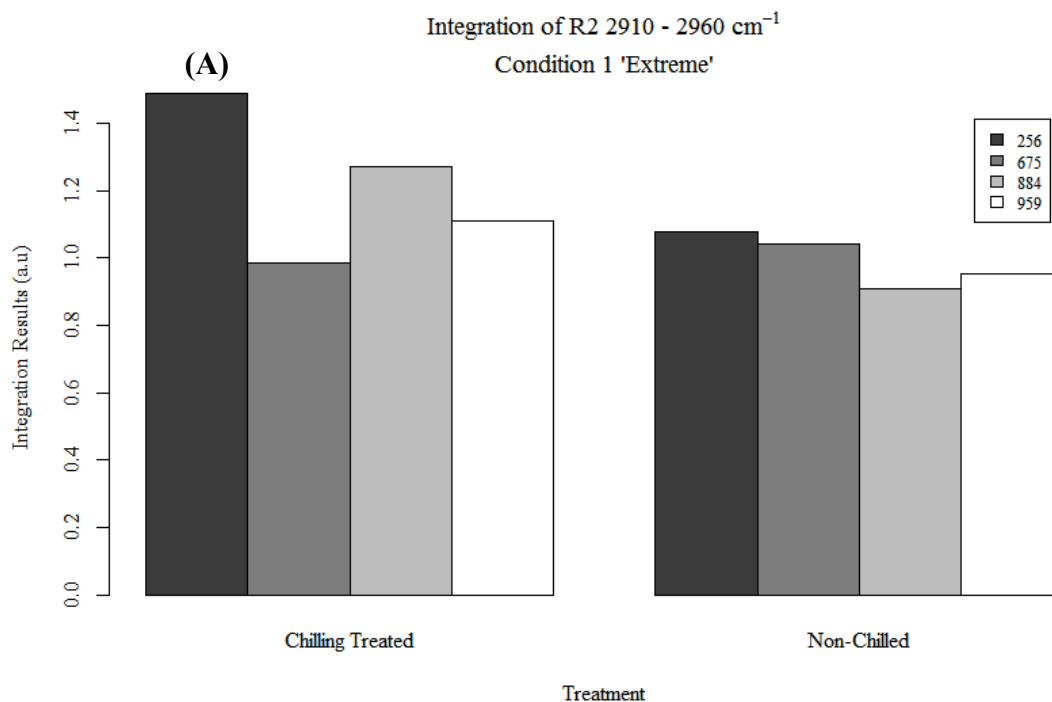


Figure B.3 Peak area integration (a.u.) of asymmetrical CH₂ bend (region 2; 2910-2960 cm^{-1}) of leaf (V6; adaxial side) 'extreme' chilling condition mature corn by genotype (256, 675, 884 and 959) and treatment (chilling treated, non-chilled) using ATR-FTIR; spectra scan average 512; min. five spectra replicates (A) Barplot demonstrates difference between genotypes; (B) Interaction plot illustrating the response of the area beneath integration region two to different combinations of factors (genotype, treatment).

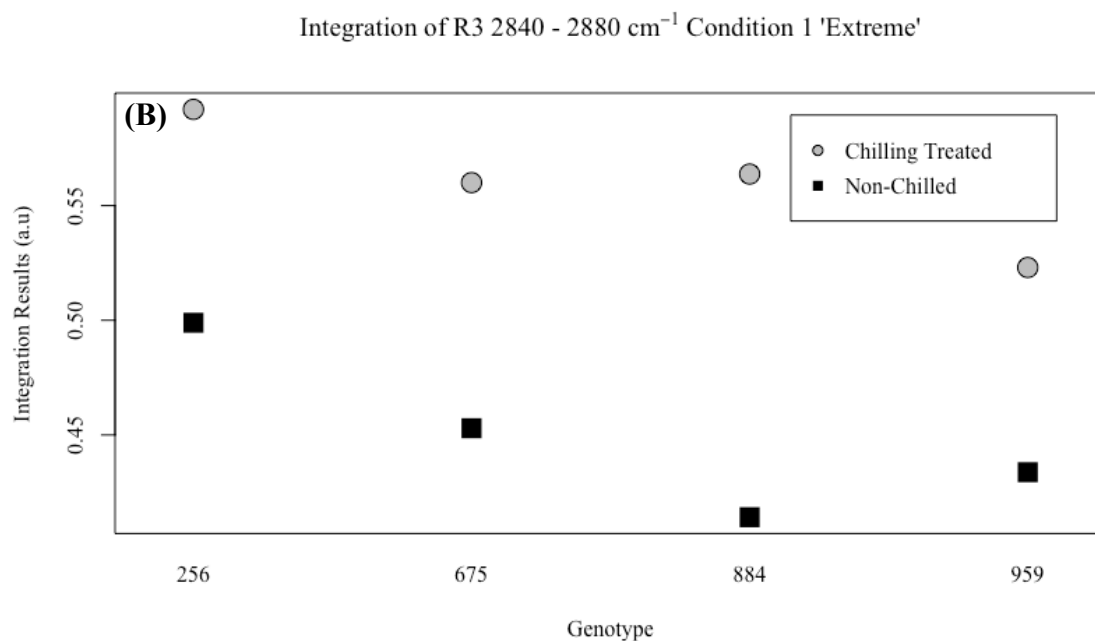
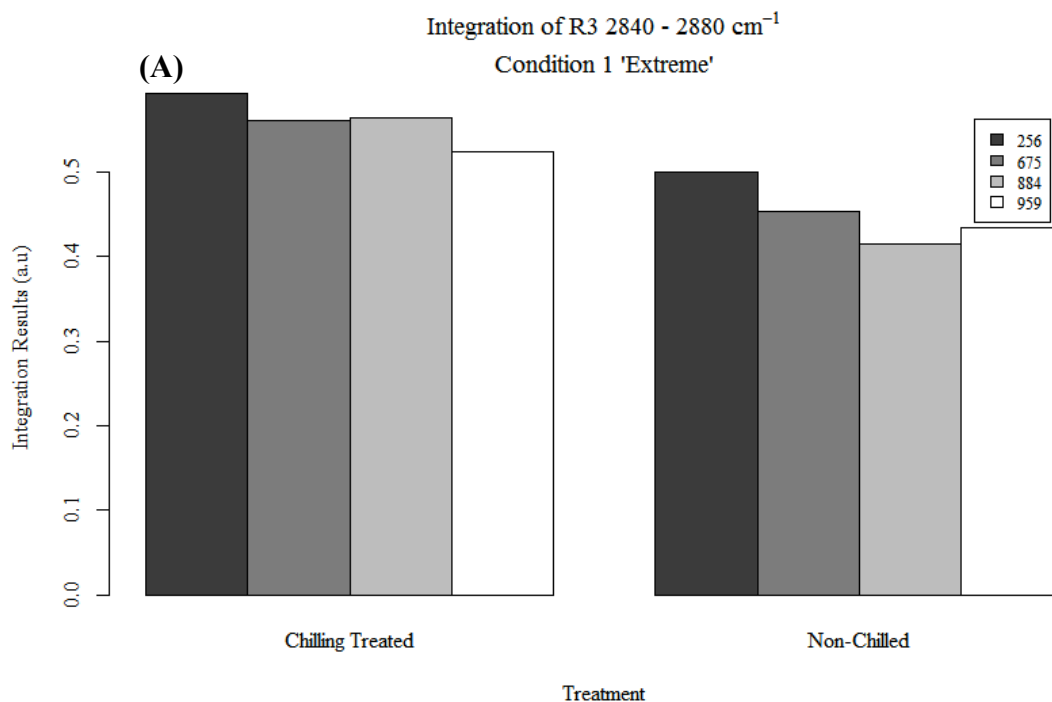


Figure B.4 Peak area integration (a.u.) of symmetrical CH_2 bend (region 3; 2840-2880 cm^{-1}) of leaf (V6; adaxial side) 'extreme' chilling condition mature corn by genotype (256, 675, 884 and 959) and treatment (chilling treated, non-chilled) using ATR-FTIR; spectra scan average 512; min. five spectra replicates **(A)** Barplot demonstrates difference between genotypes; **(B)** Interaction plot illustrating the response of the area beneath integration region three to different combinations of factors (genotype, treatment).

B.1.3 'Extreme' Chilling Conditions – Integrations by Treatment

Treatment effect under 'extreme' condition closely aligns, in regions 1 and 2, with the findings of 'mild' condition (4.3.4 'Mild' Controlled Environment Chilling Condition – Integrations by Treatment) which indicated there is strong treatment effect ($p < 0.05$) in the CH_3 group (Figure B.5A) and moderate treatment effect ($P < 0.10$) at the asymmetrical bend (Figure B.5B). Unlike the 'mild' condition, the symmetrical CH_2 bend in 'extreme' condition shows a significant increase in peak integration area following chilling pre-treatment (Figure B.6).

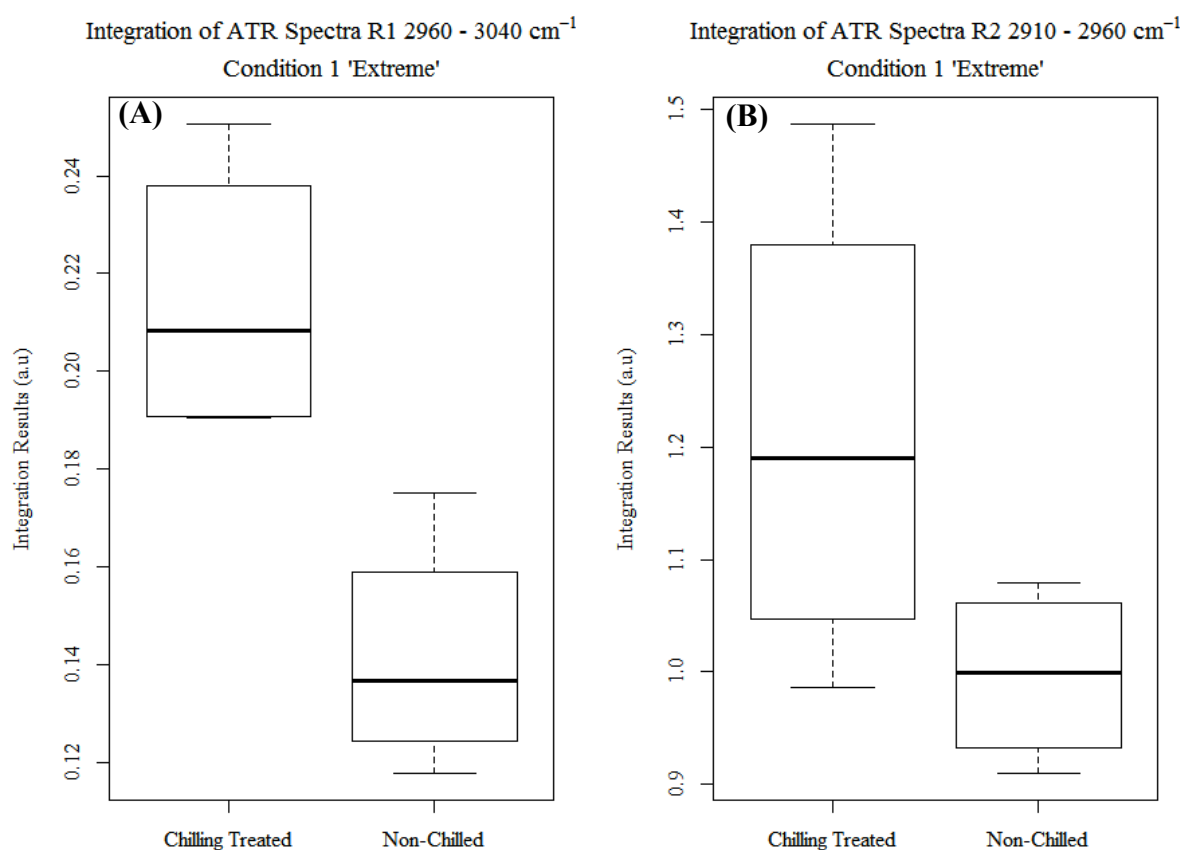


Figure B.5 Boxplot of peak area integration (a.u.) of asymmetrical CH_2 bending groups of leaf (V6; adaxial side) 'extreme' chilling condition mature corn by treatment (chilling treated, non-chilled) using ATR-FTIR; spectra scan average 512; **(A)** Bar plot of the CH_3 group (region 1; $2960\text{-}3040\text{cm}^{-1}$) by treatment. Total $F_{0.05}(1,6) = 14.63$, $p < 0.01$; NC $\mu = 0.142$, $\sigma = 0.025$; CT $\mu = 0.214$, $\sigma = 0.029$; **(B)** Bar plot of asymmetrical CH_2 bend (region 2; $2910\text{-}2960\text{cm}^{-1}$) by treatment; Total $F_{0.05}(1,6) = 3.542$, $p = 0.109$; NC $\mu = 0.997$, $\sigma = 0.078$; CT $\mu = 1.21$, $\sigma = 0.22$;

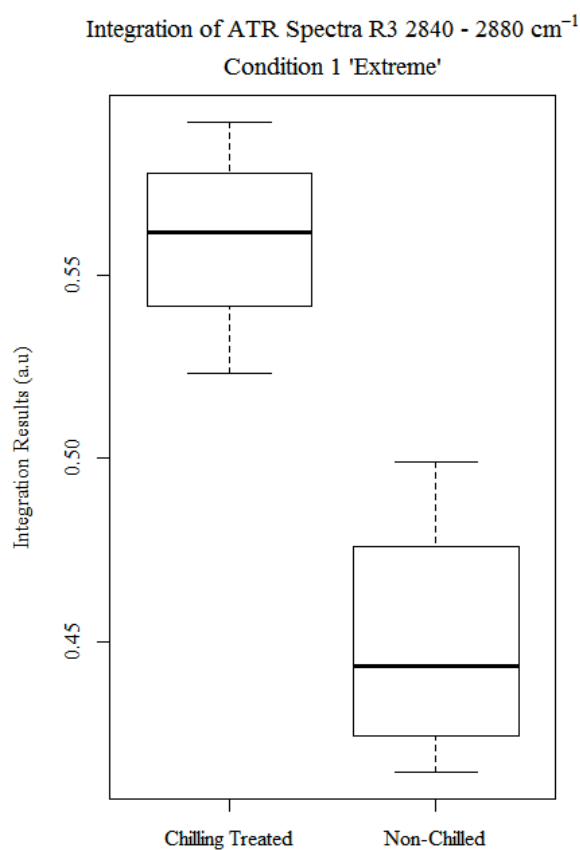


Figure B.6 Boxplot of peak area integration (a.u.) of symmetrical CH_2 bending group (region 3; $2840\text{-}2880\text{cm}^{-1}$) of leaf (V6; adaxial side) 'extreme' chilling condition mature corn by treatment (chilling treated, non-chilled) using ATR-FTIR; spectra scan average 512; Total $F_{0.05}(1,6) = 22.75$, $p < 0.01$; NC $\mu = 0.450$ $\sigma = 0.036$; CT $\mu = 0.560$, $\sigma = 0.028$;

APPENDIX C FOCAL PLANE ARRAY MAPPING

C.1.1 FPA-FTIR Sample Preparation

Mounted dried epidermal peel: Mature corn at the reproductive growth stage (Figure 3.2) with sampling of V6 leaf (Figure 3.1) was selected for adaxial epidermal peels. The peels were mounted between a set of Barium Fluoride (BaF_2) windows (Crystran Ltd., Dorset, Poole, UK) and dehydrated in a Desiccator unit with Silica Gel. Leaf Samples were collected from within 30cm of the tip of the leaf. Each sample was taken from a separate plant of same age.

C.1.2 FPA-FTIR Mapping Spectromicroscopy

Desiccated adaxial epidermal peels of mature corn at the reproductive growth stage with sampling of leaf V6 (adaxial side)(Figure 3.1) were evaluated through non-destructive leaf cuticle surface evaluation using a Fourier Transform Infrared Spectrometer to map the distribution with greater specificity following the ATR technique on a small sample set. Each sample was from a separate plant. The endstation for this testing was the Bruker Vertex 70v/S spectrometer with a Hyperion 3000 microscope equipped with a 64x64 Focal Plane Array (FPA) MCT Detector $2560 \times 2560 \mu\text{m}^2$ (Bruker Optics, Ettlingen, Germany)(Figure 4.4C). A gold background sample was collected at the start of each run to provide a reference of a clean and highly reflected surface.

C.1.3 CLS Experimental Design

FPA-FTIR Design

Focal Plane Array (FPA) Spectromicroscopy was performed on 8 samples (four genotypes by two environments (chilling treatment and non-chilled, Chapter 3). Each sample was measured at each point with 128 scans. The measurements were evaluated to determine the interaction effects between genotypes and chilling regimes.

FPA-FTIR Analysis

The spectra from the FPA-FTIR (Vertex 70V) were evaluated using OPUS Software (v. 7.0 Pro, Bruker Optics, Ettlingen, Germany) and R-Studio to generate compositional maps to distinguish the compositional contribution of cuticular wax through peak area integration across the lipid fingerprint region. FPA-FTIR maps were created in 1X1 (64x64 pixel) tiles representing chilling treated and non-chilled in two genotypes (884, 959). The maps represent the lipid integration across the three regions, as described in 4.2.14 Spectra CH₂ Regions Defined. The integration area of the spectra were analyzed with respect to two independent variables (genotype, treatment) with the response variable being the cuticular wax differences measuring using the lipid peak area integration across the region.

C.1.4 ‘Mild’ Chilling Condition FPA Mapping Results

Chilling treated samples of genotype 884 expressed an increase in spectral intensity over each of the three regions (Figure C.1). Genotype 959 did not appear to have a change in spectral intensity in the three regions (Figure C.1). Region 1 results look hotter due to scale of intensity. It was not possible to put Region 1 on the same scale as 2 and 3. Overall, there were no significant or notable differences in this test.

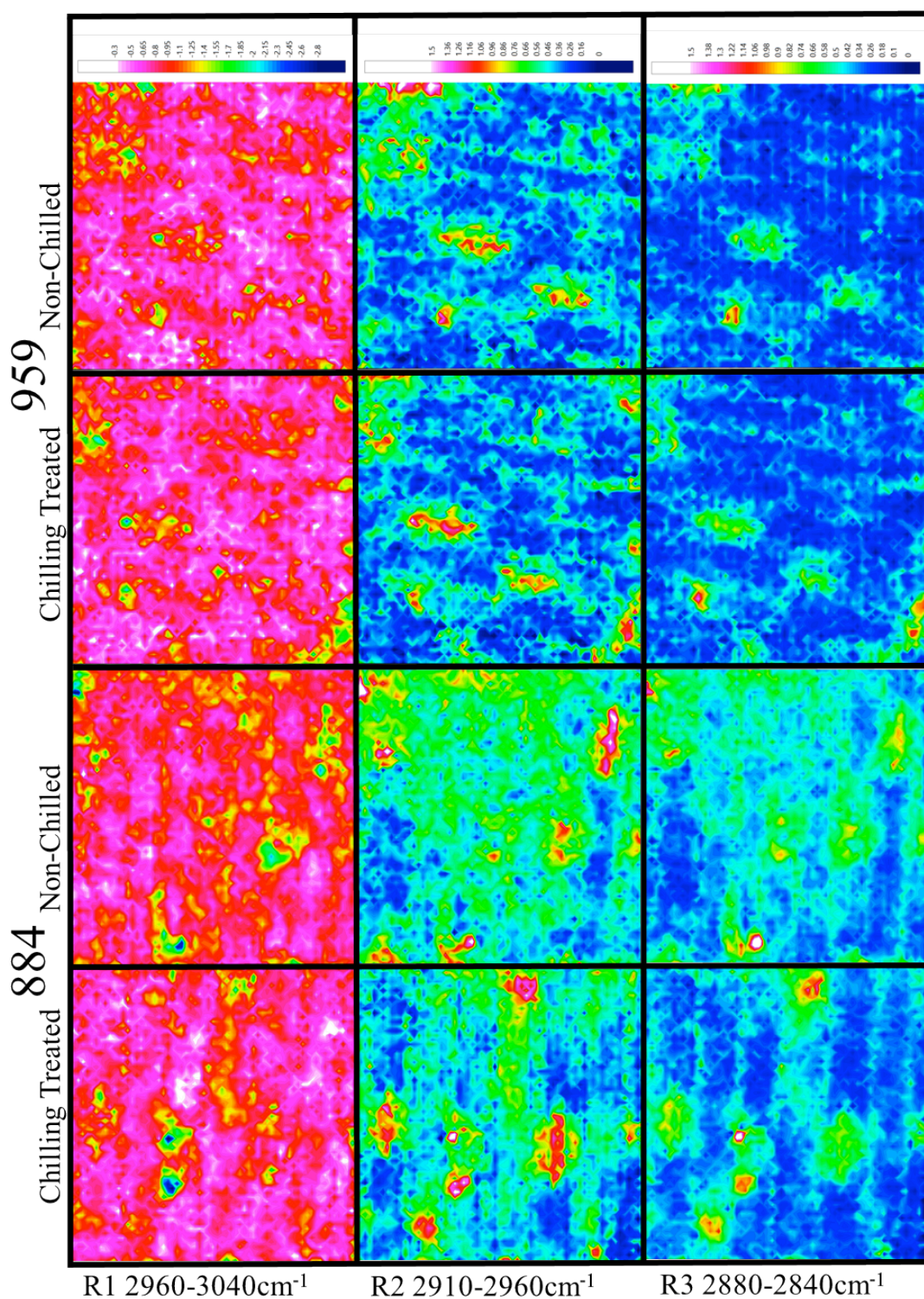


Figure C.1 Heat map of 'mild' chilling treated and non-chilled 884 and 959 over three regions of integration. The color scale represents intensity of the spectra (warm colors; high intensity, low values; cool hues).

APPENDIX D. 10 DAY 'CHILLING TREATED' MATURE CORN PLANTS



Figure D.1 (L to R): Early Golden Bantam, 3 (256), 3 (675), 3 (884), 3 (959)

APPENDIX E PRELIMINARY ULTRASTRUCTURAL STUDIES.

Hypothesis

There is a physical cuticular trait linked to frost resistance.

Objective (Trichome): To determine if differences in leaf ice nucleation are related to trichome length, density or type.

Objective (Stomata): To determine if differences in leaf ice nucleation are related to stomatal aperture.

Materials and Methods

Plants for Trichome Analysis

Sump imprints were collected from 4 genotypes (Table E.1.1).

Table E1.1: Material for trichome analysis

GENOTYPE	SENSITIVITY	TREATMENT	PLANTS PER TREATMENT	REPS
278	S	NA	3	4
675	S	NA	3	4
893	R	NA	3	4
959	R	NA	3	4
278	S	ACC	3	4
675	S	ACC	3	4
893	R	ACC	3	4
959	R	ACC	3	4

SUMP Sample Collection for Trichomes and Stomata

Samples will be collected using the Sukuzy's Universal MicroPrinting method (SUMP) (SUMP method, SUMP Laboratory, Tokyo)(Konoshima 1962, Tanaka et al. 2005). The leaf imprints will be analyzed by using Dinocapture software (AnMo Electronics Corporation, New Taipei City, Taiwan) or Matlab.

SUMP Image Acquisition and Analysis

SUMP imprints were imaged using an Evos inverted digital microscope (Thermo Fisher Scientific Inc., Waltham, MA, USA). Images were captured at different magnifications (4x, 10x and 20x). All images were analyzed using ImageTool (ImageTool version 3.0, UTHSCSA Dental Diagnostic Science, San Antonio, USA) and the Evos scale was calibrated into ImageTool. Images taken at 4x were used to count the number of trichomes by type (papillary, filiform and glandular capitate). Density of these trichomes per square millimeter of leaf area was measured. Images at 10x and 20x were used to calculate the length of the trichomes from the base to the tip on the filiform types. SUMP imprints also captured stomata aperture and for this response, all imprints were taken at night when the probability of a frost event is high.

Results

Corn trichome type by genotype

Figure E.1.1 shows that in this set of genotypes 675, 278, 959, 893, there are few differences between trichome frequencies. The only significant difference is within the

glandular capitate trichome type between genotypes 675 and 278, both of which are considered sensitive type based on chilling experiments.

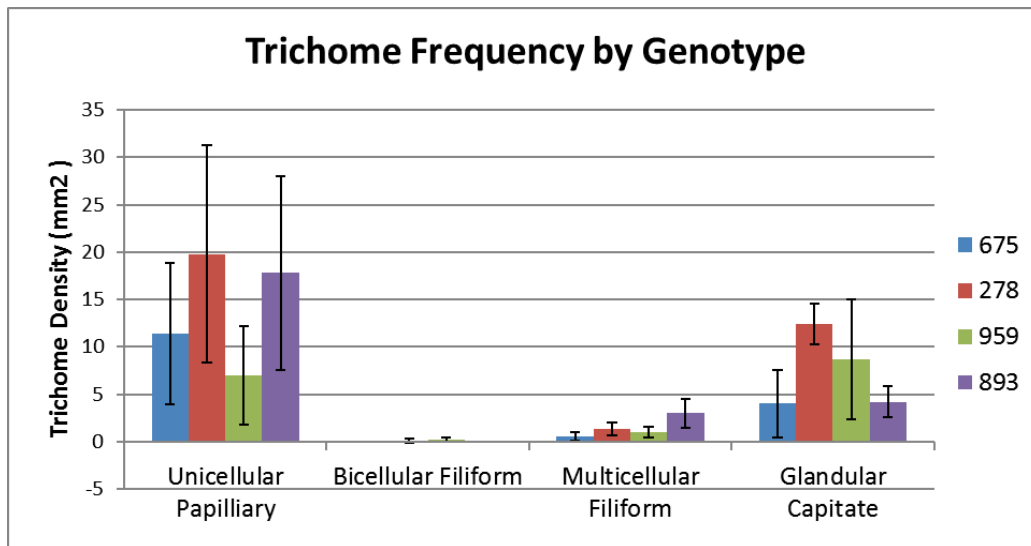


Figure E.1.1: Genotypic analysis of trichome type in grain corn

Trichome type distribution

The results for the trichome distribution across the leaf (Figure E.1.2) show that the unicellular papillary trichome type is most prevalent at the tip of the leaf and by contrast the base of the leaf has the largest number of glandular capitate trichomes. The mid portion of the leaf has an intermediate prevalence of unicellular papillary and glandular capitate trichome types. The filiform types were present in low quantities overall and showed no significant difference between leaf sampling location.

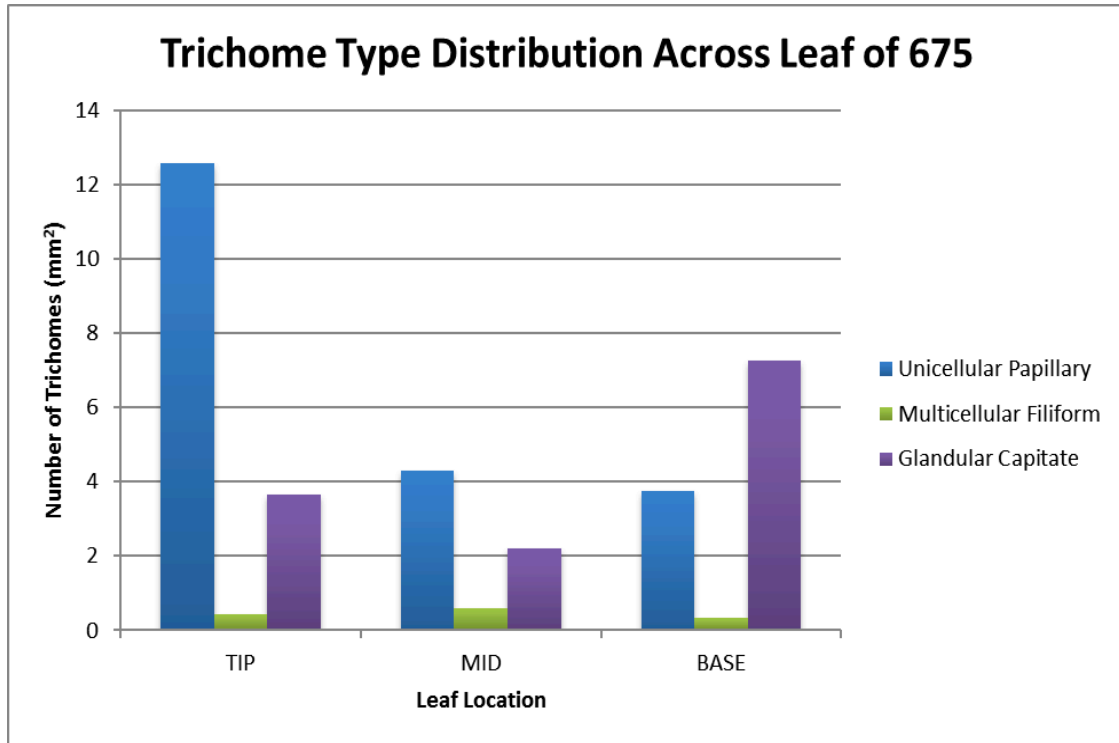


Figure E.1.2: Leaf location effect of 675 by trichome type

Stomatal Aperture

SUMP imprints across genotypes taken at night indicated all stomatal remained closed (Figure E.1.3). Since the probability of frost is greatest at night when the temperatures are lowest, and since closed stomata will not allow ice to penetrate through the stomatal aperture, we concluded that stomata were not involved in allowing ice propagation to occur across genotypes. There were no genotypic differences observed.

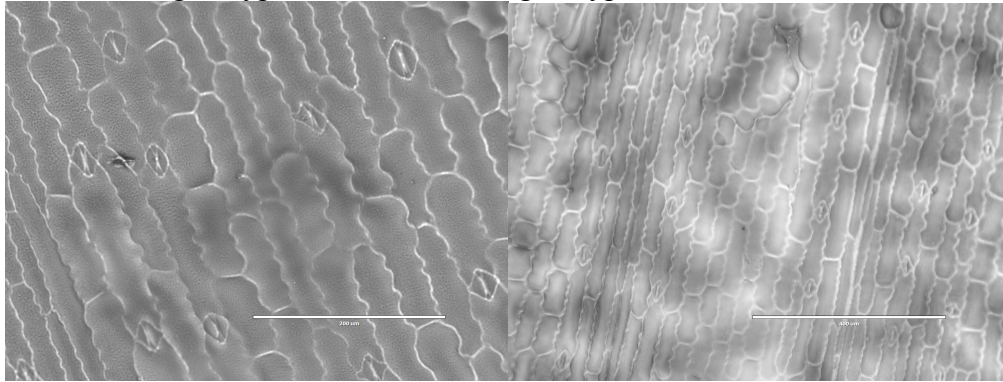


Figure E.1.3: SUMP Imprints showing closed stomata at 20X and 10X